Geological and human influences on groundwater flow systems in range-and-basin areas: the case of the Selva Basin (Catalonia, NE Spain)

Ph.D. Dissertation
2010

Albert Folch i Sancho

Advisors

Dr. Josep Mas-Pla
Universitat de Girona

Dr. Albert Soler i Gil
Universitat de Barcelona

Tutor

Dr. Joan Bach i Plaza
Universitat Autònoma de Barcelona

Unitat de Geodinàmica Externa i Hidrogeologia
Departament de Geologia

UAB
Universitat Autònoma de Barcelona

Geological and human influences on groundwater flow systems in range-and-basin areas: the case of the Selva Basin (Catalonia, NE Spain).

Programa de Doctorat en Geologia

Memòria realitzada per Albert Folch Sancho, sota la direcció del Dr. Josep Mas-Pla, del Grup Consolidat de Recerca en Geologia Aplicada i Ambiental (GAiA) de la Universitat de Girona, i el Dr. Albert Soler i Gil, del Grup de Mineralogia Aplicada i Medi Ambient de la Universitat de Barcelona, i sota la tutorització del Dr. Joan Bach Plaza, de la Unitat de Geodinàmica Externa i Hidrogeologia de la Universitat Autònoma de Barcelona.

Josep Mas-Pla Albert Folch i Sancho Albert Soler i Gil

Joan Bach i Plaza

Bellaterra, abril de 2010.

Als meus pares i als meus germans

Agraïments

En primer lloc m'agradaria donar els meu sincer agraïment als meus directors de tesi. A Josep Mas-Pla, del Grup Consolidat de Recerca en Geologia Aplicada i Ambiental (GAiA) i Geocamb de la Universitat de Girona, especialment, per impulsar-me a viatjar i a aprendre a l'altre punta del món, i sobretot per animar-me quan en un principi les coses no van sortir com esperava; per no limitar-me en la meva iniciativa "investigadora", sempre respectant-me i considerant-me tan si estava encertat o com si no ho estava; i per obrir-me les portes a la meva formació més enllà d'aquesta tesi. A Albert Soler, del Grup de Mineralogia Aplicada i Medi Ambient de la Universitat de Barcelona, especialment, per donar-me una altra visió de la hidrogeologia, per ensenyar-me la importància de la geoquímica més enllà d'aquesta tesi i per mostrar-me sempre el teu suport en tot moment. I sobretot, agrair-vos a tots dos per fer-me créixer tant a nivell professional com personal.

Agraeixo també el suport rebut pels professors de la Unitat de Geodinàmica Externa i Hidrogeologia, especialment a Joan Bach per tutoritzar-me la tesi en aquesta última etapa. M'agradaria extendre el meu agraïment a Mario Zarroca i Joan Estalrich pel suport rebut en diferents aspectes relacionats amb el treball que aquí es presenta.

A Anna Menció de la Universitat de Girona i Roger Puig de la Universitat de Barcelona, per la seva ajuda en l'elaboració d'aquesta tesi amb qui he compartit intenses jornades de camp.

To Mike Edmunds, professor at the University of Oxford and a magnificent geochemist. For his help in the interpretation of hydrochemistry data and for giving me new ideas about the use of groundwater tracers. And more than that, for showing me a wider point of view about groundwater and its importance in the world.

To T. C. Jim Yeh, professor at the University of Arizona. For his advise in groundwater flow modeling which I have applied in further contexts than this dissertation. For being so strict with me and respect my opinions. To Kris Kuhlman, a great engineer and PhD student at the University of Arizona, for his patience with me and for teaching me some of the most relevant tricks of groundwater flow modeling.

A la resta del professorat i personal del Departament de Geologia de la Universitat Autònoma de Barcelona. Especialment a Mercé Corbella pel seu suport i ànims sobretot aquest últims

mesos, a Esteve Cardellach per les discussions sobre les relacions Cl/Br, a Eliseo Tesón i Julien Babault per ajudar-me en diferents aspectes "gràfics" de la memòria que aquí es presenta.

Al Servei de Triti i C-14, al Servei d'Anàlisi Química i al Grup de Tècniques de Separació de la Universitat Autònoma de Barcelona per la seva gran professionalitat, i especialment a Maria Teresa Robles, Josep Maria Paulís, Alba Eustaquio, Ignasi Villaroya i Gustavo Pérez.

Als Serveis Cientificotècnics de la Universitat de Barcelona a on s'han realitzat les anàlisis isotòpiques, de F, TOC i metalls, i especialment als tècnics Rosa Maria Marimon, Eva Aracil, Laia i Jaume de la Unitat de Medi Ambient.

A en Josep Maria Niñerola, a la Oihane Astui i a l'Alfredo Perez de l'Agència Catalan de l'Aigua, per les xerrades que hem tingut sobre diversos temes relacionats amb aquesta tesi i la seva continuació.

A Jordi Font del Institut de Diagnosi Ambiental i Recerca de l'Aigua (IDAEA) i Xavi Sánchez-Vila de la Universitat Politècnica de Catalunya, amb qui he discutit diversos aspectes sobre la modelització i la importància del flux en fractures. A Jesús Carreras del IDAEA, per la importància que han tingut algunes de les seves classes i comentaris en el desenvolupament d'aquest tesi. A Fidel Ribera de la *Fundación Centro Internacional de Hidrología Subterránea*, per recordar-me que amb el meu esforç he aconseguit arribar a conèixer el *com* i el *perquè*.

Vull fer constar la meva gratitud a l'Enric Viñals i també a Joan Carbó de Perforacions Sacot S.L, per la informació geològica i hidrogelògica aportada per aquest estudi.

A la Paula Rodríguez, per ajudar-me en la maquetació i el format d'aquest treball.

A tots el propietaris que molt amablement m'han obert les portes de casa seva i els quals la seva ajuda i comentaris han contribuït significativament a la realització d'aquesta tesi.

A tots els alumnes que he tingut durant aquest pocs anys d'experiència docent, per fer-me plantejar coses que ni tan sols se m'havien passat pel cap abans de tenir-los a classe.

A tots els meus amics, que durant tots aquest anys m'han "aguantat" en els moments bons però també dolents. Per donar-me ànims contínuament i per estar sempre al meu costat.

Especialment a la meva família, i no només pel suport rebut aquests últims anys sinó també per tota l'ajuda que m'han donat durant tota la meva vida d'estudiant. A la meva mare, que a base de dedicar-hi moltes hores i molta paciència va aconseguir que no deixés mai el camí correcte. Al meu pare, que sempre m'ha animat i m'ha ajudat ens tots els aspectes lligats a la meva educació i formació. Als meus germans, per dedicar-me el seu temps, esforç i motivació quan més ho necessitava.

Al Ministeri de Educación y Ciencia que ha finançat aquesta tesi mitjançant els següents projectes CICYT del Programa Nacional de Recursos Hídricos: REN2002-04288-C02-01 i 02; MCYT CGL2005-08019-C04-02 i 01/HID i CGL2008-06373-C03-03 i 01/BTE). Dins aquestes ajudes s'inclou una beca FPI (BES-2003-2407) i dues ajudes per estàncies breus de recerca, una als Estats Units i una altra al Regne Unit. Parcialment també ha estat finançada per l'ajut 2009-SGR-103 de la Generalitat de Catalunya de suport al Grup Consolidat de Mineralogia Aplicada i Medi Ambient de les Universitats de Barcelona i Autònoma de Barcelona.

Abstract

Groundwater hydrodynamics in range-and-basin areas are essentially determined by their geology, including the tectonic structure and the basin sedimentary infilling. Their study requires a large-scale approach to determining the location of the recharge and discharge areas of each flow system providing the basin with water resources. Furthermore, most of these areas have undergone heavy human development that can modify groundwater quantity and/or quality in different ways. Understanding geological and human influences on groundwater flow in these areas is a key aspect in achieving an adequate water resources management and therefore its future availability.

In this dissertation, the Selva Basin has been studied as a paradigmatic case of a range-and-basin area with severe human pressure on its groundwater resources.A conceptual hydrogeological model emphasizing the role of the main fault zones has been developed and tested using numerical flow modeling as a first step. Groundwater flow has been simulated in a range-and-basin area affected by a significant fault zone, which may drain or recharge an overlying alluvial aquifer. Various hydraulic conductivity values for the range rocks, the fault-zone, and the sedimentary infilling of the basin are considered, as well as different fault-zone widths and boundary conditions. The results show that upward and downward fluxes develop in the upper part of the fault zone controlled by the action of the alluvial aquifer, and even through the basement floor, which influence the recharge of the sedimentary infilling of the basin.

Second, the Selva range-and-basin hydrogeological system is described using potentiometric, hydrochemical, and isotopic data ($\delta^{18}O$, δD) taken from different field surveys, in order to achieve a twofold objective: (i) to describe a hydrogeological system in which tectonic elements play a significant role in the flow dynamics, and (ii) to show the influence of groundwater exploitation on the hydrodynamics of the system. Hydraulic head data indicate the relationships between the geological formations in the range areas and the sedimentary infill of the basin. In this context, fault zones and a fracture network have a direct effect on the recharge, and allow an upward vertical flow from the basement to the sedimentary aquifers. Hydrochemical and isotopic data support this observation. The use of fluoride (up to 15 mg/l) and nitrate (up to 217 mg/l) as tracers for the contribution of deep and shallow flow systems respectively provides a detailed portrait of the effects of pumping on the flowpath distribution. Isotopic data depict seasonal trends in groundwater captured by wells. Two distinct flow

systems are differentiated: a regional, large-scale, long residence time system, originating in the surrounding ranges, and a local flow system constituted by infiltration in the lower areas of the basin. The two systems contribute differently to the resources that are withdrawn, and their specific contributions define the potential for sustainable future water exploitation in the basin.

The final part of this hydrogeological study is a more specific description of the geochemical processes that determine the hydrochemical characteristics of groundwater across the Selva basin, based on the interpretation of major, minor and trace elements (such as fluoride, bromide, lithium, TOC, and their ratios to some major elements), and isotope data ($\delta^{18}O_{H2O}$, δD, tritium, $\delta^{34}S_{SO4}$, $\delta^{18}O_{SO4}$). It defines two different regional flow systems and different water qualities of local recharge anduses this specific data to corroborates the overall hydrogeologic conceptual model for the Selva range-and-basin area. From a methodological perspective, this chapter explores the use of minor elements and isotopes in the interpretation of regional scale system hydrodynamics. It also discusses their use as tracers of the distinct ground water flows originating in distinct recharge areas and influenced by an intricate tectonic setting.

The results of this dissertation describe the flow system of the Selva basin. In this basin, structural control defines the local, intermediate and regional flow systems responsible for the large-scale hydrodynamics of the basin and, more importantly, the recovery of drawdown after the main withdrawal period (summer). The origin of the recharge of the large-scale, regional flow systems is assigned to the Transversal range on the northern side and to the Guilleries range, especially in the western part. These hydrogeological systems include a groundwater flow within the basement and an upward vertical recharge from the basement to the overlying Neogene sedimentary layers. The local and intermediate flow systems originate in the basin itself or in the less-elevated surrounding ranges, and the fault system has a minor effect on their flowpaths. Human development modifies the flow paths mixing the different flow systems and changing the water quality along the year seasons.

From a broader point of view, this highlights the value of using different methodological insights in the study of these hydrogeological systems, as well as addressing the problem of water management in complex geological environments. First, it presents the outcome of various methodologies ranging from field work to numerical modeling, together with the analysis of hydraulic head, hydrochemical and isotopical data. Second, it shows the relevance of potentiometric evolution in different geological settings, and the treatment of the

hydrochemical/isotopic features and related geochemical processes that define groundwater samples and therefore each of the recharge end-members (local, intermediate, and regional) that participate in the overall flow systems. Finally, it identifies the effect of human pressures even on large-scale flow systems, as true alterations of natural behavior. The recognition of these effects, together with an integrated characterization of the hydrogeological system, provides the necessary knowledge for formulating specific strategies for assessment focusing on sustainability of water resources management in these geological contexts.

In specific terms, these strategies must be based on the importance of the groundwater flow terms in the water balance for a given hydrological basin. These terms are usually overlooked, yet they play an important role, especially when groundwater resources from deep confined (or leaky) aquifers are exploited. In the case of the Selva basin, identifying this contribution is fundamental in establishing potential future exploitation rates that further socio-economic developments may generate. This dissertation shows the scope of several approaches to describing this term in the water budget in range-and-basin areas in order to determine the availability of water resources therein, as a first essential step towards sustainability.

Resum

El comportament hidrodinàmic de les aigües subterrànies en conques intramuntanyoses ve condicionat principalment per la geologia, i especialment pel context estructural i els materials sedimentaris que reomplen la conca. L'estudi d'aquestes àrees requereix un enfocament a gran escala per poder determinar les zones de recàrrega i descàrrega dels diferents sistemes de flux que conformen els recursos hídrics de la zona. Aquestes zones solen estar afectades per un fort desenvolupament humà que pot donar lloc a una modificació de la quantitat i la qualitat de l'aigua subterrània de diferents formes. En aquest sentit, en conques intramuntanyoses és un aspecte clau entendre la importància de la geologia i de les pressions humanes en el flux d'aigua subterrània per arribar a assolir una gestió correcta dels recursos hídrics, així com per assegurar llur disponibilitat a llarg termini.

En aquesta tesi s'ha estudiat la depressió de la Selva com a un cas paradigmàtic on té lloc una important pressió sobre els recursos hídrics subterranis. Per tal d'estudiar el paper hidrogeològic que juguen les falles regionals en conques intramuntanyoses, en primer lloc, s'ha realitzat un model hidrogeològic conceptual a partir de la modelització del flux subterrani. Per fer-ho, s'ha dut a terme una simulació d'una zona de falla subjacent a una formació al·luvial, on la falla pot recarregar o drenar l'aqüífer al·luvial. S'han considerat diferents valors de permeabilitat per la zona muntanyosa, la zona de falla i els materials sedimentaris, així com diferents gruixos de falla i condicions de contorn. Els resultats mostren que es poden produir fluxos verticals ascendents i descendents a la part superior de la zona de falla degut a l'acció de la formació al·luvial, i fins i tot a través del sòcol, influenciant per tant la recàrrega dels materials sedimentaris de la depressió.

En segon lloc, s'ha caracteritzat el sistema hidrogeològic de la depressió de la Selva mitjançant mesures del nivell piezomètric i dades hidroquímiques e isotòpiques ($\delta^{18}O$, δD) al llarg de diverses campanyes de camp amb un doble objectiu: (i) caracteritzar un sistema hidrodinàmic on els elements tectònics juguen un paper important en la hidrodinàmica subterrània, i (ii) descriure la influència de l'explotació d'aigües subterrànies en la hidrodinàmica del sistema. Els resultats piezomètrics han posat de manifest la relació existent entre les formacions situades a les zones de muntanya que envolten la depressió i els materials sedimentaris que rebleixen aquesta. Les zones de falla tenen un efecte directe en la recarrega, permetent l'existència de fluxos verticals ascendents des del sòcol cap a diferents aqüífers sedimentaris. Les dades hidroquímiques i isotòpiques han validat aquestes observacions. En aquest sentit l'ió

fluor (< 15 mg/l) i nitrat (< 217 mg/l) han estat usats com a traçadors dels fluxos profunds i superficials respectivament i han permès posar de manifest l'efecte dels bombejos en la distribució de les línies de flux. La composició isotòpica de la molècula de l'aigua ($\delta^{18}O_{H2O}$, δD) ha evidenciat canvis estacionals en les aigües captades pels pous posant de manifest l'existència de dos sistemes de flux: un sistema de flux regional amb llargs temps de trànsit i originat a les zones circumdants més elevades, i un sistema de flux local recarregat a la zona de la depressió. Els dos sistemes contribueixen de manera diferent als recursos hídrics que s'estan explotant, i la seva aportació específica defineix el potencial de la depressió per una explotació sostenible a llarg termini.

S'han caracteritzat les aigües des d'un punt de vista hidroquímic a partir de la composició en elements majoritaris, minoritats i traça (fluor, brom, liti, TOC) i de dades isotòpiques ($\delta^{18}O_{H2O}$, δD, triti, $\delta^{34}S_{SO4}$, $\delta^{18}O_{SO4}$). Aquesta caracterització ha permès una descripció acurada dels processos geoquímics que defineixen les fàcies hidroquímiques de l'aigua subterrània al llarg de la depressió de la Selva. Així, s'han definit dos sistemes de flux regional i diferents qualitats de l'aigua associada a la recarrega local, i alhora s'ha corroborat el model hidrogeològic conceptual de la depressió de la Selva.

Des d'un punt de vista regional, a la depressió de la Selva el control estructural defineix sistemes de flux locals, intermitjos i regionals, els quals son responsables de la hidrodinàmica a gran escala, fins al punt que aquests son responsables de la recuperació dels descensos del nivell piezomètric després del període de màxima extracció (estiu). A la zona d'estudi, l'origen de la recarrega, a escala regional, és atribuïda a la serralada Transversal, a la zona més septentrional de la conca, i a les Guilleries, especialment a la zona oest. Aquests sistemes hidrogeològics impliquen un flux vertical ascendent des del sòcol que recarrega els nivells aqüífers neògens de la depressió. Els sistemes de flux locals i intermitjos s'originen a la pròpia depressió o a les zones circumdants més properes, els quals estan menys afectats per les zones de falla. La pressió antròpica crea una barreja entre els diferents sistemes de flux modificant la qualitat de l'aigua al llarg de l'any.

Els resultats d'aquest estudi mostren que en conques intramuntanyoses per obtenir una caracterització integrada del sistema hidrogeològic i el coneixement necessari per formular estratègies específiques cap a una gestió sostenible dels recursos hídrics, i en concret a la depressió de la Selva, és necessari:

i) la utilització de diferents metodologies per abordar l'estudi d'aquests tipus de sistemes hidrogeològics. Així, en el present treball primerament s'aborda des de la caracterització de camp fins a la modelització numèrica passant per l'estudi de nivell piezomètrics i dades hidroquímiques e isotòpiques;

ii) caracteritzar l'evolució piezomètrica de les diferents formacions geològiques juntament amb les característiques hidroquímiques/isotòpiques i els processos geoquímics relacionats que defineixen les mostres d'aigua, i per tant, cada un dels extrems de barreja de la recarrega (local, intermitja i regional) que participen en el conjunt del sistema de flux;

iii) finalment, identificar les pressions humanes, fins i tot en els sistemes a més gran escala, com una verdadera alteració al comportament natural.

Aquesta tesi defineix els sistema hidrogeològic de la depressió de la Selva com a exemple de funcionament hidrodinàmic sota pressions antròpiques aplicable a altres conques intramuntanyoses. Aquest coneixement és necessari per formular estratègies de gestió dels recursos hídrics des d'un punt de vista quantitatiu i qualitatiu, com a eina indispensable per satisfer la demanda lligada a una millora socioeconòmica sense produir un empitjorament de la qualitat ambiental a llarg termini.

Summary

Chapter I

Introduction

Groundwater use is of vital importance for meeting rapidly expanding urban, industrial, and agricultural water requirements in several places around the world. As groundwater and surface water are parts of, and interact, in the hydrological cycle, awareness of their hydrodynamics and regulating their uses is important. The European Water Framework is the regulatory framework for water management in the European Union. It establishes that water management, based on basin hydrological plans, must focuson good conditions of the water bodies. To achieve these objectives, these basin plans must include mechanisms to integrate water withdrawals and make them compatible with environmental, economical and social issues in order to achieve a sustainable regime.

To achieve appropriate aquifer management, the groundwater behaviour of each body of water must be recognised. The first step in this task is to determine the recharge areas and establish the groundwater hydrodynamics for each flow system. To understand and describe this, it is necessary to focus hydrogelogical studies on two main issues: a) a description of the natural and/or predevelopment behaviour of the groundwater systems, mainly in terms of its geological context; and b) a definition of human influences upon the same system under development conditions.

The influence on the hydrogeological system of groundwater withdrawal varies depending on the hydrogeological context and human demands for water; but in any case, human effects are a major force for consideration as a potential pressure on the entire flow system. Furthermore, it can produce a potential alteration that may affect the availability of the total water resources in quantitative and qualitative terms.

In range-and-basin areas, apart from the site-specific geological context, one of the most important geological influences comes from the occurrence of regional faults. This structural aspect produces upward vertical flows (Forster and Smith, 1988a,b; Marler and Shemin, 2003; Bense and Van Balen, 2003, 2004; Bense and Person, 2006) that adds an extra recharge that changes the quality and quantity of groundwater and even surface water. The role of fault zones is therefore a key factor that must be considered and described in as much detail as possible.

In these mountain basins, the easiest way to detect human influence on the flow systems is through drawdown, and the inclusion of pollutants in the water systems. Seasonal drawdown,

especially in the summer or driest months, and its subsequent recovery, show the system's response to groundwater withdrawal. It is also interesting to look for pollutants in local as well as in regional flow systems, as indicators of the level of alteration of natural behaviour by human pressures, in temporal as well as spatial terms.

Bredehoeft (2002) and other previous authors (Theis 1940, Brown 1963, and Sophocleous 2000; as the main references) noticed the importance of studying aquifers' responses to the impact of wells in terms of sustainable development. According to them, the sustainable situation is accomplished not by pumping stresses in equilibrium with "natural" recharge (when streams, marshes, and springs may dry up), but by pumping conditions in equilibrium with discharge.It is therefore important to determine the mechanisms that enable a groundwater system to reach a new equilibrium after capture has begun. How capture occurs in an aquifer is a thus a dynamic process that must be taken into consideration when achieving a sustainable yield in equilibrium with environmental, social and economic issues.

Human activities therefore add an extra difficulty to knowledge of groundwater dynamics, which are complex even under predevelopment conditions because of their inherent geological heterogeneity. Several hydrogeological tools and information must be applied simultaneously in order to understand this hydrodynamic complexity. Each approach is based on whether potentiometric, hydrochemical, and/or isotopical data provides a partial answer to the hydrogeological problems. However, by combining several sources of information – i.e. methodologies - the necessary integrated knowledge of groundwater hydrodynamics can be obtained.

This dissertation attempts to provide an integrated approach to the various questions and problems mentioned above.The Selva basin in the NE of Spain, is therefore an appropriate area for testing such a combined methodology. Previous studies (Vehí 2000, Vilanova 2004, Menció 2006 and Piqué 2008) pointed out the hydrogeological features of this area, and its suitability for achieving this objective. It is a range and basin area that is recharged with different flow systems related to its tectonic context, where agriculture, industry and domestic supply generate intense groundwater demand (Menció et al. 2010).

The main objective of this dissertation is therefore to characterize the flow systems that make up the hydrogeological system of the Selva basin, as an approach to evaluating recharge areas

and their contribution to the basin water balance, indicating whether they are a guarantee of available water resources. To accomplish this objective, three main considerations have been taken into account:

- The task needs to be accomplished by means of integrating various approaches,
- Structural/geological features are a key point for identifying recharge in a range-and-basin area,
- Human influences are indeed a major factor in modern hydrodynamic processes.

1.1. Dissertation content

This dissertation is organized in five main chapters. In addition to this introduction (Chapter 1), Chapter 2 deals with numerical groundwater flow modeling in range-and-basin areas affected by significant fault zones, which may drain or recharge the basin under the influence of an overlaying alluvial aquifer. The work carried out shows the hydrological efficiency of fault zones as preferential flow, and it also analyzes the constraints that determine groundwater recharge rates to the surrounding basins.

In Chapter 3, the Selva range-and-basin hydrogeological system is described using potentiometric, hydrochemical and isotopic ($\delta^{18}O_{H2O}$, δD) data obtained in various field surveys, in order to realize a twofold objective: 1) to describe a hydrogeological system where tectonic elements play a significant role in the flow dynamics, and 2) to show the influence of groundwater exploitation on the system's hydrodynamics. The second goal is significant in that the field data collected must be seen as representative of of a natural system's response to human pressures. Fluoride and nitrate are used as tracers of the contribution of deep and shallow flow systems, with an occurrence that shows the effects of pumping on the flow path distribution.

Chapter 4 presents a detailed description of the geochemical processes that determine the hydrochemical characteristics of ground water across the Selva basin, based on the interpretation of major, minor and trace elements (such as fluoride, bromide, lithium, TOC, and their ratios to some major elements), and isotope data ($\delta^{18}O_{H2O}$, δD, tritium, $\delta^{34}S_{SO4}$, $\delta^{18}O_{SO4}$). It provides a robust support for the evidence from the various flow systems described in the previous chapter and corroborates the overall hydrogeologic conceptual model for the

Selva range-and-basin area. From a methodological perspective, this chapter explores the use of minor elements and isotopes in the interpretation of regional scale systems hydrodynamics. It also discusses their use as tracers of the various ground water flows originating in the different recharge areas and influenced by an intricate tectonic setting.

Chapter 5 contains the general conclusions based on the results presented in the three previous chapters.

Annex include the papers already published from the work developed for this dissertation.

1.2. Previous research

As mentioned above, each chapter focuses on to specific subjects or themes. References to previous work are specifically discussed in each section. Nevertheless, several studies carried out in the Selva basin are the basis for this hydrogeological study.

Many of the local and regional studies related with geology, groundwater and surface water have been summarized in the PhD dissertation by Menció (2006). However, the following works warrant a particular mention due to their hydrogeological relevance:

- Various hydrogeological studies analyze groundwater resources in the Selva basin in past decades, especially between the 1970s and the 1990s, such as as MOPU (1971b and 1985) and IGME (1984 and 1993).
- Vehí (2001) studies various geological aspects related to human activitites, one of which is the hydrogeology of the main geological formations.
- A hydrogeological study of the surface aquifers related to the Santa Coloma river is presented by Folch and Roldán (2003).
- Vilanova (2004) investigates the geological structure and the recharge of the Neogen sediments surrounding the Gavarres Range.
- Menció (2006) analyzes the geological, hydrogeological, ecological and social aspects related to water resources in the area and its sustainable development.
- Piqué (2008), characterizes the mineralogy, fluid geochemistry and processes releasing arsenic in groundwater in the Caldes de Malavella geothermal field.

1.3. References

Agència Catalana de l'Aigua (ACA), 2002. Model de Gestió del sistema hidrològic de naturalesa granítica del sistema Montseny-Guilleries. Generalitat de Catalunya. Barcelona. Unpublished.

Bense, V., Balen R., 2003. Hydrogeological aspects of fault zones on various scales in the Roer Valley Rift System. Journal of Geochemical Exploration 78-79: 317-320.

Bense V, Balen R., 2004. The effect of fault relay and clay smearing on groundwater flowpatterns in the Lower Rhine embayment. Basin Research 16: 397-411.

Bense VF, Person MA., 2006. Faults as conduit-barrier systems to fluid flow in siliciclastic sedimentary aquifers. Water Resources Research 42, W05421. DOI:10·1029/2005WR004480. http://www.agu.org/pubs/crossref/2006/2005WR004480.shtml.

Bredehoeft, J.D., 2002. The Water Budget Myth Revisited: Why Hydrogeologist Model. Groundwater 40, 340-345.

Brown, R.H., 1963. The cone of depression and the area of diversion around a discharging well in an infinite strip aquifer subject to uniform recharge. U.S. Geological Survey Water-Supply Paper 1545C.

Folch, A., Roldán, R., 2003. *Estudio hidrogeològico de los acuíferos de la riera de Santa Coloma de Farners.* Fundación Centro Internacional de Hidología Subterránea. Barcelona.

Forster, C.B., and Smith, L., 1988a. Groundwater Flow Systems in Mountainous Terrain. 1. Numerical Modeling Technique. Water Resources Research 24, 999-1010.

Forster, C.B, and Smith, L., 1988b. Groundwater Flow Systems in Mountainous Terrain. 2.Controlling Factors . Water Resources Research 24, 1011-1023.

Instituto Geológico y Minero de España (IGME), 1984. Proyecto de investigación Geotérmica en el Vallès mediante sondeos de reconocimiento y síntesis hidrogeotérmica. Síntesis Hidrogeológica de la Selva. Madrid.

Instituto Geológico y Minero de España (IGME), 1993. Estudio para le evaluación de las aguas minero-medicinales, minerales naturales, de manantial, termales y minero-industriales en el territorio de Catalunya. El macizo granítico de les Guilleries-el Montseny (Girona y Barcelona). Primer informe final. Madrid.

Marler, J., Shemin, G.,2003. The Permeability of the Elkhorn Fault Zone, South Parck, Colorado. Groundwater 41, 321-332.

Menció, A., 2006. Anàlisi multidisciplinària de l'estat de l'aigua a la depressió de la Selva. PhD dissertation, Universitat Autònoma de Barcelona. http://www.tdx.cesca.es/TDX-0718106-140651/

Menció, A., Folch, A., Mas-Pla, J., 2010. Analysing hydrological sustainability through water balance. Environmental Management. DOI 10.1007/s00267-010-9461-y.

Ministerio de Obras Públicas y Urbanismo (MOPU), 1971b. Estudio de los recursos subterráneos de la zona de la Selva (Gerona). Estudio de los recursos hidráulicos totales del Pirineo Oriental (zona norte). Dirección General de Obras Hidráulicas. Madrid (Spain).

Ministerio de Obras Públicas y Urbanismo (MOPU), 1985. Plan Hidrológico del Pirineo Oriental. E.E.2 Estudio complementario sobre aguas subterráneas. Zona 5 - La Selva. Síntesis Hidrogeológica. Dirección General de Obras Hidráulicas. Madrid (Spain).

Piqué, A., 2008. Insights into the geochemistry of F, Ba and Zn-(Pb) hydrothermal systems: examples from northern Iberian Peninsula. PhD dissertation. Universitat de Barcelona.

Sophocleous, M. , 2000. From safe yield to sustainable development of water resources: The Kansas experience. Journal of Hydrology 235, 27–43.

Theis, C.V., 1940. The source of water derived from wells: Essential factors controlling the response of an aquifer to development. Civil Engineer 10, 277–280.

Vehí, M., 2001. Geologia Ambiental de la Depressió de la Selva. PhD dissertation. Universitat Autònoma de Barcelona. http://www.tesisenxarxa.net/TDX-0321102-144158/

Vilanova, E., 2004. Anàlisi dels sistemes de flux a l'àrea Gavarres-Selva-Baix Empordà. Proposta de model hidrodinàmic regional. PhD dissertation, Universitat Autònoma de Barcelona. http://www.tesisenxarxa.net/TDX-1217104-145328/

Chapter II

*Hydrogeological interactions between fault zones and alluvial aquifers in regional flow systems**

* this chapter is an extended version of the paper *Folch, A., Mas-Pla, J., 2008. Hydrogeological interactions between fault zones and alluvial aquifers in regional flow systems. Hydrological Processes 22, 3476-3487.*

2.1. Introduction

Regional groundwater flow paths have a strong influence on the recharge of aquifers located in tectonic basins, which are sometimes disregarded in local water balances because of their large scale. These flow paths were described in early conceptual studies by Hubbert (1940) and Tóth (1963), who pointed out that groundwater infiltrating in mountain areas may develop different scale flow systems according to the regional topography and the location of the recharge/discharge areas.

Faults profoundly affect patterns and rates of fluid flow systems occurring at the upper part of the Earth's crust at scales ranging from the microscale to basins of tens of kilometers wide (Nesbit and Meuhlenbachs, 1989; Bethke, 1985; Ge and Garven, 1994). A fault zone with different hydraulic properties may act as a conduit for flow, a barrier to flow, or a complex conduit/barrier body that will control the water flow regime (Smith *et al*., 1990; Bredehoeft *et al*., 1992; Antonellini and Aydin, 1994; Haneberg, 1995; and Caine *et al*., 1996). In this way, fault zones are recognized as discrete intervals with particular lithologies and hydraulic properties (Forster *et al*., 1994, Scholz and Anders, 1994; Caine *et al*., 1996). Different studies (Forster and Smith, 1988a,b; Evans *et al*., 1997; Marler and Shemin, 2003; Bense and Van Balen, 2003, 2004; Bense and Person, 2006) show the importance of considering faults as hydrogeologic entities in the study of faulted flow systems. In particular, Bense and Van Balen (2003, 2004) show the influence of different fault structures on sedimentary deposits and how groundwater flow may be enhanced in the relay zones of normal faults.

Furthermore, the geomorphologic occurrence of streams and related alluvial aquifers following the fault direction is usual in range-and-basin areas where structural factors control the development of drainage networks. This creates an interaction between surface water-table aquifers and deep flow systems that can be complex (Novakowski et al., 2000). In a regional context, these alluvial formations may then play an important role in the hydrogeology of the system depending on the stream discharge and the hydraulic properties of the underground geological formations; that is, those of the fault zone and the surrounding range and basin areas. In a broad sense, this type of relationship between water-table aquifers and fault zones can be assimilated to the stream-aquifer association that provides river base-flow or aquifer recharge (Winter et al., 1998); and define a kind of alluvial gain or loss depending on the direction of the recharge with respect to the underlying fault zone.

In this study, our objective is to use numerical modeling to characterize the role of zone faults in the recharge of tectonic basins in range-and-basin aquifers, considering the occurrence of an upper alluvial aquifer as an additional feature in this particular hydrological system (Figure 2.1). Although fault influence on the groundwater flow has been widely recognized, flow line distribution and water balances are usually hard to estimate, as they will depend on the geometry of the geological formations and the variability of their hydrological properties. Furthermore, the existence of a stream recharged alluvial aquifer on the top of the fault zone adds a complementary element that disturbs the hydrological behavior of the system.

Recent research carried out at the Empordà and Selva basins (NE Spain; Figure 2.2) by Vilanova and Mas-Pla (2001), and more extensively by Vilanova (2004) and Menció (2006), provided motivation for this exercise. Their research used potentiometric as well as hydrochemical and isotopical data to show that faults located at the boundaries of these basins, in addition to fractures existing in its basement below the sedimentary infil, are responsible for a significant recharge in these formations. Upward vertical flow through fractures was then clearly stated. The occurrence of a large alluvial aquifer on the top of the fault zone adds an environmental interested as this upward flow from the fault zone may actually help to maintain its groundwater reserves and the stream base-flow. However, the possible recharge from the alluvial/surface water towards the aquifer constitutes an extra input that may bias groundwater hydrochemical and isotopical interpretations.

We conduct numerical simulations to reproduce and evaluate the different flow systems that outcome from distinct geological settings. In this way, we consider several conceptual models, multiple combinations of hydraulic conductivity values, changes in the fault zone width, and stratigraphic layering of the basin-fill sediments. Results are then discussed with the aim to understand possible field observations from these geological environments.

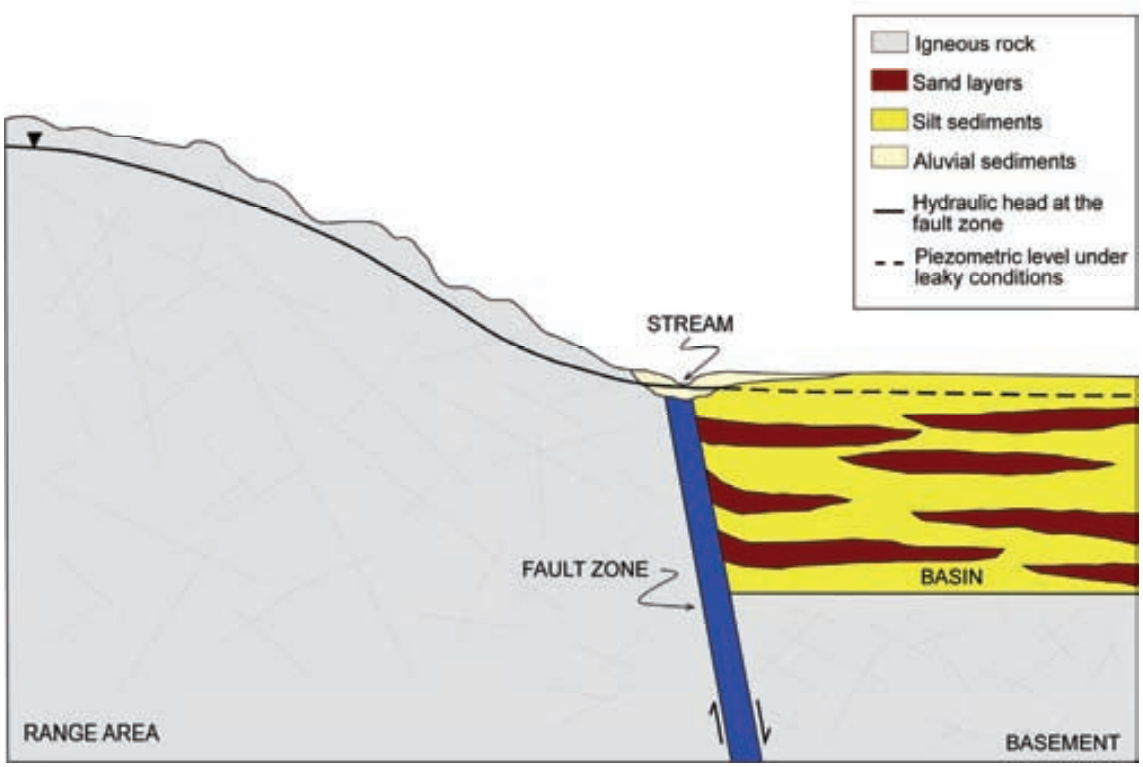

Figure 2.1. Hydrogeological scheme of the conceptual model.

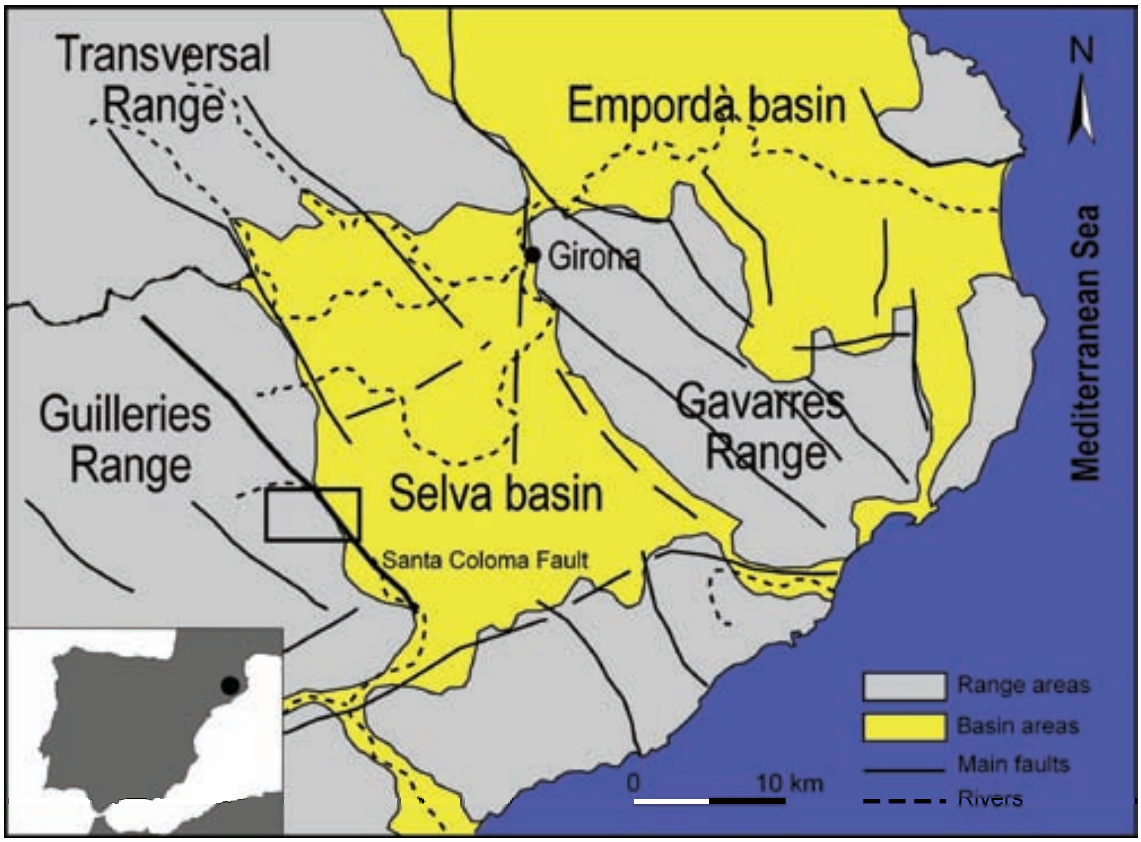

Figure 2.2. Geographical situation of the reference area. The simplified geological cross-section in Figure 2.1 correponds to the framed area.

2.2. Geological and hydrogeological setting

The Selva basin is a tectonic basin surrounded by the Guilleries (1,202 m asl), Gavarres (535 m asl) and Transversal (998 m asl) ranges located in the province of Girona (NE Spain) (Figure 2.2). Main fault direction in the area is NW-SE, with other relevant faults oriented NE-SW and N-S. This basin was created during the distensive periods after the Alpine orogenesis, and it has a Neogene sedimentary poorly-consolidated infil. Surrounding ranges consist of Paleozoic igneous and metamorphic rocks in the Guilleries and Gavarres, and pre-Alpine Paleogene sedimentary rocks (mainly, limestone and sandstone) in the Transversal range. Mean annual precipitation in this zone is approximately 700 mm.

In particular, the reference zone chosen for this modeling exercise is located along the Santa Coloma fault on the west side of the Selva Basin (Figures 2.1 and 2.2). The Santa Coloma Fault constitutes the tectonic boundary between the Guilleries Range and the Selva Basin. This fault zone has multiple planes showing a strike-slip movement coupled with a vertical normal component. Horizontal displacement is of several kilometers and vertical displacement is in the order of tens to hundreds of meters. Fault planes are basically vertical (Duran, 1985), although no description at short scale of this fault zone is available. In particular, the alluvial formation placed upon the Santa Coloma Fault zone is constituted by the fluvial deposition of the weathering products of the Guilleries Range rocks.

2.3. Modeling methodology

2.3.1. Hydrogeological model

A conceptual model for groundwater flow in the study area has been developed based on field investigations completed in the Guilleries domain (IGME, 1993; ACA, 2002) and recent field-work in the Selva Basin (Folch, 2005; Menció, 2006). In general, the Guilleries Range acts as the main recharge area. Groundwater discharge has a divergent pattern towards the eastern boundary of the range; i.e., the Selva basin. This flow system develops at different depths, generating a regional and a local flow system. Regional systems are of larger geographical extent than the study area. They take place through the granitic basement, and are responsible for the thermal springs occurring within the Selva basin. Local flows originate from

the range area to the basin sediments, as a lateral recharge, and from the uppermost parts of the basement as well. In this model, we address this local flow system to evaluate the effect of the limiting faults on their flow line distribution and the interaction with the upper alluvial aquifer. The hydrologic role of the alluvial formation developed along the Santa Coloma Fault zone is then considered in this work as a relevant hydrological domain. The perennial character of the stream suggests a strong relationship with local groundwater flow systems.

Hydrogeologically, we differentiate four geological domains in the study area (Figures 2.1 and 2.2); namely, the Guilleries Range and the basement of the depression, the sedimentary basin formations at the Selva, the Santa Coloma Fault zone, and finally, the upper alluvial formation. Their potential geometric and hydraulic properties constitute the basis of the conceptual model.

I. Guilleries range domain

This domain consists mainly of igneous rocks affected by foliation and fissures. Isotopic studies carried out in this zone (ACA, 2002) show that this range constitutes a whole unconfined aquifer that recharges on its entire surface. Potentiometric maps show that hydraulic head produces a smooth surface topography (Figure 2.3). Some deep wells, however, may show a confined type behavior according to structural characteristics, fault geometry, and scaling.

The hydraulic characteristics of these materials were studied by IGME (1993). Various pumping tests were carried out at between 36 and 300 m depth showing that the granite hydraulic conductivity and the storativity are determined by a dense joint system. Pumping-test interpretation shows a relative hydrodynamic homogeneity that can be represented as an equivalent continuous porous media. Hydraulic conductivity values vary only two orders of magnitude; from 10^{-2} to 1 m/day. The smallest hydraulic conductivity value corresponds to the fissured granite without the influence of fractures; whereas the largest value is associated with the influence of faults. Those hydraulic values can potentially be extrapolated to the granitic basement underlying sedimentary basin infil (Stober and Bucher, 2007).

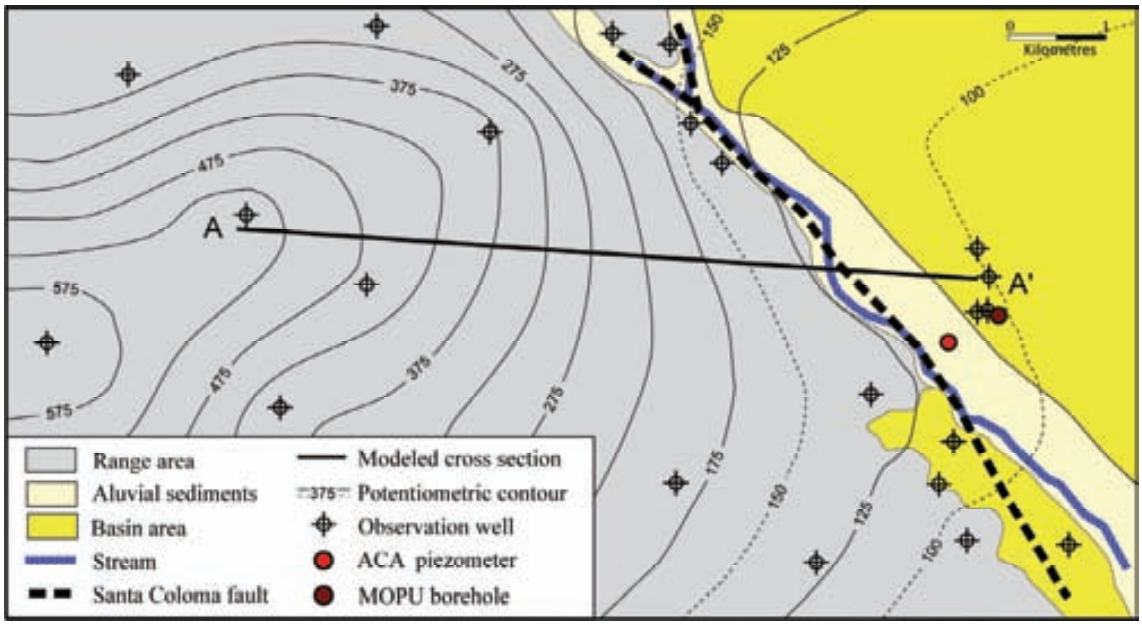

Figure 2.3. Geological features and hydraulic head distribution within the framed area in Figure 2.2. In particular, Figure 2.1 represents the geological cross section A-A'.

II. Sedimentary basin-fill materials of the Selva domain

Geophysical studies reveal a mean sediment thickness of 200 m near the western limit of the basin along the Santa Coloma Fault (MOPU, 1971). A particular borehole of 180 m shows a heterogeneous alternation of silt and sand layers. Sand layer thickness is between 2 and 5 m. Such a succession produces a multilayer aquifer with an unconfined behavior at the surface and a leaky behavior deeper down. The hydraulic conductivity geometric mean of the sand materials was obtained from pumping tests carried out at every layer in a single well, and it offers a value of 3 m/day (MOPU, 1971). Hydraulic conductivity for the silt layers was taken from literature. Then, the horizontal effective hydraulic conductivity of the sedimentary infil have been estimated being of about 1.3 m/day, considering the thicknesses of sand and silt layers in the borehole and their hydraulic conductivity, These experimental data become a reference for the conductivity values in this domain.

III. Santa Coloma fault zone domain

Structural studies of the area indicate that fault zones consist of multiple facture planes (Duran, 1985). Field work and borehole data from the area suggest a maximum width of the fault zone of 300 m. Three fault widths of 30, 100 and 300 m are used in the hydrological simulations to investigate the relevance of the fault geometry upon the flow system. As this fault is associated to the Guilleries Range lithology, the minimum hydraulic conductivity value

considered is 1 m/day, corresponding to the maximum value of the granitic unaltered rock. The maximum conductivity value attributed is 10 m/day, as is the maximum conductivity value given for this type of media (Sinhal and Gupta, 1999). Such high hydraulic conductivity values are consistent with those referred by Domenico and Schwartz (1998), Tiedeman and Hsieh (2001) and Stober and Bucher (2007).

Boreholes drilled in the fault zone do not differentiate a damage belt and a fault core in their records. From this lack of evidence and the mentioned structural characteristics of the fault zone, the fault zone can thus be considered an equivalent porous medium (Caine et al., 1996). We interpret from field data that no sudden changes in the hydraulic heads on either side of the fault suggest that vertical anisotropy is of small relevance.

IV. Santa Coloma alluvial formation domain

A final domain consists of the alluvial sediments along the Santa Coloma Fault. From a geomorphologic point of view, drainage network in the area is controlled by the tectonic structure, and streams tend to set their courses and their sedimentary deposits along structural lines in a rectangular drainage pattern. This is the case of the Santa Coloma Stream, which has developed an alluvial body 15-20 m thick and about 500 m wide over the fault zone outcrop (Figure 2.2).

Hydraulic head at the alluvial aquifer show a slight oscillation less than 3 m wide (ACA, 2007), related to seasonal variations without evidencing the intense groundwater withdrawal and the drought periods occurred in the last decades. Such behavior suggests an additional groundwater recharge from the underlying formations. Therefore, it shall be included as a hydrogeological domain in the model in spite of its reduced volume with respect to other domains.

2.3.2. Conceptual and numerical model

The conceptual and numerical model has been constructed despite a lack of detailed geological information and historical head records which allow a meaningful calibration of data. Nonetheless, our goal consists in describing flow patterns in a wide range of hydrologic

configurations that control recharge patterns to the basin area, and the fault zone and alluvial interaction. We just attempt a generic model of the Guilleries-Selva area.

For these reasons, we propose a two-dimensional numerical model simulating a cross section from the Guilleries Range to the Selva Basin (Figure 2.3 and 2.4). Measured potentiometric lines show a recharge towards the fault zone. Flow in the third direction (i.e., orthogonal to the modeled section) is assumed negligible.

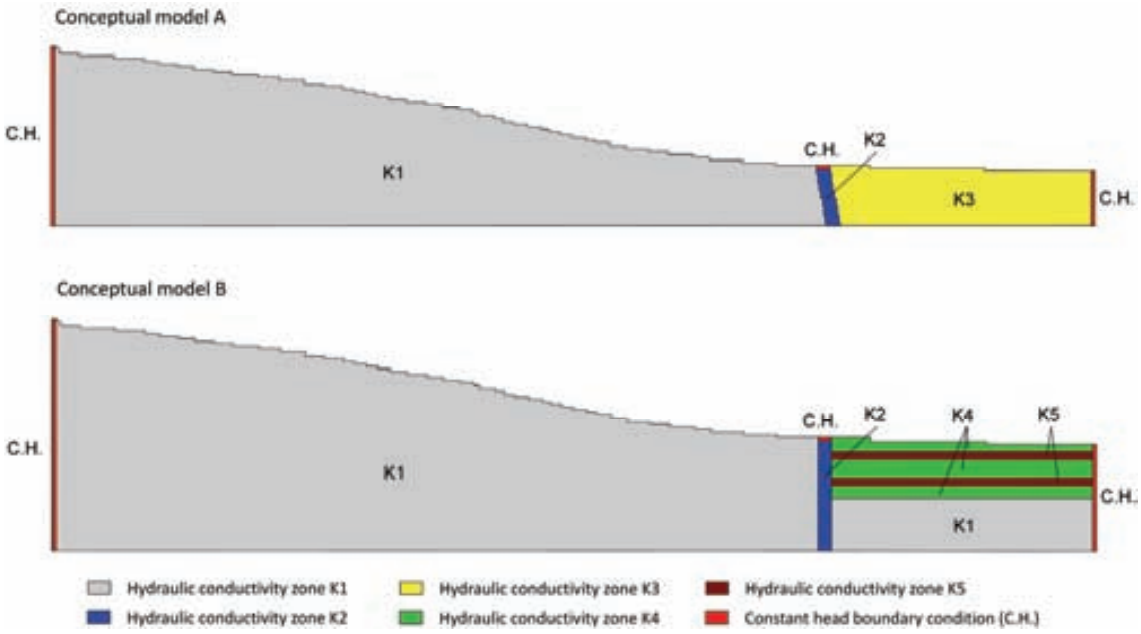

Figure 2.4. Examples of conceptual models A and B. In this figure, model A represents a specific case with a inclined fault zone, and a homogeneous and isotropic sedimentary domain. Model B, which includes a basement, represents a case study with a layered configuration of sedimentary materials and a vertical fault zone.

In order to constrain the number of cells in the model grid, geological and hydrological features have been simplified so that only a portion of the range and the basin domains is included. Specifically, the grid does not incorporate the parts of these domains where no influence of the fault on the water flow is expected. Each domain in our model consists of a homogeneous isotropic zone, simulating an equivalent porous media. In fractured media, this approximation is reasonable when fracture density is sufficiently high and the length and the space of the individual fractures are much smaller than the range scale (Forster and Smith, 1988a). Geometry and grid spacing have been designed to represent the three domains previously described. A similar analytical model was presented by Haneberg (1995), where the piezometric level at the fault zone was determined by the length of the fault zone and its surrounding areas, the hydraulic head of every zone, and the hydraulic conductivity values.

Two different conceptual geometries are considered in this modeling exercise. In the first setup, namely conceptual model A, the base of the sedimentary materials of the Selva basin is represented as an impervious boundary. In the second configuration, conceptual model B, which simulates a more realistic geological setup, a granitic basement is considered below the sedimentary basin-fill formation. In addition, different arrangements have been simulated for each conceptual model A and B to depict the influence of certain structural factors upon the flow lines; in particular different fault width and dip, and layering in the sedimentary domain. Figure 2.4 illustrates two specific models used in the simulations. In this figure, conceptual model A shows a specific case with a vertical fault and a homogeneous sedimentary domain. Conceptual model B adds the basement below the tectonic basin and the layering defined within the sedimentary formation. Model execution includes executing both conceptual models for every particularity described. Specifically, models A and B are studied both as homogeneous and layered basin-fill sediments, as well as with a vertical and an inclined fault zone. Although fault zones are assumed vertical, an inclination of 18º is also considered as a modeling option.

The finite-difference groundwater flow model MODFLOW (MacDonald and Harbaugh, 1988) and the graphical environment "Groundwater Vistas" (Rumbaugh and Rumbaugh, 2003) are used in this exercise. All simulations are run in a steady-state condition.

2.3.3. Grid construction

Grids for the two conceptual models A and B consist of 288 columns. Conceptual model A presents 65 rows, and between 9,433 and 9,477 active cells, depending on the fault zone width that varies the number of columns. Conceptual model B, which considers only a 100 m fault zone width, has 85 rows and 14,905 active cells.

The modeled section represents 7,580 m length in X-direction, and a vertical length of 650 m (model A) and 850 m (model B) in Y-direction. Topographic elevation at the highest point (column 1) is of 550 m asl. A unit thickness in the orthogonal direction is assumed for water mass-balances estimation. Grid construction has been adapted to field data procuring that the extremes were located near observation wells (Figure 2.3).

Cell size varies for each domain. The greatest cells are situated in the Guilleries domain, where the flow behavior is less important for the study purpose. Horizontal cell size is between 20 and 40 m. Mesh refinements have been implemented in the fault zone depending on its width, its horizontal cell size being 5, 10 and 20 m for 30, 100 and 300 m fault zone width, respectively. Finally, at the sedimentary domain, horizontal size grid is 20 m. Transition cells between two rows with different width present the average size with respect to the surrounding cells. All cells have a uniform 10 m vertical size.

2.3.4. Boundary conditions

The following boundary conditions are defined in the model (Figure 2.4):

- Constant-head boundaries are located in the sides of the model area, those of the granitic domain in the left-hand boundary, and of the sedimentary domain at the right-hand. The top of the fault zone overlaid by the alluvial deposit is also represented by a constant-head boundary.
- No-flow boundaries are placed at the bottom and top of the model.

The highest constant-head boundary condition is located in the granitic domain (column 1), with a value of 550 m. It corresponds to water table elevation at the boundary as reported by ACA (2002). Despite seasonal and annual head variations, we assume this has a slight influence on the overall results. Indeed, results arising from a lower head at the boundaries did not account for significant variations on the final mass balance. Since the modeled cross section represents the lower part of the range front, the horizontal flow pattern resulting from this specific model setup is consistent with a major recharge at the range highest elevations.

The second constant-head boundary condition has been situated at the last column, which represents the hydraulic head of the sedimentary multilayered aquifer. In this zone, the maximum head oscillation is between 4 to 10 m, depending on the observation well. The value represented in this boundary condition is 100 m, corresponding to the average value of one observation well near the section studied.

The third constant-head boundary condition is located at the top of the fault zone and it physically represents the occurrence of the alluvial formation. This boundary condition is supported, first of all, by the previously mentioned steadiness of the water table elevation. A

water table head oscillation less than 3 m wide since 1986 indicates that no major hydrologic changes occur in this aquifer. Secondly, hydraulic conductivity of the alluvial is some orders of magnitude larger than that of the fault zone, which permits an efficient flow from or to the fault zone towards the alluvial aquifer. In fact, we assume that the alluvial formation is able to drain off all the flux supplied by the fault zone through subsurface and surface discharge. Likewise it is capable of fully supplying surface water to the fault zone if a downward hydraulic gradient develops. Next, we define a constant-head value of 115 m that corresponds to the hydraulic head value of the alluvial aquifer in the section studied (Folch and Roldan, 2003).

Flow through this boundary will be of interest for the hydrological implications of the modeling results. In a similar way to the stream-aquifer interactions (Winter et al., 1998, Sophocleous, 2002), we define as a losing alluvial those simulations that transfer water from the alluvial aquifer to the fault zone and flow is defined as positive. Otherwise, a gaining alluvial represents those cases where water flows from the fault zone to the alluvial formation and flow is then defined as negative (Figure 2.5). Total flow is estimated by multiplying the flux (volume per unit area) given by the numerical flow model for the constant-head boundary cells that define the top of the fault zone, times the cell length and width (i.e.; a unit width).

No-flow boundary conditions are defined at the bottom and top of the modeled section. In conceptual model A, this represents the base of the sedimentary basin unit. In model B, it stands for the base of the granitic basement. A second no-flow boundary condition is defined at the top of the grid, except on the cells with a constant-head boundary. This boundary condition implies that infiltration does not occur through the water table. In the range area recharge takes place mainly in the highest summits of the Guilleries range, which are not included in the modeled section. Because the reproduced section only considers a small fraction of the whole hydrologic watershed, infiltration in this area is just a small volume of total recharge. Therefore, it will not significantly modify the flow field controlled by the whole basin. Similarly, infiltration upon the sedimentary aquifers has been described to recharge the uppermost layers of the sedimentary infil (Menció, 2006), and therefore it has no significance on the water balance of the overall sedimentary domain. Moreover, defining water table as a no-flow boundary avoids undesired and unrealistic model calibrations that would difficult the scope of these simulations, that is, the evaluation of the potential flow systems that outcome in range-and-basin areas from different combinations of domain hydraulic conductivities and fault geometries.

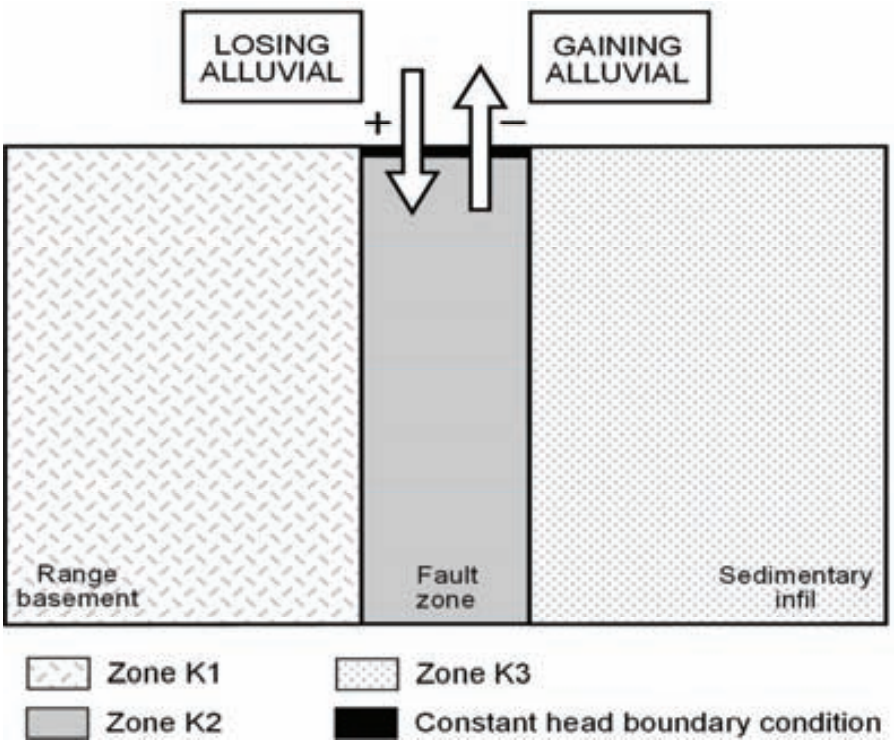

Figure 2.5. Fault zone/alluvial aquifer hydraulic relationships. Arrows indicate flow direction with the associated sign of the boundary mass-balance

2.3.5. Hydraulic properties and zonation

In accordance with the conceptual model we define three hydrogeological zones (Table 2.1): the fractured-fissured igneous domain (named K1), the fault zone (K2), and the bulk sedimentary basin materials (K3). In particular, conductivity zone K1 is located in the range area (conceptual models A and B), and in the granitic basement of the tectonic depression (model B). Its length is 5,500 m. Zone K2 presents different widths depending on the modeled fault zone width.

Table 2.1. Set of hydraulic conductivity values used for each domain.

Hydrogeologic domain	Zone	K (m/day)
Granite	K1	0.01 - 0.1 - 1
Fault zone	K2	1 - 10
Sedimentary materials (homogeneous)	K3	0.1 - 1.0 - 4
Sedimentary materials (layered)	K4	0.011 – 0.25
	K5	0.9 – 6.5

Finally, the K3 zone corresponds to the homogeneous sedimentary infil of the basin. Its length is 1,900 m. When considered as a layered unit, two distinct hydraulic conductivity values are considered, representing silt and sand layers that are called zones K4 and K5, respectively. According to well logs, sand levels represent between 10% and 60% of the total sedimentary column. Models with a layered structure of the basin sediments, with zones K4 and K5, have the same effective hydraulic conductivity value as the models build with the homogeneous zone K3.

Additionally, a specific extreme case with several K2 values up to 1,000 m/day (although possibly unrealistic) is considered with the aim of estimating the effect of exceptional K values at the fault zone on the flow distribution.

2.4. Results

For each conceptual model and fault geometry representing every possible hydrogeological model as described above, there is a set of 18 simulations that result from the combination of the different hydraulic conductivity value of every zone. Results are analyzed based on the main observed flow distributions, which are described and graphically presented. Flow exchange between the fault zone and the alluvial aquifer for each simulation is considered as an indicator of the influence of the distinct modern setups upon the behavior of the system. Overall mass balance results are not discussed as they simply represent total water volumes in a schematic geological setup, and therefore do not provide valuable contribution to the flow system description.

Simulations show the occurrence of a dual behavior in the relationship between the fault zone and the alluvial aquifer. Using conceptual model A, Figure 2.6 illustrates the flow distribution originated by distinct K1 values, with constant K2 and K3, in a 100 m fault zone width and an homogeneous sedimentary formation. As shown, for small values of K1 a losing alluvial situation arises (Figure 2.6A), whereas for larger values of K1 the opposite situation, a gaining alluvial, prevails (Figure 2.6B). The occurrence of such behavior is thus related to the recharge capability of the range zone (K1), as already stated by Haneberg (1995), and controlled by the boundary conditions at the top of the fault zone and the sedimentary materials (right-hand side of the model, Figure 2.4). The plot of the vertical flow magnitude (v_y) illustrates the zones where fault-zone and alluvial aquifer interacting becomes more significant.

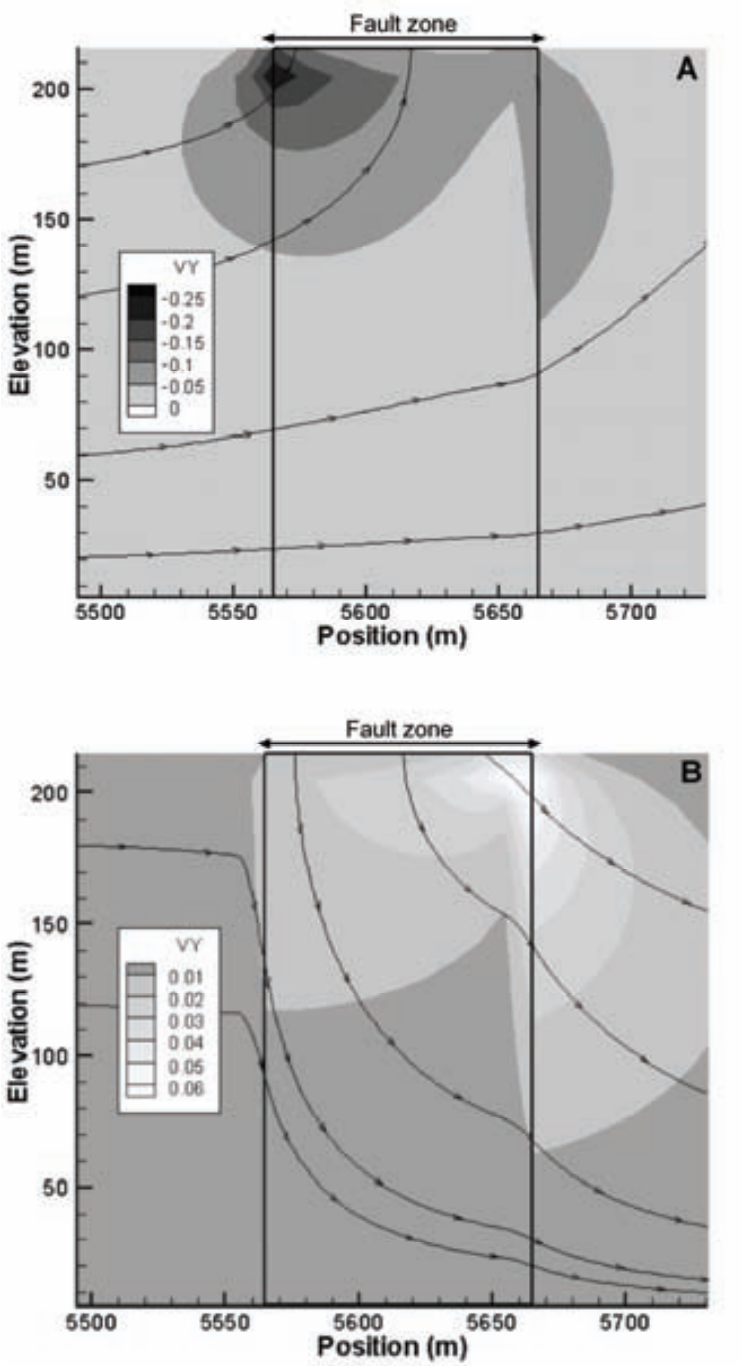

Figure 2.6. Vertical flow component (Vy) distribution and flow paths, based on conceptual model A and a 100 m fault zone width. A) Gaining alluvial case with K1 = 1 m/day, K2 = 1 m day^{-1}, K3eff. = 4 m/day (K4 = 0.25 m/day and K5 = 9 m/day). B) Losing alluvial case with K1 = 0.01 m/day, K2 = 1 m/day, K3eff. = 4 m/day (K4 = 0.25 m/day and K5 = 9 m/day).

Figure 2.7 presents the variation of flow values at the top of the fault zone for all model combinations. It can be observed that this dual behavior is observed independently of the fault zone width. Losing alluvial conditions (flow > 0) take place for small values of K1 and large values of K3, which gives the maximum contrast between the range and basin areas conductivities. It does not show a significant influence of K2, and is even less important as the

fault width increases. It is also noticeable that, for small K1 values, the flow magnitude entering the fault zone (losing alluvial) does not change significantly as a function of the fault zone width. In particular, the estimated magnitude of 5 m^3/day per unit length seems consistent for regular streams as that on the Santa Coloma alluvial formation. Santa Coloma River is a non-gauged stream; nevertheless, a nearby gauging station of a hydrologically-like watershed (Onyar River) has a mean annual flow of 1.8 m^3/s, and minimum mean flow of 0.46 m^3/s in summer. For instance, the estimated steady flow magnitude would imply a stream discharge of 0.40 m^3/s along an estimated stream reach of 7 km, which can be understood as a base flow; being then in fair agreement with actual discharge data.

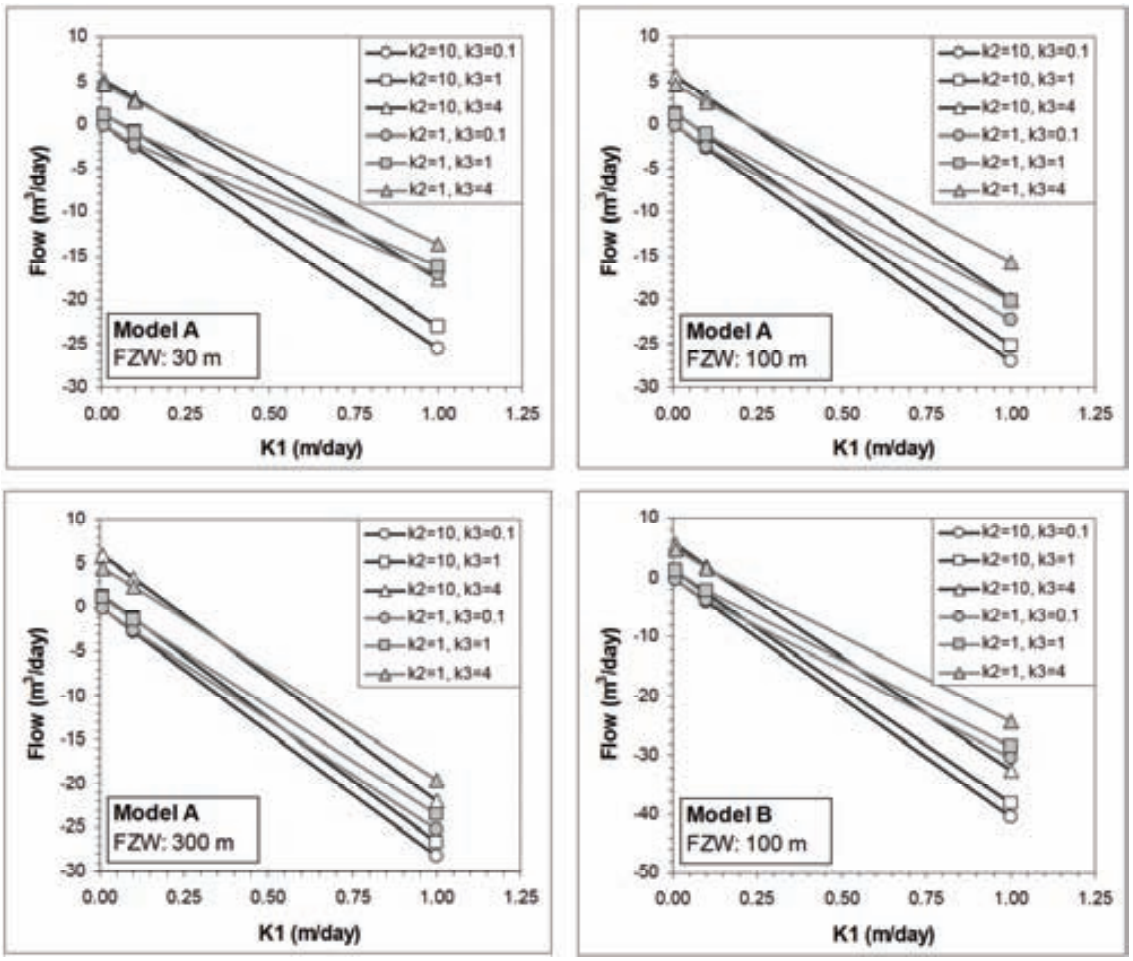

Figure 2.7 Flow magnitude at the fault zone related to different K values for each domain. FZW D fault-zone width.

On the other hand, in gaining alluvial conditions (flow < 0) the flow magnitude recharging the alluvial for large values of K1 tends to unify with the increase of the fault zone width. In this case, groundwater outflows to the alluvial increases for small values of K3, and for large values of K2. Finally, it can also be observed in Figure 2.7 that the influence of the fault zone conductivity, K2, diminishes as the fault zone width increases.

For most of the usual, realistic conditions, a gaining alluvial aquifer situation will occur. For K1 values larger than 0.1 m/day, and K3 values smaller than 1 m/day, groundwater flow will feed alluvial aquifer through an upward vertical recharge. Hydraulic conductivity values and flow magnitudes are dependent on the physical constraints of the model, and they do not represent actual observations. Those relationships, however, permit an identification of the possible hydrodynamic arrangements in such a geological environment.

More interestingly, for a particular combination of conductivity values and fault zone width equal to 100 and 300 m, a double behavior coexists at the top of the fault zone, where its portion close to the range area acts as a gaining alluvial, and the rest of the boundary, closer to the basin, behaves as a losing alluvial (Figure 2.8). This mixed behavior only occurs for low values of K1 (0.1 m/day), and it has only been reproduced in a few simulations.

These examples point out that hydrological recharge of the basin aquifers may have different sources, and in specific cases it may result from a mixing of surface and groundwater. For instance, Figure 2.6 illustrates that the basin zone recharge may result only from deep circulation from the range area when a gaining alluvial situation occurs. In a losing alluvial situation, basin recharge results from a mixing of water originated at the range area and at the upper alluvial formation. In these examples as well as in the specific setup that crafts the double behavior shown in Figure 2.8, it becomes obvious that basin recharge may originate from different depths within the range area. Therefore it may mix waters with distinct residence times as well as with different qualities. This fact becomes more extreme when surface water contributes to recharge through the alluvial formation.

The possible origins of water recharge into the basin sediments becomes better represented when layers of distinct hydraulic conductivity are introduced in the model, likewise a multilayer leaky aquifer. Figure 2.9 reproduces the same setup as Figure 2.6, except that the homogeneous basin aquifer has been replaced by a layered system with the same effective hydraulic conductivity. The effect of layers with distinct conductivity produces a modification of the flow lines. These tend to concentrate towards the high-conductivity layers (K5), as indicated by the distribution of horizontal flow magnitude (v_x) contoured in the chart. Moreover, numerical results indicate that in gaining or losing alluvial conditions, the flow is always greater in the deepest high conductivity layer. The variation of water volume recharging each layer attenuates as the fault zone conductivity (K2) increases.

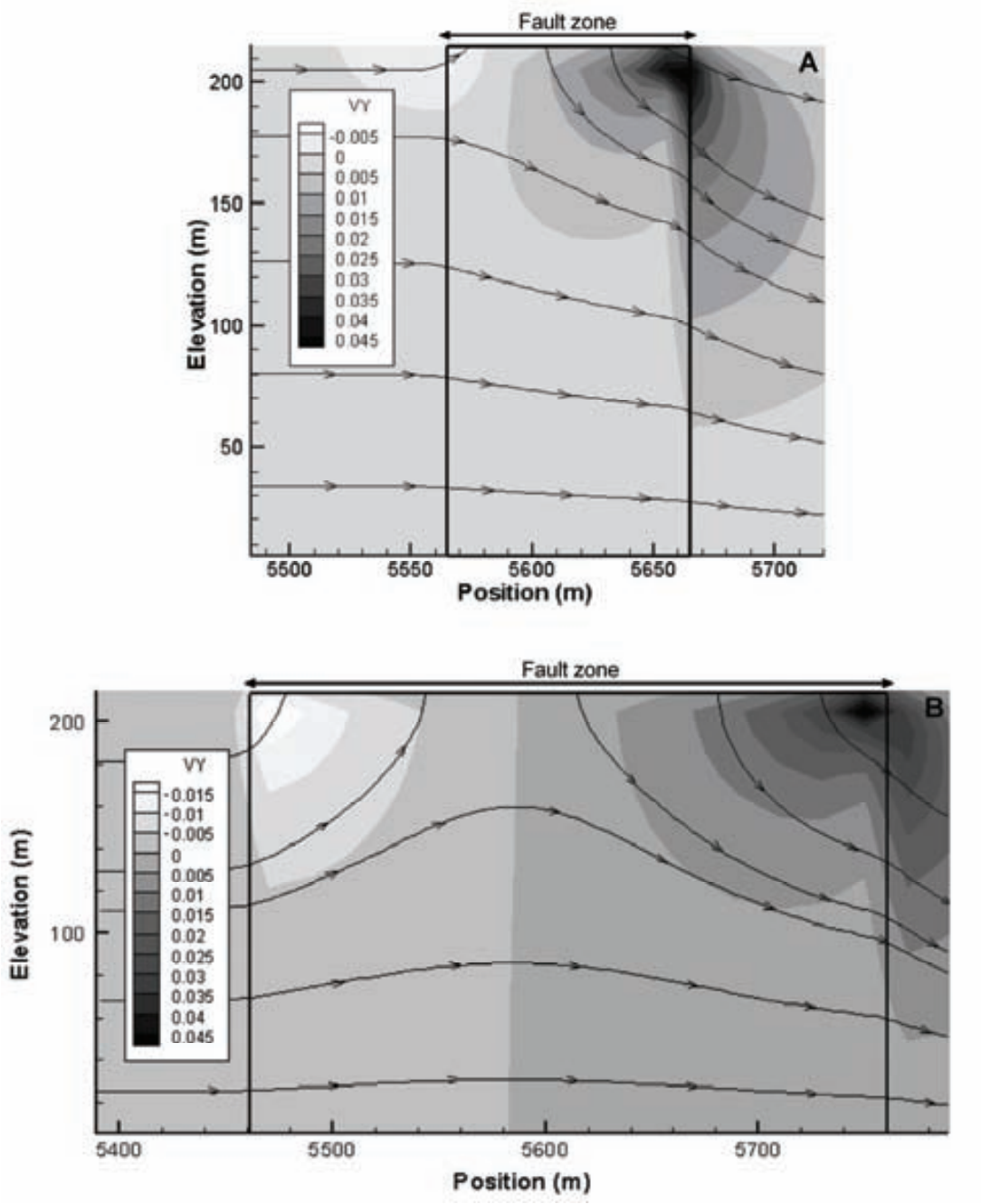

Figure 2.8. Effect of two distinct fault zone widths on flow distribution and flow paths, based on conceptual model A with K1 = 0.1 m/day, K2 = 1 m/day and K3 = 4 m/day. (A) Fault zone width: 100 m. (B) Fault zone width: 300 m. (Vy is the vertical flow component).

Some relevant observations concerning the recharge of the basin aquifer can be derived from Figure 2.9. For instance, the upper sedimentary layers may get their recharge mainly from deep flow lines in a gaining alluvial condition, whereas the lower layers can receive water from the alluvial if a losing alluvial situation occurs. It is relevant to notice that those flow line distributions can not be derived from a usual two-dimensional plain-view potentiometric map and they can hardly be identified in the field without a dense network of head data at several depths.

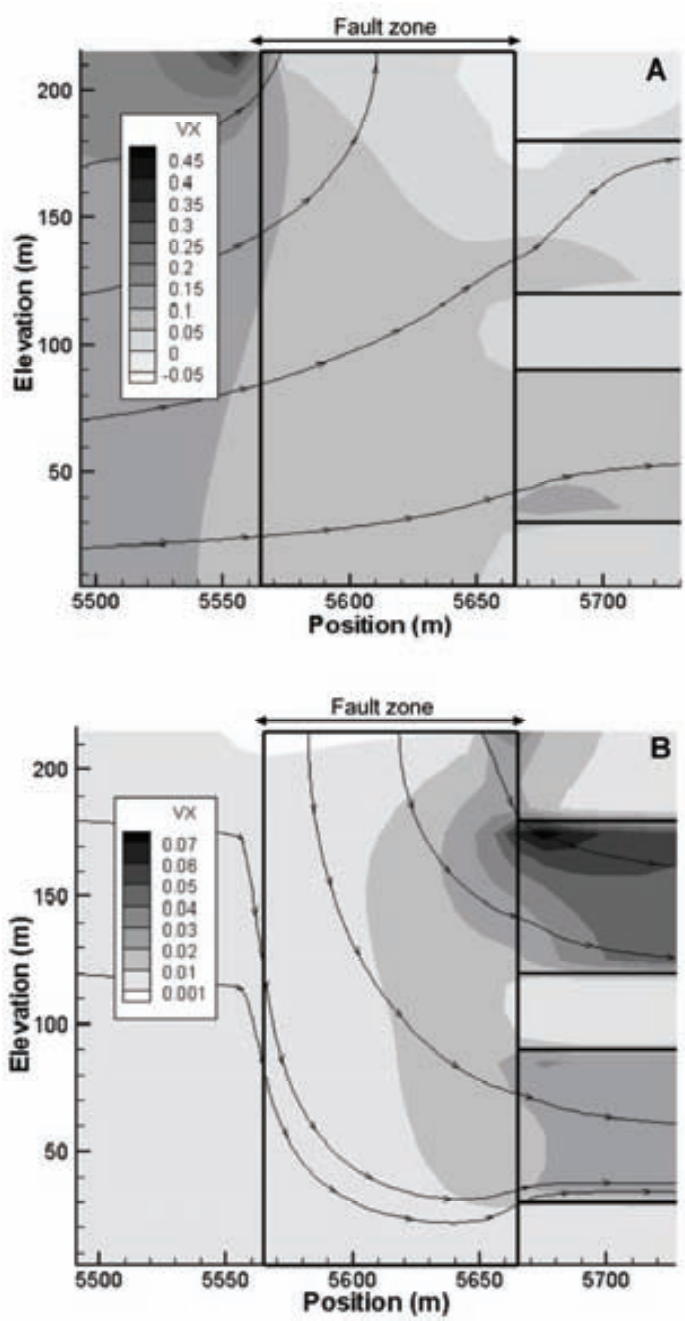

Figure 2.9. Effect of distinct K1 magnitude on flow distribution and flow paths, based on conceptual model A with a 100 m fault zone width, and a layered sedimentary domain. (A) Gaining alluvial. K1 = 1 m/day, K2 = 1 m/day and K3eff. = 4 m/day (K4 = 0.25 m/day and K5 = 9 m/day). B) Losing alluvial. K1 = 0.01 m/day, K2 = 1 m/day, K3eff.= 4 m/day (K4 = 0.25 m/day and K5 = 9 m/day). (Vx is the horizontal flow component).

When considering a dipping fault zone of 18º with respect to the vertical and towards de basin, the overall behavior is similar to those simulations with a vertical one. Main differences relate to the flow line location, which are displaced to a lower position by only 10-20 m, and to the discharge through the fault zone with small variations of 3-5% in the homogeneous case and

about 8-12% in the layered setup. Such results suggest that inaccuracies in the fault dip may not represent a serious handicap for regional aquifer modeling.

Conceptual model B incorporates a 200 m thick granitic basement. All simulations have been performed using a single fault zone width value of 100 m. In general, observed qualitative behavior is similar to those of conceptual model A. Obviously, an increase of the inflow cross-section in the left-hand side of the model modifies the overall mass-balance of the system and, in particular, water exchange at the fault zone top boundary. For instance, in the losing alluvial case (flow>0), the maximum reduction of water infiltrating from the alluvial to the fault zone is estimated to be less than 3% (Figure 2.7), and infiltrating flow lines do not reach the same depth as in model A. However, water exchange differences at the fault zone are larger in the gaining alluvial case (flow <0), reaching a maximum difference of 32% (Figure 2.7).

An additional remark refers to the behavior of flow lines through the granitic basement. Figure 2.10 shows two simulations based on model B, with a layered basin, and different values of K2. It can be observed that deep flow lines from the range area reach the sedimentary aquifer located about 100 m above. Even deeper flow lines cross the fault zone and continue through the basement in an ascending direction. Those flow lines will produce an upward vertical recharge to the sedimentary layers. The slope of these flow lines depends on the ratio of hydraulic conductivity values of all domains. Such observation is consistent with current vertical recharge identified using geochemical data (Vilanova, 2004; Menció, 2006). It can be related to large scale flow systems whose paths are modified by structural factors. Moreover, fractures in the basement rocks constitute an additional factor of flow path disturbance, which may certainly result in a more efficient recharge of the overlaying formations. According to the tangent law, the ratio between K2 and K3 controls the flow path from the fault zone to the basement below the basin. For those cases with very high K2 (K2>>K3), flow lines tend to be horizontal in the basement, and therefore the vertical recharge to the overlaying basin is limited.

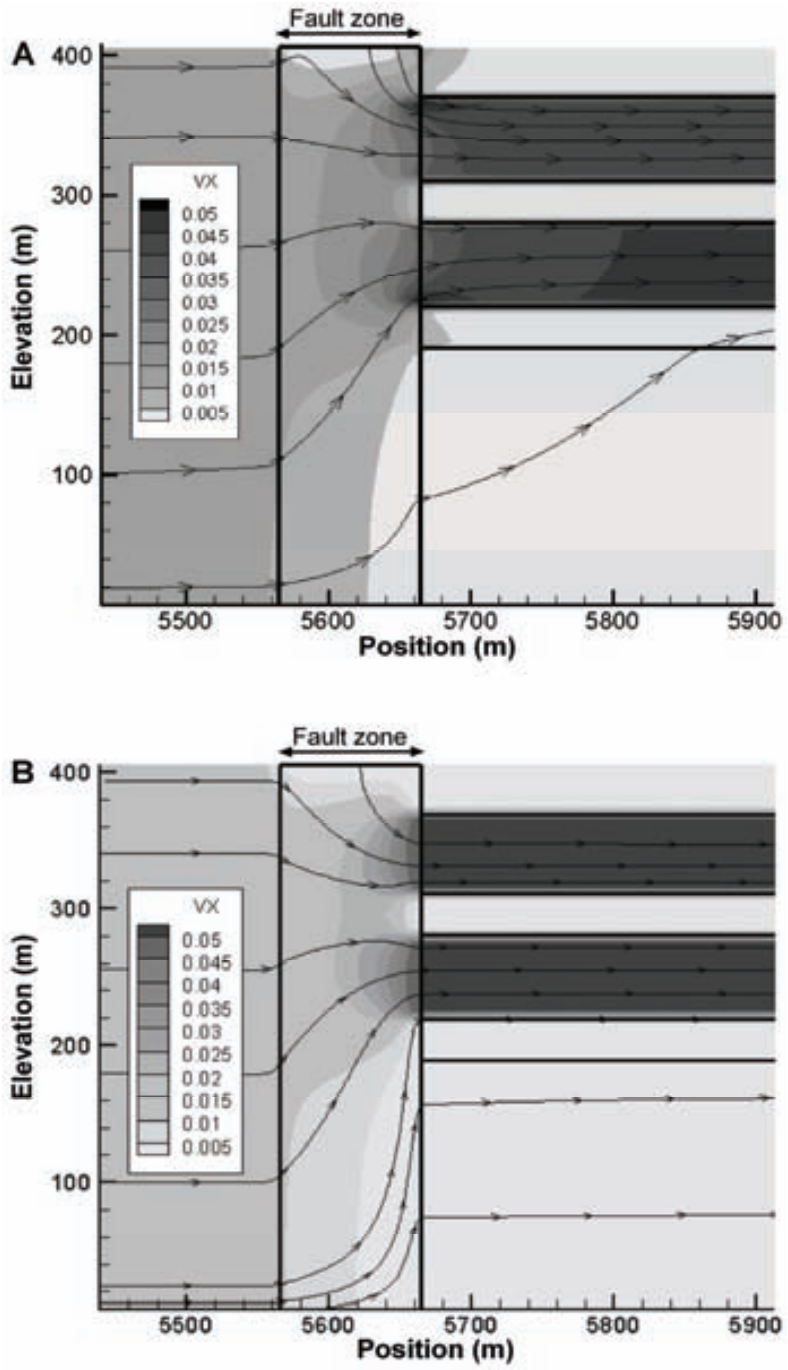

Figure 2.10. Effect of distinct K2 magnitude on flow distribution and flow paths, based on conceptual model B with a 100 m fault zone width, and a layered sedimentary domain. K1 = 0.1 m/day, K3eff. = 4 m/day (K4 = 0.25 m day_1 and K5 = 9 m/day). (A) K2 = 1 m/day. (B) K2 = 100 m/day (Vx is the horizontal flow component).

The influence of fault zone conductivity has been studied using a wider range of K2 values: up to 1,000 m/day. Two distinct simulations were conducted: the first one, with K1=0.01 m/day ensures a losing alluvial behavior, whereas the second case, with K1=0.1 m/day allows a gaining alluvial (Figure 2.11). In both cases, the absolute flow magnitude increases significantly in the K2 rank up to 150 m/day. For larger values of K2 no substantial modification of the flow magnitude occurs, indicating that the influence of the fault zone conductivity above this

reference value is of little importance. This observation can be valuable in those cases where the occurrence of open fractures may efficiently control groundwater flow pattern.

As a final point, simulation using conceptual model B is even less modified by the inclination of the fault. The fact of considering larger domain results in smaller influence on mass balance through the boundaries and in the modification of the flow paths.

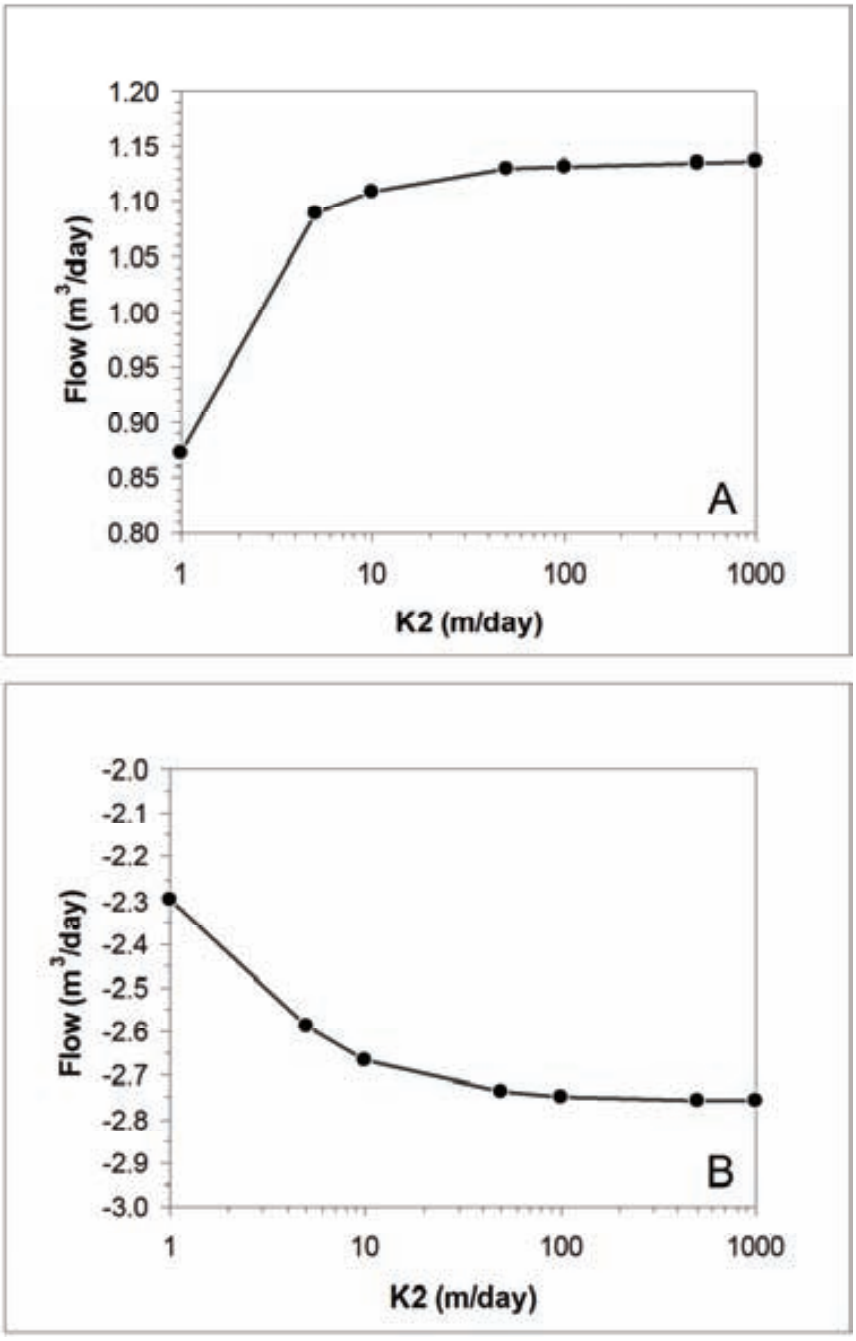

Figure 2.11. Flux at the upper fault zone boundary condition (i.e. the alluvial aquifer) as a function of K2 value for (A) a losing alluvial case: K1 = 0.01 m/day and K3 = 1 m/day, and (B) a gaining alluvial case: K1 = 0.1 m/day and K3 = 1 m/day.

2.5. Conclusions

A comprehensive numerical modeling exercise has been conducted to illustrate the control exerted by regional faults in range-and-basin areas where overlaying alluvial formation occurs. In this chapter, we address the case for several possible hydrological scenarios with the aim to depict flow paths within these geological systems. Geomorphic relationship between the fault zone and an overlaying alluvial formation has proved to be a relevant hydrological factor.

A suite of numerical simulations allow the identification of distinct flow behavior depending on the ratio of hydraulic conductivity values in the three geological domains, namely range, basin and fault zone; and the fault zone width. The presence of an alluvial formation on top of the fault zone defines two opposite hydrologic flow systems: (1) a gaining alluvial, in which there is a recharge from the fault zone towards the alluvial, and therefore to surface discharge, and (2) a losing alluvial behavior that allows infiltration of groundwater from the alluvial within the fault zone and the basin sedimentary infil. The habitual pattern in most of the simulations that cover realistic ranks of conductivity values is that of the gaining alluvial; however, a loosing alluvial takes place when recharge from the range area is limited by its low hydraulic conductivity, and externally controlled boundary conditions in the basin edge force this recharge. In some specific cases both types of behavior may coexist.

Results point to the fact that the flow line distributions and the relationship between the overlaying alluvial aquifer are basically controlled by the hydraulic conductivity differences between the domains, while the fault-zone width basically exerts its influence upon the mass balance with the alluvial formation. A small fault-zone dip up to 18^{o} does not substantially modify the flow system, indicating that the exact inclination may not be relevant in numerical simulations that consider vertical faults.

Conceptual model B, which accounts for a basement below the tectonic basin, and layering of the basin-filling sedimentary domain, provide a more realistic reproduction of the geological setting and offers a more reasonable interpretation of hydrological dynamics. As a result, these results contribute to understanding recharge processes of sedimentary tectonic basins that are controlled by hydraulically effective faults.

In particular, the set of flow-paths plots allow the identification of these recharge patterns. They point out that, according to the combination of conductivity values, recharge may come from distinct origins (Figure 2.12); for instance, only from deep circulation from the range area in the case of a gaining alluvial, or from a mixing coming from surface water and range inflow in losing alluvial circumstances. Additionally, different layers may also have different sources of recharge, and upward vertical recharge from the basin basement to the sedimentary aquifer outcome even in the case of a homogeneous basement.

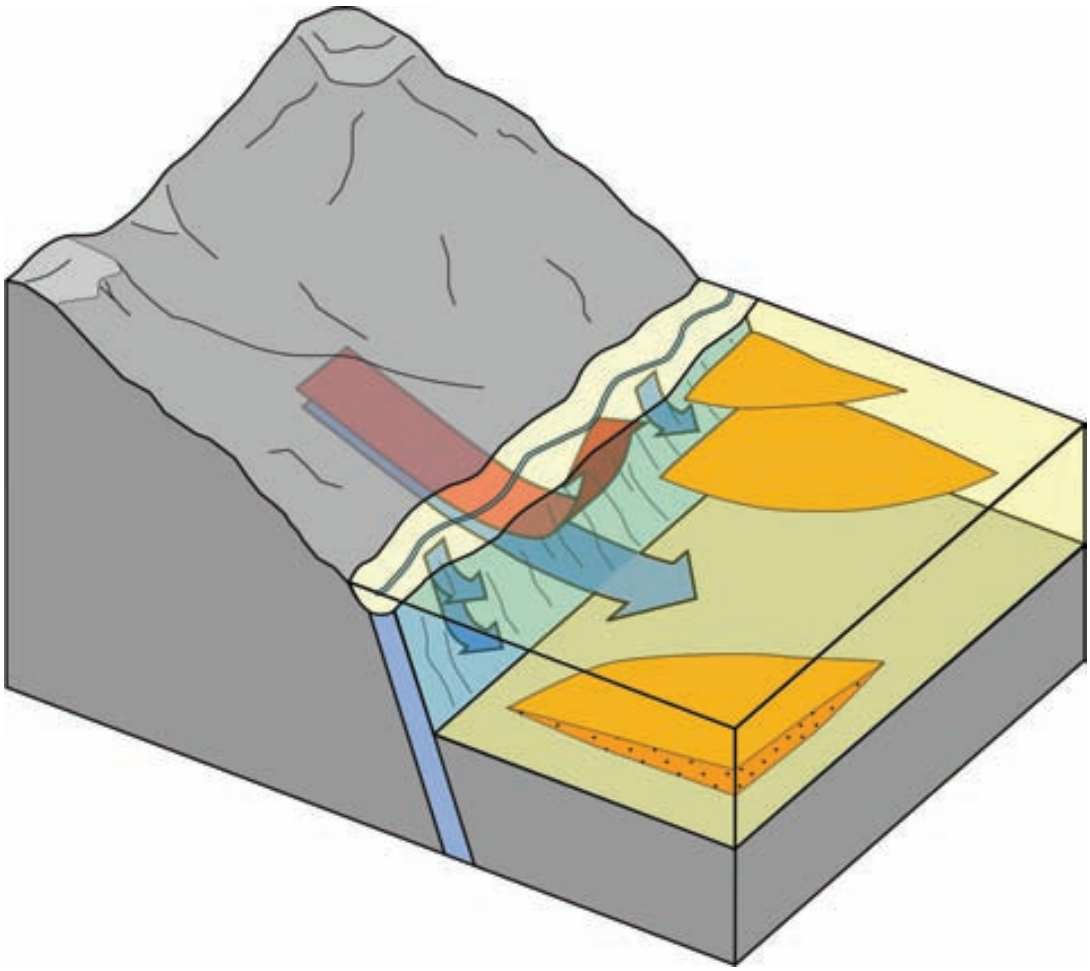

Figure 2.12. Hydrogeological conceptual model of regional faults in range-and-basin areas where overlaying alluvial formation occurs.

These conclusions illustrate possible hydrologic dynamics that are not easily drawn from field data. They also remind us of the need for caution in the hydrological interpretation of hydrochemical and isotopic data of basin groundwater samples, which may result from a mixing of waters from distinct quality and residence times within the regional hydrogeological system.

2.6. References

Agència Catalana de l'Aigua (ACA), 2002. Model de Gestió del sistema hidrològic de naturalesa granítica del sistema Montseny-Guilleries. Generalitat de Catalunya. Barcelona.

Agència Catalana de l'Aigua (ACA), 2007. Hydraulic head records. http://mediambient.gencat.net/aca/en/inici.jsp.

Antonellini, M., Aydin, A., 1994. Effect of faulting on fluid flow in porous sandstones: Petrophysical properties. American Association of Petroleum Geologist Bulletin 78, 355-377.

Bense, V., Balen, R., 2003. Hydrogeological aspects of fault zones on various scales in the Roer Valley Rift System. Journal of Geochemical Exploration 78-79, 317-320.

Bense, V., Balen, R. 2004. The effect of fault relay and clay smearing on groundwater flowpatterns in the Lower Rhine Embayment. Basin Research 16, 397–411.

Bense, V. F., Person, M. A., 2006. Faults as conduit-barrier systems to fluid flow in siliciclastic sedimentary aquifers. Water Resources Research. 42, W05421, doi:10.1029/2005WR004480.

Bethke, C. M., 1985. A numerical model of compaction-driven ground-water flow and heat transfer and its application to paleohydrology of intracatonic sedimentary basins. Journal of Geophysical Research 90, 6817-6828.

Bredehoeft, J.D., Belitz, K., Sharp-Hansen, S., 1992. The hydrodinamics of the Big Horn Basin: A Study of the Role of Faults. American Association Petroleum Geologists Bulletin 76, 530-546.

Caine, J.S., Evans, J.P., Forster, C.B., 1996. Fault zones architecture and permeability structure. Geology 24, 1025-1028.

Domenico, P.A., Schwartz, F. W., 1998. Physical and chemical hydrogeology. Wiley, 502 pp.

Duran, H., 1985. El paleozoico de Les Guilleries. PhD thesis, Departament de Geologia, Universitat Autònoma de Barcelona.

Evans, J. P., Forster C.B., Goddard, J.V., 1997. Permeability of fault related rocks, and implications for hydraulic structure of fault zones. Journal of Structural Geology 19, 1393-1404.

Folch, A., Roldán, R., 2003. Estudio hidrogeológico de los acuíferos de la riera de Santa Coloma de Farners. Fundación Centro Internacional de Hidrología Subterránea. Barcelona.

Folch, A., 2005. Modelització de flux en zones de fractura: implicacions en la recàrrega de depressions intramuntanyoses. Master thesis, Department de Geologia, Universitat Autònoma de Barcelona.

Forster, C.B., Smith, L., 1988a. Groundwater Flow Systems in Mountainous Terrain. 1. Numerical Modeling Technique. Water Resources Research 24, 999-1010.

Forster, C.B., Smith, L., 1988b. Groundwater Flow Systems in Mountainous Terrain. 2.Controlling Factors . Water Resources Research 24, 1011-1023.

Forster CB, Goddard JD, Evans, J.P., 1994. Permeability structure of a thrust fault . In The Mechanical Involvement of Fluids in Faulting, eds Hickman, S., Sibson, r. and Bruhn, R., USGS Open FileReport 94-228, 216-223.

Ge, S., Garven, G., 1994. A theoretical model for thrust-induced deep groundwater expulsion with application to the Canadian Rocky Mountains. Journal of Geophysical Research 99, 13851-13868.

Haneberg, W.C., 1995. Steady state groundwater flow across idealized faults. Water Resources Research 31, 1815-1820.

Hubbert, K.M., 1940. The theory of groundwater motion. Journal of Geology 8, 785-944.

Instituto Geológico y Minero de España (IGME), 1993. Estudio para la evaluación de las aguas minero-medicinales, minerales naturales, de manantial, termales y minero-industriales en el territorio de Catalunya. El macizo granítico de les Guilleries-el Montseny (Girona y Barcelona). Primer informe final. Madrid.

McDonald, M.G., Harbaugh, A.W., 1988. A modular three-dimensional finite difference ground-water flow model. U.S. Geological Survey Open-File Report 83-875. Washington.

Marler, J., Shemin, G., 2003. The Permeability of the Elkhorn Fault Zone, South Parck, Colorado. Groundwater 41: 321-332.

Menció, A., 2006. Anàlisi multidisciplinària de l'estat de l'aigua a la depressió de la Selva. PhD dissertation, Universitat Autònoma de Barcelona. http://www.tdx.cesca.es/TDX-0718106-140651/

Ministerio de Obras Públicas y Urbanismo (MOPU), 1971. Estudio de los recursos subterráneos de la zona de la Selva (Gerona). Estudio de los recursos hidráulicos totales del Pirineo Oriental (zona norte). Dirección General de Obras Hidráulicas. Madrid.

Novakowsky, K., Oxtobee, J.P.A., Kriger, P.W., 2000. Potential discharge of Lockport groundwater into Twenty Mile Creek downgradient from the CWML site, Smithvile, Ontario. Final Report to the Smithville Phase IV Bedrock Remediation program.

Nesbit, B. E., Meuhlenbachs, K., 1989. Origins and movement of fluid during deformation and metamorphism in the Canadian cordillera. Science 246, 733-736.

Rumbaugh, J.O., Rumbaugh, D.B., 2003. Groundwater Vistas: Guide to using. Environmental Simulations, Inc. 266 pp.

Scholz, C. H., Anders, M. H., 1994. The Permeability of faults, in Proc. of USGS Conf. on Mechanical Involvement of Fluids in Faulting, S. Hickman, R. Sibson, R.Bruhn, USGS Open File Report 94-228, 247-253.

Sinhal, B.B.S., Gupta, R.P. 1999. Applied Hydrogeology of fractured Rocks. Kluwer Academic Publishers, 400 pp.

Smith, L., Forster, C.B., Evans, J.P., 1990. Interaction of fault zones, fluid flow and heat transfer at the basin scale: in, Neuman, S.P., and Neretnieks, I., eds., Hydrogeology of Low Permeability Environments: Int. Assoc. Hydrol. Sci., Selected Papers in Hydrogeology 2, 41-67. Verlag.

Sophocleous, M., 2002. Interactions between groundwater and surface water: the state of the science. Hydrogeology Journal 10, 52-67.

Stober, I., Bucher, K., 2007. Hydraulic properties of the crystalline basement. Hydrogeology Journal 15, 213-224.

Tiedeman, C.R., Hsieh, P.A., 2001. Assessing an open-well aquifer test in fractured crystalline rock. Groundwater 39, 68-78.

Tóth, J., 1963. A theoretical analysis of groundwater flow in small drainage basins. Journal of Geophysical Research 68, 4795-4812.

Vilanova, E., 2004. Anàlisi dels sistemes de flux a l'àrea Gavarres-Selva-Baix Empordà. Proposta de model hidrodinàmic regional. PhD dissertation, Universitat Autònoma de Barcelona. http://www.tesisenxarxa.net/TDX-1217104-145328/

Vilanova, E., Mas-Pla, J., 2001. Hydrochemical patterns of groundwater flow in the Gavarres hercinian mountains and surrounding areas (NE Spain). R. Cidu, ed.: Water-Rock Interaction – WRI-10, Balkena, pp. 601-604.

Winter, T.C., Harvey, J.W., Franke, O.L., Alley, W.M. , 1998. Ground water and surface water: A single resource. U.S.G.S. Circular 1139.

Chapter III

Groundwater exploitation effects on regional flow systems in a range-and-basin hydrogeological setting: the Selva basin (NE Spain)

3.1. Introduction

In many areas groundwater has become a primary resource for supplying human demand. In some cases, a continuous growth in demand has produced a modification in the natural flow system that varies the water cycle and, more specifically, overall recharge in terms of a water balance that defines the amount of available resources (Devlin and Sophocleous, 2005). From a holistic perspective, a conceptual approach that encompasses such human pressures must recognize the hydrogeological heterogeneity provided by the complexity of the geological scenario and the potential contributions of distinct recharge areas once groundwater withdrawal has begun (Mahlknecht et al., 2006; Palmer et al., 2007; Li et al., 2008).

Water balances are undoubtedly a delicate matter in hydrogeological research. In particular, the occurrence of groundwater flows from neighboring basins, in the form of subsurface recharge or discharge, is usually indirectly inferred or deduced though numerical simulations. Field determinations based on potentiometric, hydrochemical or isotopic data are then necessary before it is possible to think about groundwater flows between geological formations (e.g., Cunningham et al., 1998; Chen et al., 2004; Sukhija et al., 2006; Demlie et al., 2007; Aji et al, 2008; among others). These attempts, however, encounter additional difficulties where tectonic structures add complexity to the regional geological setting, and when intensive groundwater exploitation, characterized by seasonal withdrawal regimes, different exploitation depths, sparse well distribution, and so on, modifies the naturally steady flow systems under predevelopment conditions.

All these aspects coexist in the Selva basin (NE Spain), where the recent intensive development of agricultural and industrial activity and a growing urban sprawl have called into question the future availability of water resources and their sustainable management (Menció, 2006). The Selva basin is a range-and-basin area with an approximate extension of 600 km2, where groundwater exploitation meets most of the human demand (Figure 3.1).

Tectonic structures exert an important role in this hydrogeological system, as indicated by the naturally occurring thermal and/or CO_2-rich springs exploited since the Roman period. Previous research in the study area has shown that tectonic elements are responsible for a significant recharge towards the sedimentary infilling of the basin, and flow systems of different spatial magnitude have been described (Vilanova, 2004; Menció, 2006; Folch and Mas-Pla, 2008).

Nevertheless, these studies do not address the effect of groundwater withdrawal on the forced recharge towards the aquifer, and therefore the role of distinct recharge areas on the water balance of the basin. Furthermore, groundwater exploitation takes place during the irrigation season when recharge is almost nil. In this scenario, the distortion of flow systems caused by water withdrawal is relevant as it may limit inflow magnitudes leaked from other geological formations. Such alterations, described within the appropriate hydrogeological framework, are therefore of major interest in defining the availability of groundwater resources in the face of potential future demand.

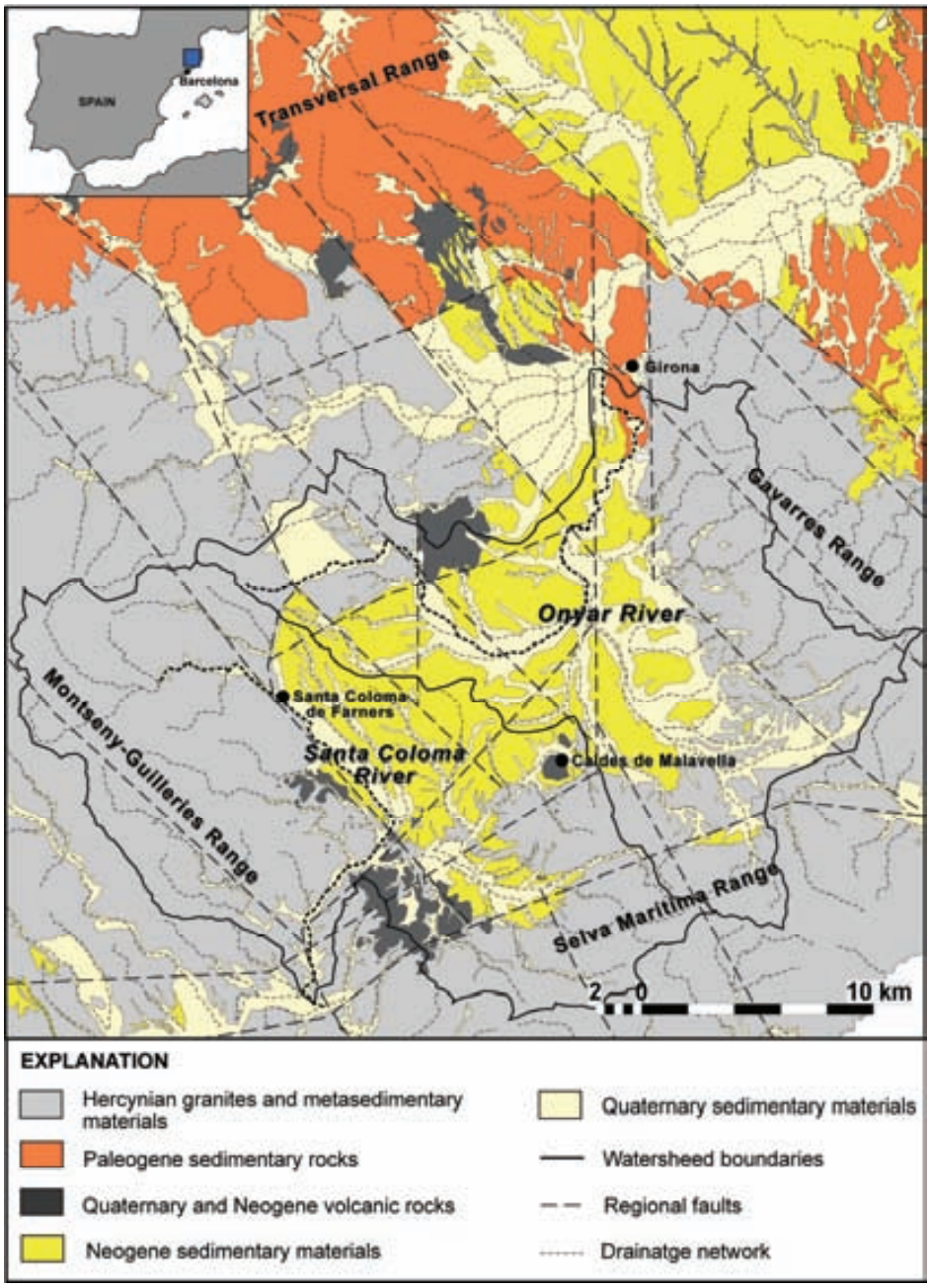

Figure 3.1. Geographical situation and geological setting of the Selva Basin.

The objective of this paper is to characterize the alteration to a hydrogeological system located in a range-and-basin area by intensive groundwater withdrawal, where tectonic elements such as fault zones are expected to contribute to the overall recharge of the aquifers. Within this context, we seek to construct a conceptual hydrodynamic framework, supported by potentiometric, hydrochemical and isotopic data, that enables us to provide a suitable description of relationships between aquifers and their seasonal variations due to groundwater withdrawal. Our contention is that understanding the alteration to natural flow systems will reveal their response to human pressures and, therefore, provide criteria for groundwater management of these water resources.

3.2. Study area and geological setting

The Selva basin is a tectonic area surrounded by the Montseny-Guilleries (1202 m asl), Gavarres (535 m asl), Selva Marítima (519 m asl) and Transversal (998 m asl) mountain ranges in the province of Girona (NE Spain) (Figure 3.1). There are two main watersheds in the study area, those of the Santa Coloma River and Onyar River basins. The Santa Coloma River Basin (SCRB) extends along the entire length of the south-western side of the Selva basin, with part of its headwaters in the Montseny-Guilleries mountains. The Onyar River basin (ORB) occupies the north-eastern side of the basin, and its headwaters are in the Gavarres and Selva Marítima ranges. An annual human demand of 27.1 hm^3 is supplied mainly by groundwater, with 16.0 hm^3 devoted to agricultural uses, primarily during the summer. Annual rainfall is approximately 700 mm, while potential evapotranspiration (as determined by the Thornwaite equation) exceeds precipitation, especially in summer.

Geomorphologically, the Selva basin constitutes a type of range-and-basin structural area. It was created during the distensive period following the Alpine orogeny during the Neogene. The main fault direction in the area is NW–SE, with other significant faults, oriented NE–SW and N–S, being responsible for the tectonic and morphological evolution of the area. The surrounding ranges consist of Paleozoic igneous and metamorphic rocks in the Montseny-Guilleries, Selva Marítima and Gavarres, and pre-Alpine Paleogene sedimentary rocks (mainly limestone and sandstone) in the Transversal range. The basin sedimentary infill consists of a layer of unconsolidated gravel, coarse and medium sand and layers of silt, deposited by alluvial fan systems during the basin formation. They can reach a total thickness of more than 200 m in the western area, varying according to the tectonic blocks that form the basin basement.

Groundwater occurs in unconfined conditions in shallow sedimentary formations, such as alluvial and weathered zones, and in confined and leaky conditions at deeper levels. Hydrogeologically, three main units can be determined: 1) the upper aquifer formed by alluvial materials associated with the main rivers, surface Neogene sedimentary layers, and weathered igneous rocks; 2) an alternation of silts, arkosic sands, gravels and conglomerates with low clay content of Neogene sediments, resulting in an intermediate multilayer aquifer with thicknesses from 20 to 300 m (MOPU, 1985; Pous et al., 1990); and 3) a deep aquifer, formed by the granite basement affected by local and regional faults and by a weathering cap in the upper zones. Wells located in the foothills of the ranges exploit weathered granite layers under unconfined conditions or, if drilled in unaltered rock, benefit from the occurrence of fractures. In particular, the Santa Coloma fault zone, located at the western boundary of the basin, has a strong regional geological, as well as hydrogeological, significance.

3.3. Methodology

Field surveys in the Selva basin were conducted from 2000 to 2006. Groundwater hydraulic head was measured in successive years: 2000 (December), 2002 (September), 2003 (February, July and December), 2004 (May and October), 2005 (May and October), 2006 (May). The number of head data measured was between 156 and 366, depending on the season and year. Hydraulic heads were measured under non-pumping conditions.

Hydrochemical data from 60 water samples were collected during May 2006. Sampling points were in the Selva basin sedimentary infill and in the surrounding ranges (Figure 3.2). Fifty-five wells between 7 and 150 m deep were sampled.. In addition, three springs in different geological settings coinciding with fault zones were analyzed, and two surface water samples from the Santa Coloma River complemented the dataset. Hydrochemical data from previous surveys are provided by Menció (2006). The isotopic data used in this study were collected during three different seasons in 2003 (May, September, and December), and in May 2006 (Figure 3.2). Environmental isotopes, oxygen-18 ($\delta^{18}O$), deuterium (δD), were analyzed. Sample numbers increased from 20 in 2003, to 60 in 2006, to enable a better characterization of the hydrogeological system.

Samples for hydrochemical and isotopic analysis were taken under pumping conditions. We ensured that at least three casing volumes of groundwater were removed from each bore

prior to sampling. The samples collected were analyzed for pH, electrical conductivity (EC), and temperature under field conditions, which were monitored until stabilization. After filtration (0.45 μm), the samples were processed in the field and stored under recommended conditions until analysis for major ions, including fluoride, and isotopes.

Groundwater hydraulic head, hydrochemical and isotopical data were all collected from private wells. These wells search for maximum productivity and are generally screened at multiple depths. Therefore, water samples are not always taken from the desired aquifer level, but from the most productive level, or they may represent a mixture of water from different layers.

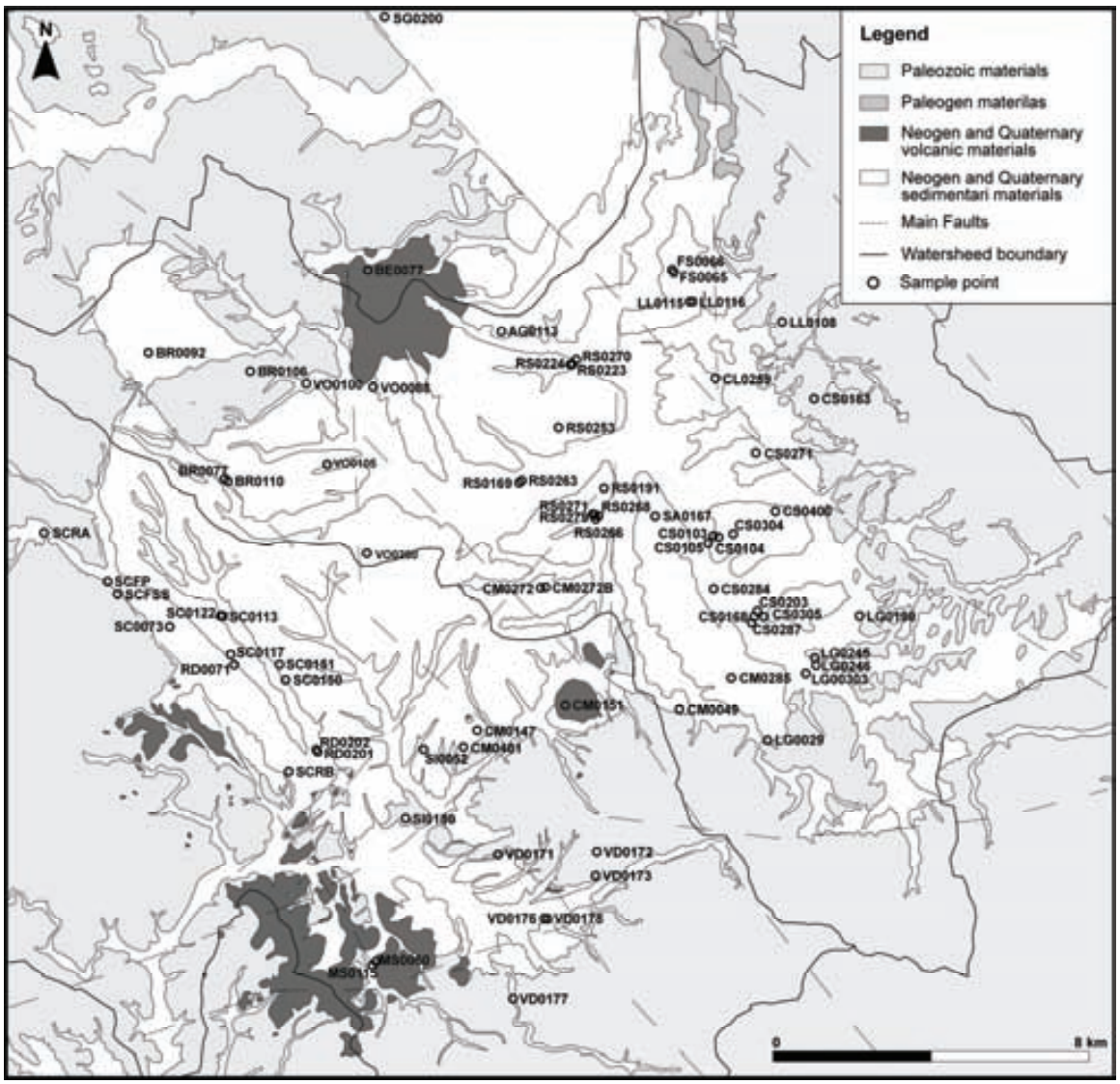

Figure 3.2. Sample points used for hydraulic head evolution and/or hydrochemical and isotopic data collection. Other wells used for head measurements are not shown for the sake of simplicity.

Because of the complexity of the available sampling points, we focused our efforts on grouping samples by their geological and hydrochemical features in an attempt to identify distinct hydrogeological systems, and to provide a complete description of the range-and-basin hydrodynamics.

3.4. Results

3.4.1. Piezometric data

Potentiometric lines were drawn separately for the upper unconfined aquifer, which includes alluvial formations and the uppermost Neogene sedimentary units, and the confined and leaky aquifers underneath (Figure 3.3). These set the boundary for both aquifer systems at a depth of 30 m, in accordance with field observations. In both maps, flow lines define two main hydrogeological units, in agreement with the hydrographic boundaries of the SCRB and ORB. According to them, the main recharge areas are located in the Montseny-Guilleries and Selva Maríitima ranges for the SCRB, and the Gavarres and Selva Marítima ranges for the ORB. Rainfall infiltration from the basin sedimentary infill surface is also significant in the upper formations.

Groundwater flow systems are south-oriented in the SCRB, and north-oriented in the ORB. Between them, a groundwater divide oriented WNW-ESE appears in the central part of the Selva basin, within the Neogene sedimentary formation, which coincides with the surface limits of both watersheds. This setting reflects a geological control of the head distribution that results in separated flow systems draining in opposite directions, controlled by the drainage pattern of the basin on the surface and by structural elements at depth. It is worth noting that altitude at the northern and southern exits of the two drainage networks is similar (approximately 65 m asl). Such a potentiometric configuration was also observed in earlier groundwater research (MOPU, 1971b), conducted under much less developed conditions.

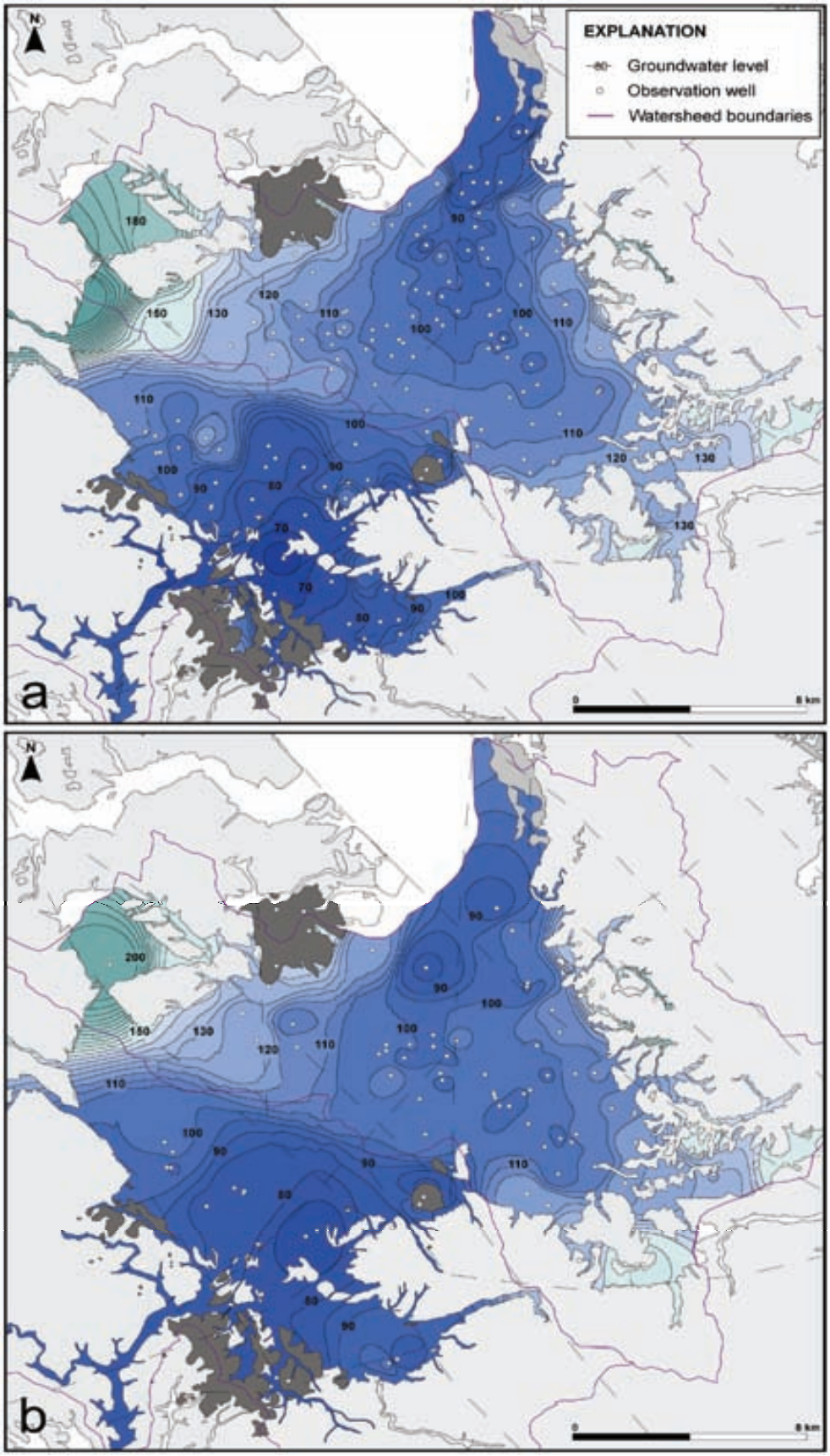

Figure 3.3. Potentiometric contour map May 2004. a) Upper unconfined aquifers (wells under 30 m deep). b) Deep confined or semi-confined aquifer (wells over 30 m deep).

Major head decline in both surface and deep aquifer levels occurs during the driest months (July and August), because of low recharge and maximum groundwater extractions (Figure 3.4, Table 3.1 and Figure 3.5;). As a result, a reduction in the water stored in the aquifer takes place. Nevertheless, head variations over time reveal specific hydrological behavior as a response to intense groundwater withdrawal. To discern the behavior of the flow system under such a development scenario, groundwater head evolution was considered in representative wells between 2000 and 2006.

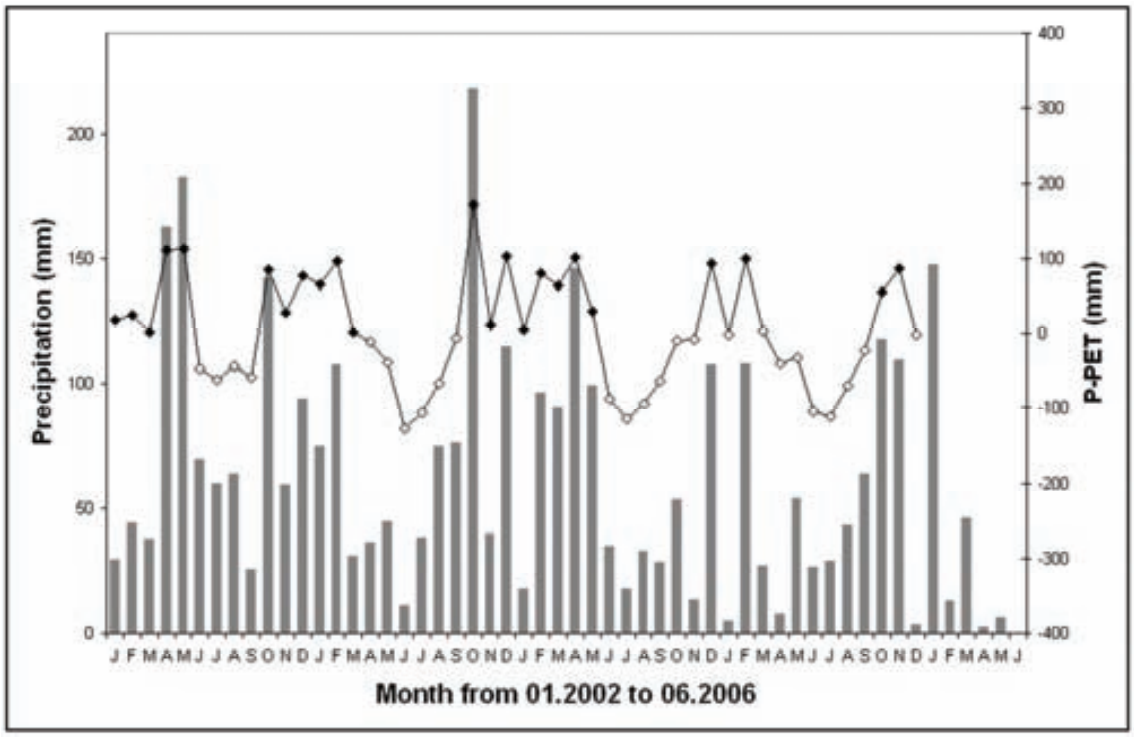

Figure 3.4. Precipitation and effective rainfall (i.e., rainfall minus potential evapotranspiration; P-PET) at the Fornells weather station. Data from Servei Meteorològic de Catalunya (http://www.meteocat.com).

Because of intensive pumping, deep wells (that is, those with a depth greater than 30 m) show larger head drops than shallow wells in the upper unconfined formations. This large drawdown occurs despite all the Neogene sedimentary infilling, tens of meters thick, and the high hydraulic conductivity of the sandy layers which, a priori, should allow significant flow rates. Such head declines suggest, therefore, a limited storage capacity of the sedimentary formations and hence a large induced recharge from the surrounding ranges where, given the structural setting, fluxes take place through fracture networks and fault zones. In addition, they recover fairly well after a rainy winter season (Figures 3.5 a, d, g, j). Regional recharge flows have so far been high enough for hydraulic heads to recover when water withdrawal stops after the irrigation season. Such behavior illustrates the significant influence of pumping

on the natural flow fields, forcing discharge from the range areas towards the intensively exploited sedimentary aquifers within the basin.

Table 3.1. Geology and hydraulic head (m.s.l) of every well for each field campaign.

Code	Geology	Depth (m)	Dec-00	Sep-02	Feb-03	Jul-03	Dec-03	May-04	Oct-04	Feb-05	May-05	Oct-05	May-06
FS0065	Neogene+Granite	26	83.4	84.1	83.9	84.6	84.1	87.1	84.8	84.6	84.6	84.1	
FS0066	Neogene	102	85.2		89.4		88.8	88.4	84.1	89.9	89.5	89.2	88.2
CS0168	Quaternary	5		103.3		103.8		106.8	103.5	106.0	104.4	106.2	105.3
CS0203	Neogene+Granite	150			97.4			97.1		88.0			75.8
CS0305	Neogene+Granite	130					101.3		95.8	103.1	103.3	102.3	104.4
CS0284	Neogene	70			102.0		101.2	103.0	100.3	102.7		101.4	
CS0287	Neogene	60				102.8		105.0	102.5	102.7	103.5		
CS0103	Neogene	39		95.2	96.4	95.2	95.7	97.6	95.7	101.4	100.9	100.1	101.2
CS0104	Neogene	8	97.8	98.2		98.6	98.6	99.5	98.7	99.1	98.8	98.4	
CS0105a	Neogene	80	96.9		99.2		97.4	99.6					
CS0105b	Neogene+granite	140							95.8	97.8		96.9	92.3
LG0245	Quaternary	9				107.7	108.5		108.6	108.6	107.5	109.4	
LG0246	Granit	>100							93.0				
LG0303	Granit	110				83.9	100.1	106.0	93.3	101.4	101.2	96.6	
LL0115	Neogene	80			99.4	99.6	99.8	100.4	100.0	100.5	100.5	100.3	
LL0116	Neogene	12				111.0	110.7	111.4	111.3	110.9	110.8	110.6	109.6
RS0223	Quaternary	10	89.1	89.1	88.7			88.9	87.2	89.2	87.8	88.7	85.8
RS0224	Quaternary	12	88.9	89.2						89.4	88.0	88.8	85.8
RS0270	Neogene	100			84.8	81.1		84.7	82.5	83.8	82.0	81.8	
RS0191	Neogene	105	95.6	94.7	98.0	91.9	97.7	99.3	95.7				
RS0266	Neogene	120			99.6		99.4	101.0	97.9	99.6	97.8	98.6	
RS0268	Neogene	65			98.9		97.6		96.4	97.9	97.5		
RS0271	Quaternary+Neogene	65			98.1			99.6	96.8	98.2	97.0	97.4	96.8
RS0279	Neogene	18				93.6			99.3	100.9	100.5	99.7	
RS0169	Quaternary+Neogene	10	96.2	97.6			99.5	100.9	95.9	98.6	98.1	97.7	
RS0263	Quaternary+Neogene	50	96.5	97.6	99.6		99.9	101.1	96.2	99.0	98.2	98.0	89.7
VD0178	Neogene	13							82.5	85.6	84.5	86.2	84.5
VD0176	Neogene	69					86.1		83.8	85.4	85.5	83.5	
SC0113	Neogene	73				83.4	102.1	102.9	93.0	103.0	99.5	100.7	97.2
SC0122	Quaternary	6							100.7	102.0	101.5	100.7	101.9
SC0117	Neogene	65				91.2	94.1	94.2	92.5	94.0	93.0	93.1	93.4
RD0071	Neogene	16		92.3	93.5	93.9	94.0	95.3	93.5	93.9	94.0	93.2	94.2

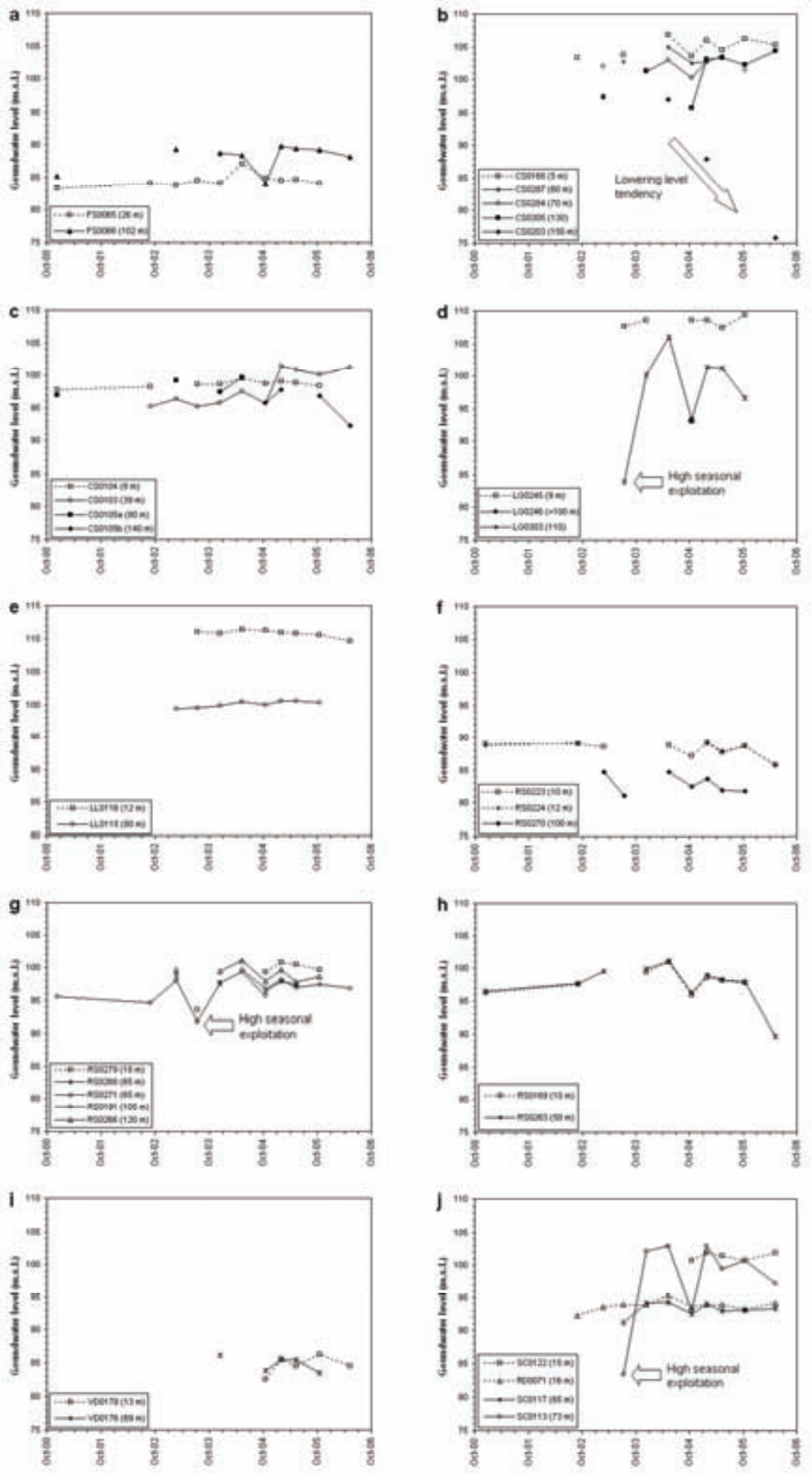

Figure 3.5. Groundwater head evolution at several wells in the Selva basin. Each plot represents two or more wells located close to each other. See Figure 2.

Different vertical relationships between surface and deep aquifer levels can be established depending on the location and the geological setting. For instance, close drawdowns are observed in both shallow and deep wells in specific areas, suggesting an effective connection between sedimentary layers that end up behaving as a single hydrogeological unit (Figure 3.5h). In other locations, distinct behaviors are identified at depth, depending on the degree of vertical connectivity between Neogene sand layers. For instance, limited connectivity results in distinct hydraulic heads but similar evolution through time (Figures 3.5b,g), while in some places deep layers act as confined aquifers with head levels above (Figure 3.5a) or below (Figure 3.5e, f) those of the unconfined aquifers. The latter case is usually found where the upper aquifers are located in topographically elevated areas. In such cases, head differences reflect a practically nil vertical downward leakage between the aquifers.

Head distribution points to there being a lateral hydraulic connection between the range-front areas and the basin aquifers, which indicates an effective recharge through fault zones and fracture networks within the basement (Figure 3.3). Similar behavior can also be said to occur at the contact between the sedimentary infill of the basin and the basement, although the magnitude of the recharge will depend on distinct geological features such as the hydraulic conductivity of the lowest Neogene sediments, the thickness of the weathered granite on the top of the basement, the fracture networks, and the vertical head gradient generated by pumping rates. This means that deep wells located in the vicinity of regional fault zones (e.g., CS0203 in Figure 3.5b, and LG0303 in Figure 3.5d) are the most productive, and will even have a distinct hydrochemical facies. In particular, well CS0203 showed a lowering tendency during the later surveys that was related to fault zones with high storage capacity, but limited recharge.

Wells CS0103, CS0104 and CS0105 (Figure 3.5c) also reflect the spatial heterogeneity that controls the relationship between the basement and the overlying sedimentary layers. For instance, well CS0105 exploited the sedimentary layers at a depth of 80 m until October 2004 and is named CS0105a in the plot. The borehole was then drilled down to 140 m, the last 60 m being within the granitic basement, and renamed as CS0105b in the plot. Well productivity increased from 80 m^3/h to more than 200 m^3/h, pointing to the significant productivity of the basement fracture and fault networks in comparison with the Neogene sedimentary layers. As a result of this new scenario, well CS0103, which is located in sedimentary layers at 39 m from the surface, raised its hydraulic head by approximately 10 m, making it even higher than those of CS0105 and CS0104, the latter being in the upper unconfined aquifers. As CS0103 kept its

pumping rates, such an observed head increase suggests there are interesting features of the recharge of the sedimentary formations from the basement and the range-front boundaries. In particular, it shows that the basement rocks may endure intensive pumping rates with an almost nil hydraulic influence on the overlaying sedimentary layers. Moreover, the recovery of the potentiometric levels in the sedimentary aquifers (observed after drawdown caused by CS0105a stopped in October 2004 whilst CS103 kept on pumping) suggest an efficient recharge of the Neogene sedimentary layers. Since water-table levels in CS0104 remained fairly steady, unaffected by pumping in the deeper aquifers, we conclude that regional flow systems originating in the surrounding ranges, and flowing through tectonic elements that define the geological setting of the system, have a major influence on the recharge of the basin sedimentary infill.

The last type of interaction is the seasonal change in the relative groundwater level between surface and deep aquifers (Figure 3.5 a, i, j). Throughout the wet season, deep aquifers show higher water levels than the shallow ones. Upward vertical flows towards the upper formations depend on leakage magnitude across the overlying aquitards. Conversely, at the end of the dry season, deep aquifer levels decrease because of intensive groundwater withdrawal and show a water level below the upper unconfined aquifers.

To summarize, then, the two hydrogeological units show differences in the origin of their recharge. The upper unconfined aquifer unit gets superficial recharge through direct rainfall and river infiltration, while deeper aquifer levels are recharged by lateral flow systems and, more importantly, by upward vertical flows from the basement. In addition, lateral flow from the surrounding range areas is also significant. At the same time, hydraulic head data indicate a vertical connection between sedimentary aquifer levels at various depths, which allow distinct vertical connections between the Neogene sedimentary aquifer layers.

Discharge from the system is also different in both units. The upper aquifer mainly drains off through the river network as base flow from the alluvial formations (Figure 3.1 and Figure 3.3) and as a result of pumping. Deep aquifer discharge is also related to water withdrawal, though potentiometric data from the deepest wells suggest an efficient outflow from the basin through regional faults at its south-eastern margin. Evidence of such deep flows is encountered in CO_2-rich springs located at the tectonic boundary between the Selva Marítima and Gavarres ranges (Vilanova, 2004; Vilanova et al., 2008).

The behavior of and the interactions between distinct hydrogeological units are thus seen to be diverse and dependent on location, geological setting, seasonal variation, and pumping rate. The differences observed between aquifer head levels and productivity indicate the occurrence of recharge fluxes from the range front and the basement. Groundwater capture by pumping modifies natural flow paths and the recharge/discharge relationships between large-scale hydrogeological units. Such a degree of interaction affects groundwater quantity as well as its quality, and ultimately the vulnerability of the Selva basin water resources.

3.4.2. Hydrochemistry

Each geological environment in the Selva basin has a different hydrochemical facies based on its rock lithology and hydrogeological flow path. For instance, Stiff diagrams (Figure 3.6) corresponding to the May 2006 survey identify low salinity groundwater samples on the western side of the SCRB with a mean electrical conductivity of 618±99 μS/cm, whereas those samples from the ORB and eastern SCRB commonly show a higher salinity, with an electrical conductivity mean value of 879±29 μS/cm. Such a general difference can be attributed to the fingerprint of distinct recharge areas, as already suggested by hydraulic head data and potentiometric maps (Figure 3.3).

Specifically, groundwater samples from aquifers in Neogene sediments, regardless of their depth, have a Ca-HCO_3 facies (VO0280, SC0117, RS0191, RS0263, CM0272), some of them with a significant chloride content of up to 30-40%, as indicated in the Piper diagram (Figure 3.7). Samples from wells in weathered or fractured igneous rocks also have a Ca-HCO_3 facies (e.g., CS0304, SC0117, and SC0113), although in some cases, especially in those wells totally or partially drilled in granite, the chloride content increases up to 60%, which defines a Ca-HCO_3-Cl facies (VD0173; VD0172, CS0183).

Sodium content is about 20-40% of the cation proportion in many samples (Figure 3.7). Sodium-rich hydrochemical facies, such as Na-HCO_3 and Ca-Na-HCO_3, are thus encountered in deep wells in Neogene materials (RS0270, VD0176) and in granites (VD0177, LG0246, BR0092), provided they are in the vicinity of main fault zones. Some of these samples, for instance, have high chloride concentrations without being Na-Cl rich, (FS0066, LG0190, VD0172). Some springs located at the basin border also have sodium-rich hydrochemical facies (SCFP, SG0200).

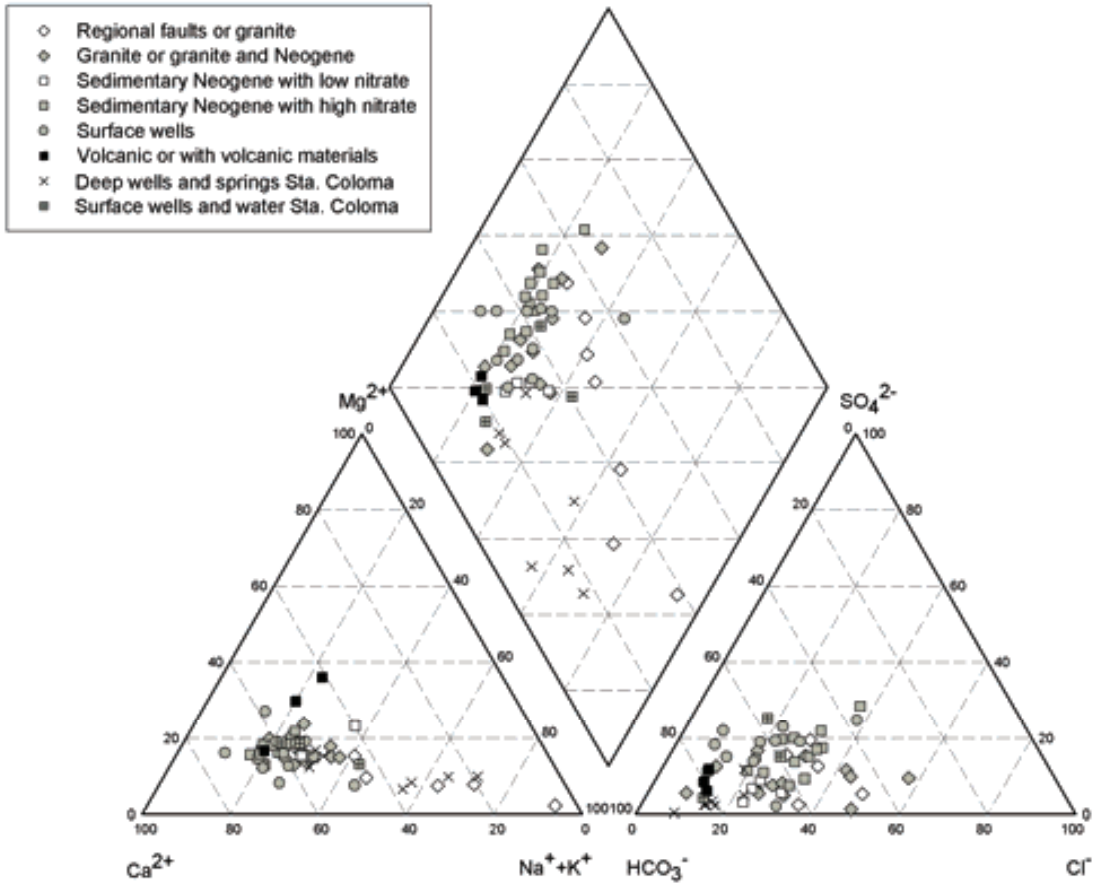

Figure 3.6. Piper diagram of May 2006 survey showing hydrochemical groups. See text for explanation.

Hydrochemical facies allow distinct groundwater sources to be differentiated in the main aquifers of the Selva basin. Based on their chemical composition, Na-HCO_3 and chloride-rich facies can be attributed to regional flow systems with long residence times at the subsurface (Gascoyne, et al., 1987; Tóth, 1995, 2000; Beucaire, 1999; and Carrillo et al., 2007). Those samples also have a high fluoride content of up to 15 mg/L, and low nitrate concentrations. Conversely, local flow systems have Ca-HCO_3 facies with high nitrate, sulphate and chloride concentrations related to pollution sources. This type of facies indistinctively shows a low fluoride content (< 2.0 mg/L). Among them, Ca-HCO_3 facies with significant sodium content may be attributed to intermediate flow systems, with sulphate and nitrate concentrations lower than samples from local flow regimes. Some enrichment in chloride may be related to evaporation processes in the unsaturated zone, as revealed by isotopic data shown later in the paper.

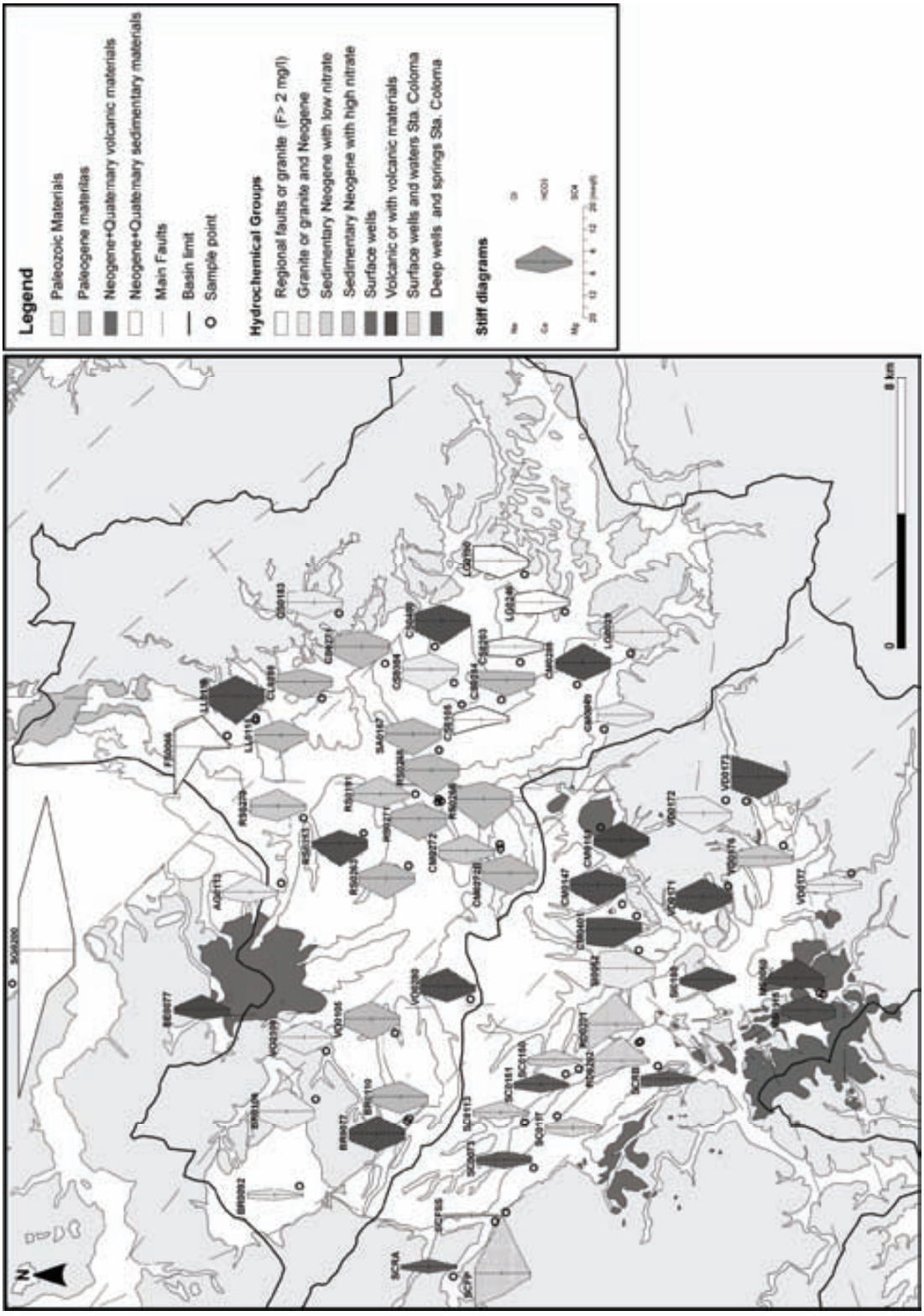

Figure 3.7. Stiff diagram distribution in the May 2006 field campaign. Refer to text for hydrochemical groups description.

Fluoride and nitrate act as valuable tracers that define the origin of groundwater recharge within the basin. High nitrate samples seldom coincide with high fluoride content, and thus define distinct end-members in the recharge of the Selva basin: inflow from rainfall infiltration within the basin will present nitrate pollution, while vertical upward inflow from the granitic basement, or lateral inflow from the range-front as in the Santa Coloma fault zone, will present a significant fluoride concentration (Table 3.2). It is worth noting that the occurrence of fluoride is limited to wells located along the main fault areas, suggesting an efficient flow path through tectonic structures.

Previous studies indicated the occurrence of mixing processes between distinct flow systems (Vilanova 2004, Menció 2006, Folch and Mas-Pla, 2008). In this dataset, some wells present high fluoride concentrations as well as a moderated nitrate content (CM0151, SC0117, and CS0304; Table 3.2). Such hydrochemical composition could also be attributable to mixing caused by the cones of depression inside the aquifer, or simply to the existence of several screened intervals in the borehole. All the same, these samples illustrate the impact of withdrawal on the quality of pumped groundwater.

In summary, hydrochemical facies permit a classification of groundwater samples in different groups according to their geological origin in the ORB and eastern SCRB (Table 3.3):

1. Samples related to *regional fault zones and granitic aquifers* with fluoride concentrations higher than 2 mg/L, except in the case of SG0200 which, being located on the northern edge of the study area, can be understood to have a hydrochemistry mainly affected by the sedimentary formations of the Transversal range, which do not contain fluoride-rich minerals.
2. Samples from wells in *granitic rocks that may also exploit Neogene sedimentary formations*, usually have a Ca-HCO3 facies, some of them with high chloride content.
3. Samples from *Neogene sedimentary layers with low nitrate content*, below 37.5 mg/L NO_3, indicate sources from regional or intermediate flow systems, and a minimum contribution from local recharge. Nitrate threshold values of 37.5 mg/L NO_3, and 50.0 mg/L in Group 4, are set based on actual field data values, although they coincide, respectively, with the standard point for pollution trend reversal actions and the quality standard for nitrate defined in the European Groundwater Directive (Directive 2006/118/EC).

4. Samples from *Neogene sedimentary layers with high nitrate content*, usually above 50.0 mg/L NO_3, show the influence of groundwater withdrawal at moderate depth from or below shallow aquifer units. Pumping in the Neogene layers forces a downward flow that conveys nitrate from the surface soil. Such hydrochemical features are common in areas where the Neogene sedimentary unit is homogeneous in its depth, that is with insignificant aquitard formations as depicted by well cores and also reflected by potentiometric data.
5. Samples from *surface wells*, whether in alluvial, in the uppermost Neogene layers, or in weathered granite outcrops, have a characteristic Ca-HCO_3 facies, and are likely to present high nitrate concentrations in the eastern SCRB and in the ORB.
6. Samples located totally or partially in *volcanic rock* may reach a depth of 80 m, and be related to local aquifers and/or deeper system flows.

Finally, two types of wells can be distinguished in the western SCRB with features different to those already described, such as lower salinity content. Accordingly, we differentiate between:

1. Samples from s*urface wells and stream water in the SCRB,* with a lower nitrate content than those of the ORB, as a result of various human pressures and agricultural land-use distribution, and
2. Samples from *deep wells and springs in the Santa Coloma River basin,* also with a significant fluoride content and low nitrate concentration.

One of the main outcomes of the dataset is that surface wells are seen to have a wide range of hydrochemical facies. This can be attributed to the effect of aquifer lithology and pollution impacts, mainly from the intensive use of manure as fertilizer. Specifically, groundwater samples from the Santa Coloma River unconfined aquifer have a similar hydrochemistry to that of stream waters, indicating effective hydrological connectivity between river and aquifer. Stream recharge to the aquifer also explains the low nitrate content observed in the aquifer (in all samples but one, less than 20 mg/L). Samples from the unconfined aquifer have a Ca-HCO_3 facies, although deep wells and springs associated with fault zone hydraulics are characteristically of the Na-HCO_3 type.

Nitrate is also found in some deep wells in the ORB, which indicates the occurrence of a continuous hydrogeological unit consisting of the surface layers and the underlying Neogene sedimentary formations.

Wells placed in granitic rocks may present distinct mineralization levels according to residence time and the extent of granite weathering processes. Nitrate may occasionally occur, although in these cases it is attributable to a downward flux from the surface caused by pumping in the igneous unit.

Fluoride, as a specific component of this hydrogeological system, is found in specific locations within the Selva basin, in particular in the vicinity of the main fault zones (e.g., FS0066, CS0105, LG0190, and others in the ORB; and SCFP and RD0201 in the SCRB; Table 3.2). As fluoride origin is related to fluoride-bearing minerals recognized in veins in the Montseny-Guilleries range (Piqué et al., 2008), its occurrence must be related to upward vertical flows occurring from the basin basement whose recharge areas are located at the summit of the surrounding ranges and have acquired the required hydraulic gradient. However, not all the samples from springs or wells associated with fault zones present noteworthy fluoride concentrations. Some of the samples at the SCR watershed are low in fluoride, and therefore its origin must be linked to a distinct flow path with a different mineralogical composition. Based on the location of fluoride-rich groundwater samples, it can be assumed that fluoride mineralization is probably associated with particular fracture networks, especially those of the most regional significance, developed during specific stages of the basement's geological history. This may explain why only samples from the basement have a high fluoride content despite all of them being related to flow into fractures.

Flow systems of different magnitude and scale (regional, intermediate, and local) are thus identified in the Selva basin according to their hydrochemical facies and the geological location where they occur. The SCRB presents a major recharge associated with the Montseny-Guilleries range, governed by the Santa Coloma fault zone that controls the flow towards the Neogene sedimentary materials that fill the basin as well as to the upper surface (alluvial) aquifers (Folch and Mas-Pla, 2008).

In the ORB, two recharge poles are identified. One of them represents infiltration from rainfall recharge within the lower basin area. This pole is defined by high nitrate content. The second pole is related to fault zones within the basement, which contribute through a recharging flow

path originating far away, on a regional scale, in the Transversal range, and also possibly in the Montseny-Guilleries range. Faults located in the E and SE of the basin limits, on the boundaries with the Gavarres and Selva Marítima ranges, also represent flow zones that provide a lateral, intermediate-scale flow contribution to the basin's Neogene sedimentary aquifers. These regional and intermediate flow systems are frequently characterized by significant fluoride content.

Table 3.2. Hydrochemical data of the May 2006 field campaign.

Sample	Group	Geology	Depth (m)	Data	Cond.µS	T ºC	pH	Alkalinity as mg/l HCO3	Cl mg/l	SO4 mg/l	NO3 mg/l	F mg/l	Ca mg/l	Mg mg/l	Na mg/l	K mg/l
CS0105b	Regional faults or granite	Neogene+granite	80	06/05/2006	767	16.8	7.31	274.3	73.0	58.1	30.0	6.2	50.8	8.0	125.0	3.6
CS0203	Regional faults or granite	Neogene +granite	150	09/05/2006	751	17.2	7.04	205.0	70.7	62.8	34.8	2.0	76.0	16.0	76.2	7.6
FS0066	Regional faults or granite	Neogene+granite	102	06/05/2006	1533	19.7	7.78	653.9	221.1	21.0	< 0,5	15.4	18.7	5.3	397.8	1.8
LG0190	Regional faults or granite	Granite	120	05/05/2006	963	17.4	7.25	314.8	196.1	29.6	0.5	2.3	133.7	24.8	71.8	1.4
LG0246	Regional faults or granite	Granite	>100	05/05/2006	786	17.7	7.27	263.5	103.0	50.3	13.4	3.0	81.5	10.7	94.7	4.3
SG0200	Regional faults or granite	Spring not determined	0	05/05/2006	4790	17.2	6.49	3220.8	651.9	238.4	< 0,5	0.0	319.5	74.1	1249.8	30.1
AG0113	Granite or granite and Neo.	Neogene+granite	70	16/05/2006	556	18.2	7.21	329.4	19.7	17.1	4.5	0.7	77.7	11.6	47.8	1.5
BR0092	Granite or granite and Neo.	Quaternari+granite	80	16/05/2006	361	17	6.28	122.0	29.8	11.3	24.4	0.2	36.1	8.1	29.0	< 1
BR0106	Granite or granite and Neo.	Granite	83	23/05/2006	974	16.8	7.01	478.2	136.2	30.0	9.0	0.5	143.7	32.3	68.3	2.1
CM0049	Granite or granite and Neo.	Granite	121	19/05/2006	681	17.2	7.19	270.8	73.9	28.1	26.9	0.5	89.9	15.8	50.8	1.2
CS0183	Granite or granite and Neo.	Granite	60	06/05/2006	825	-	6.9	251.3	133.1	49.8	30.7	1.3	117.6	17.6	55.2	1.2
CS0304	Granite or granite and Neo.	Neogene+granite	116	06/05/2006	1046	17.7	6.96	344.0	115.6	77.7	119.8	2.8	156.8	20.9	84.6	1.1
LG0029	Granite or granite and Neo.	Wheathered granit+granite	110	09/05/2006	970	17.3	7.43	541.7	114.9	33.7	< 0,5	0.5	135.8	38.3	74.0	2.4
SI0052	Granite or granite and Neo.	Wheathered granite	50	10/05/2006	1217	16.3	6.87	385.5	213.6	64.7	79.0	0.5	159.3	29.4	129.5	1.4
VD0172	Granite or granite and Neo.	Wheathered granit+granite	50	23/05/2006	921	19.3	7.22	329.4	184.1	7.5	0.5	0.4	153.0	25.7	50.6	< 1
VD0173	Granite or granite and Neo.	Wheathered granite	20	23/05/2006	1136	-	7.24	275.7	277.7	62.1	7.1	0.2	162.4	27.6	101.0	1.4
VD0177	Granite or granite and Neo.	Granite	80	10/05/2006	612	16.5	7.04	214.7	37.9	44.2	66.7	0.2	66.9	12.8	60.2	< 1
VO0100	Granite or granite and Neo.	Quaternary+granite	80	16/05/2006	783	16.9	7.06	317.2	29.6	42.0	155.9	0.3	126.8	25.0	44.4	1.5
CM0272	S. Neogene with low nitrate	Neogene	90	23/05/2006	682	18	6.76	322.1	62.2	24.3	32.6	0.3	94.0	15.6	54.9	< 1
RS0191	S. Neogene with low nitrate	Neogene	90	11/05/2006	765	18.6	6.87	370.9	67.0	13.1	20.5	0.3	99.8	20.2	55.3	1.9
RS0270	S. Neogene with low nitrate	Neogene	100	23/05/2006	803	16.9	6.93	361.1	75.3	37.8	37.3	0.9	109.7	18.4	73.3	1.2
VD0176	S. Neogene with low nitrate	Neogene+volcanic	69	10/05/2006	710	17.9	7.37	256.2	71.0	17.9	< 0,5	0.7	67.7	23.9	70.4	1.8
BR0110	S. Neogene with high nitrate	Quaternary+Neogene	70	11/05/2006	894	17.0	6.93	319.6	94.8	30.9	86.7	0.6	118.0	28.7	58.6	1.4
CL0259	S. Neogene with high nitrate	Neogene	75	06/05/2006	891	17.2	6.92	244.0	85.7	54.8	104.4	0.4	130.0	24.4	57.5	< 1
CM0272B	S. Neogene with high nitrate	Neogene	40	09/05/2006	1004	16.9	6.86	380.6	131.8	49.3	78.3	0.2	154.2	24.9	66.3	< 1
CS0271	S. Neogene with high nitrate	Neogene	80	09/05/2006	1049	16.3	6.76	334.3	134.6	94.5	113.8	0.2	163.1	28.2	74.8	< 1
CS0284	S. Neogene with high nitrate	Neogene	70	09/05/2006	856	16.2	6.55	178.6	110.7	115.7	87.9	0.5	122.3	23.7	55.5	3.2
LL0115	S. Neogene with high nitrate	Neogene	80	06/05/2006	763	17.2	6.96	319.6	53.6	41.4	67.4	0.2	125.1	14.9	46.7	< 1
RS0263	S. Neogene with high nitrate	Neogene	50	10/05/2006	887	16.5	6.79	329.4	79.5	89.4	70.3	0.2	151.9	18.4	54.4	1.1
RS0266	S. Neogene with high nitrate	Neogene	120	23/05/2006	1171	-	6.87	368.4	143.0	135.4	138.4	0.2	221.2	31.1	62.8	< 1
RS0268	S. Neogene with high nitrate	Neogene	65	23/05/2006	1045	16	6.79	341.6	129.3	91.1	97.5	0.2	183.5	24.7	59.4	2.7
RS0271	S. Neogene with high nitrate	Neogene	65	23/05/2006	948	15.9	6.89	327.0	91.6	96.0	94.6	0.2	156.6	27.2	52.3	< 1
SA0167	S. Neogene with high nitrate	Neogene	80	19/05/2006	895	-	6.89	329.4	98.9	62.5	114.7	0.1	154.9	22.7	51.1	1.1

Sample	Group	Geology	Depth (m)	Data	Cond.µS	T ºC	pH	Alkalinity as mg/l HCO3	Cl mg/l	SO4 mg/l	NO3 mg/l	F mg/l	Ca mg/l	Mg mg/l	Na mg/l	K mg/l
VO0105	S. Neogene with high nitrate	Neogene	150	11/05/2006	916	16.5	6.8	366.0	77.1	48.5	94.2	0.2	147.7	26.5	56.5	< 1
BR0077	Surface wells	Quaternary	11.3	11/05/2006	999	16.4?	6.84	373.3	66.0	90.0	99.9	0.2	128.9	28.1	53.6	38.9
CM0147	Surface wells	Neogene	7	10/05/2006	1011	14.7	6.79	336.7	78.6	111.2	128.0	0.2	151.8	24.6	50.0	34.7
CM0285	Surface wells	Neogene	14.7	09/05/2006	835	15.4	7.82	402.6	43.0	66.8	88.0	0.4	133.7	25.8	52.0	2.8
CM0401	Surface wells	Neogene	14.6	10/05/2006	1124	14.8	6.83	248.9	147.5	130.3	170.4	0.2	132.3	12.8	122.5	31.1
CS0400	Surface wells	Neogene	12	09/05/2006	1078	15.3	6.86	339.2	104.0	96.8	138.9	0.1	170.8	21.7	86.5	1.5
LL0116	Surface wells	Neogene	11.8	06/05/2006	1148	15	7.42	424.6	93.9	110.4	200.5	0.2	206.5	23.0	75.4	1.0
MS0115	Surface wells	Quaternary+volcanic	21.9	11/05/2006	735	16.7	6.84	312.3	55.9	55.1	46.6	0.2	106.9	30.0	30.2	< 1
RS0253	Surface wells	Neogene	17.1	11/05/2006	864	17.0	6.9	278.2	21.0	70.1	217.2	0.2	160.8	21.6	27.2	< 1
SI0180	Surface wells	Weathered Granite	12	11/05/2006	612	15	7.15	261.1	18.6	51.9	18.4	0.4	91.5	7.1	42.0	3.3
VD0171	Surface wells	Quaternary	80	11/05/2006	909	16.4	7.11	385.5	67.5	64.0	59.7	0.4	125.4	21.7	84.8	< 1
VO0280	Surface wells	Neogene	8	12/05/2006	805	17.0	7.03	366.0	98.4	9.3	14.7	0.5	111.5	22.6	58.0	1.4
RD0201	D. wells and springs Sta. Col.	Neogene	75	16/05/2006	1093	18.2	6.79	675.9	70.2	16.3	< 0,5	3.2	51.7	16.5	221.9	3.7
RD0202	D. wells and springs Sta. Col.	Neogene	65	16/05/2006	839	17.2	7.15	500.2	50.3	12.1	4.3	1.0	48.0	11.3	138.4	2.5
SC0113	D. wells and springs Sta. Col.	Neogene	73	11/05/2006	440	16	7.11	226.9	27.6	5.1	5.7	0.3	51.3	9.3	38.8	< 1
SC0117	D. wells and springs Sta. Col.	Neogene	65	11/05/2006	533	17.4	6.7	214.7	33.8	28.7	35.5	2.6	69.3	9.4	45.4	< 1
SC0150	D. wells and springs Sta. Col.	Neogene	80	22/05/2006	447	16.9	6.93	212.3	24.0	7.1	16.3	0.5	52.3	10.2	35.7	< 1
SCFP	D. wells and springs Sta. Col.	Spring granite	0	22/05/2006	1471	17.1	6.41	1207.8	66.2	5.8	< 0,5	3.4	161.4	17.4	273.9	4.2
SCFSS	D. wells and springs Sta. Col.	Spring granite	0	22/05/2006	131	17	6.08	51.2	9.1	2.9	< 0,5	0.8	8.9	1.3	16.9	< 1
SC0073	S. wells and waters Sta. Col.	Quaternary	9.5	22/05/2006	502	15.6	6.6	175.7	31.2	60.9	8.5	0.2	61.3	12.8	33.2	1.1
SC0151	S. wells and waters Sta. Col.	Neogene	20	22/05/2006	466	-	6.93	234.2	22.1	9.5	20.1	0.5	59.8	12.3	33.1	< 1
SCRA	S. wells and waters Sta. Col.	Stream	0	22/05/2006	358	19.2	8.07	164.5	13.3	18.7	7.7	0.4	47.4	9.2	19.8	1.1
SCRB	S. wells and waters Sta. Col.	Stream	0	22/05/2006	524	22.3	8.79	183.0	45.5	36.8	10.7	0.6	51.3	9.3	55.4	3.1
BE0077	Volcanic or with vol. materials	Volcanic+Neogene	80	11/05/2006	588	17.9	7.15	307.4	29.3	18.3	11.3	0.3	71.6	25.7	30.6	3.8
CM0151	Volcanic or with vol. materials	Volcanic	75	19/05/2006	764	18.7	7.15	390.4	31.9	46.9	67.7	1.2	127.4	20.2	42.7	3.3
MS0060	Volcanic or with vol. materials	Volcanic	60	11/05/2006	693	18.3	6.95	412.4	34.1	34.6	0.7	0.2	75.8	40.4	44.8	6.6

Table 3.3. Characteristics of each group of samples.

Group number	Group Name	Geology and type of sample point	Type of source	Sub-basin	Well depth (m)	F^- mg/l	NO_3^- mg/l
1	Regional faults or granite	Granit or granites and sedimentary Neogene	Wells and spring	Onyar	0 -150	2.01 -15.4 SG0200=0.13	<0.5 - 34.8
2	Granite or granite and Neogene	Granite, granite+sedimentary Neogene, weathered granite and/or Quaternary+granite	Wells	Onyar and South Santa Coloma	20-121	0.18-2.79	<0.5 - 155.9
3	Sedimentary Neogene with low nitrate	Sedimentary Neogene and sedimentary Neogene+volcanic	Wells	Onyar and South Santa Coloma	69-100	0.28 - 0.89	<0.5 - 37.3
4	Sedimentary Neogene with high nitrate	Sedimentary Neogene and quaternary+ sedimentary Neogene	Wells	Onyar	40-150	0.14 - 0.65	67.4 - 138.4
5	Surface wells	Quaternary, sedimentary Neogene, Neogene+volcaic and weathered granite	Wells	Onyar and South Santa Coloma	7 - 22	0.15 - 0.51	14.7 - 217.2
6	Deep wells and springs Santa Coloma	Neogene and granite (springs)	Wells and springs	North Santa Coloma	0 - 80	0.34 - 3.42	<0.5 - 35.5
7	Surface wells and water Santa Coloma	Quaternary and Neogene	Wells and surface waters	North Santa Coloma	0 - 20	0.22 - 0.55	7.7 - 20.1
8	Volcanic or with volcanic materials	Volcanic or volcanic+Neogene	Wells	Onyar and South Santa Coloma	60 - 80	0.21 - 1.15	0.7 - 67.7

3.4.3. Environmental Isotopes (δD, $\delta^{18}O$)

The contribution of isotopic data to the understanding of the hydrogeological system in the Selva basin is considered in four field surveys depicting seasonal evolution in recharge processes. Three surveys were conducted in 2003 (May, September and December), and a fourth in May 2006, which coincides with the hydrochemical dataset previously discussed. Some of the sampling locations were the same in the different surveys, whereas others were changed depending on their accessibility. The most complete dataset is that of May 2006, coinciding with the beginning of the explotation period of the study area (Table 3.4; Figure 3.8).

Two meteoric lines in Figure 3.8 represent a reference for groundwater isotopic content. A local meteoric water line (LMWL-M) presented for Neat et al. (1992) for the Montseny-Guilleries and another range in NE of Spain. This meteoric water line corresponds to $\delta D = 7.9\ \delta^{18}O + 9.8$, being considered as a representative of the range areas surrounding the Selva basin. A second local meteoric water line (LMWL-S) was constructed using isotopic data from the IAEA-GNIP database (IAEA/WMO 2006) for the "*Girona airport*" station in the central part of the Selva basin. A linear regression of monthly isotopic data results in the following expression for LMWL-S: $\delta D = 8.13\ \delta^{18}O + 6.95$, which shows some deuterium defect in comparison with the LMWL-1.

All these meteoric lines show similar slopes and diverge at the constant term, which can be explained by differences in precipitation regimes and processes of every area studied.

Groundwater samples are plotted in Figure 3.8 according to the hydrochemical categories established in the previous section. Samples are dispersed along meteoric lines indicating different areas and altitudes of recharge. In particular, groundwater from regional fault zones, granite areas and springs show low isotopic content near to LMWL-M, indicating recharge to the surrounding basin from higher altitudes. Specifically, samples straight from fault zones (i.e. SG0200, FS0066 and SCFP) show the lowest isotopic values and, therefore, confirm a relationship with regional, fluoride-rich (except SG0200, as discussed), long-residence time flow systems, and a control of the fault zones upon the flow line distribution.

Table 3.4. Environmental isotopes of each field campaign. If no other type of source is specified in the geology column, samples have been collected from wells.

Sample	Group	Geology	Deep	May-03		Sep-03		Des-03		May-06	
				$\delta^{18}O$	δD	$\delta^{18}O$	δD	$\delta^{18}O$	δD	$\delta^{18}O$	δD
CS0105a	Regional faults or granits	Neogene	80	-5.3	-35.0	-5.6	-36.4				
CS0105b	Regional faults or granits	Neogene+granit	140							-37.3	-5.3
CS0203	Regional faults or granits	Neogene +granit	150			-6.1	-37.8	-6.0	-37.4	-37.0	-5.5
FS0066	Regional faults or granits	Neogene+granit	102	-6.7	-43.5	-6.7	-43.3	-6.8	-43.9	-39.9	-6.1
LG0190	Regional faults or granits	Granit	120	-5.4	-35.0			-5.6	-36.2	-34.0	-5.5
LG0246	Regional faults or granits	Granit	>100							-35.2	-5.7
SG0200	Regional faults or granits	Source	0							-41.0	-6.6
AG0113	Granite or granit and Neo.	Neogene+granit	70							-35.5	-5.4
BR0092	Granite or granit and Neo.	Quaternari+granit	80	-5.8	-37.5	-6.0	-37.8	-6.0	-37.3	-38.6	-6.0
BR0106	Granite or granit and Neo.	Paleozoic	83	-5.5	-36.6	-5.9	-35.6			-35.4	-5.3
CS0183	Granite or granit and Neo.	Granit	60	-5.5	-36.3	-5.9	-38.6	-6.1	-39.8	-34.7	-5.1
LG0029	Granite or granit and Neo.	Wheath. granit+granit	110							-32.7	-4.9
SI0052	Granite or granit and Neo.	Wheathered granit	50							-34.4	-5.1
VD0172	Granite or granit and Neo.	Wheath. granit+granit	50			-5.9	-37.9	-6.0	-36.3	-35.4	-5.5
VD0173	Granite or granit and Neo.	Wheathered granit	20			-5.6	-35.8			-30.8	-4.2
VD0177	Granite or granit and Neo.	Granit	80			-5.6	-34.9	-5.2	-34.7	-32.1	-4.6
VO0100	Granite or granit and Neo.	Quaternary+granit	80							-40.8	-5.6
CM0049	Granite or granit and Neo.	granit	121					-5.1	-31.9	-30.0	-3.8
CS0304	Granite or granit and Neo.	Neogenee+granit	116			-5.8	-34.7			-33.0	-4.9
CM0272	S. Neogene with low nitrate	Neogene	90	-5.4	-36.4	-5.7	-36.5	-5.9	-39.1	-35.7	-4.9
RS0191	S. Neogene with low nitrate	Neogene	90	-5.3	-35.2	-5.8	-35.2	-5.9	-38.8	-33.4	-5.7
RS0270	S. Neogene with low nitrate	Neogene	100	-5.3	-34.8	-5.6	-34.0	-5.6	-35.7	-39.0	-6.0
VD0176	S. Neogene with low nitrate	Neogene+volcanic	69							-34.6	-5.3
BR0110	S. Neogene with high nitrate	Quaternary+Neogene	70							-33.9	-4.9
CL0259	S. Neogene with high nitrate	Neogene	75			-5.7	-35.2	-5.7	-35.7	-35.2	-5.2
CM0272B	S. Neogene with high nitrate	Neogene	40							-35.6	-5.0
CS0271	S. Neogene with high nitrate	Neogene	80	-5.3	-35.8	-5.6	-34.3	-5.8	-38.0	-33.7	-4.9
CS0284	S. Neogene with high nitrate	Neogene	70			-5.8	-35.6	-5.8	-35.1	-35.0	-5.4
LL0115	S. Neogene with high nitrate	Neogene	80	-5.2	-34.7	-5.6	-35.5	-5.4	-34.9	-34.5	-5.2
RS0263	S. Neogene with high nitrate	Neogene	50							-36.3	-5.4
RS0266	S. Neogene with high nitrate	Neogene	120	-5.1	-34.0	-5.6	-33.9	-5.4	-35.0	-33.6	-5.2
RS0268	S. Neogene with high nitrate	Neogene	65							-33.3	-5.3
RS0271	S. Neogene with high nitrate	Neogene	65	-5.1	-33.4					-33.9	-5.4
SA0167	S. Neogene with high nitrate	Neogene	80							-31.6	-4.7
VO0105	S. Neogene with high nitrate	Neogene	150	-5.3	-35.8	-5.8	-33.5	-5.7	-36.1	-34.1	-4.9
BR0077	Surface wells	Quaternary	11.3							-36.4	-5.7
CM0147	Surface wells	Neogene	7							-34.3	-5.1
CM0285	Surface wells	Neogene	14.7							-33.2	-4.6
CM0401	Surface wells	Neogene	14.6							-36.3	-5.2
CS0400	Surface wells	Neogene	12							-32.5	-5.3
LL0116	Surface wells	Neogene	11.8							-32.8	-5.0
MS0115	Surface wells	Quaternary+volcanic	21.9							-31.0	-4.9
RS0253	Surface wells	Neogene	17.1							-32.3	-4.8
SI0180	Surface wells	Wheath. granit	12							-35.2	-5.5
VD0171	Surface wells	Quaternary	80							-31.9	-4.5
VO0280	Surface wells	Neogene	8							-35.6	-5.3
RD0201	D. wells and springs Sta. Col.	Neogene	75							-37.7	-6.3
RD0202	D. wells and springs Sta. Col.	Neogene	65							-33.4	-5.7
SC0113	D. wells and springs Sta. Col.	Neogene	73			-6.1	-38.7	-6.1	-38.7	-38.0	-5.8
SC0117	D. wells and springs Sta. Col.	Neogene	65			-6.0	-37.9	-6.9	-43.3	-33.9	-5.2
SC0150	D. wells and springs Sta. Col.	Neogene	80							-35.9	-5.5
SCFP	D. wells and springs Sta. Col.	Spring grait	0							-40.6	-6.5
SCFSS	D. wells and springs Sta. Col.	Spring granit	0							-38.5	-5.9
SC0073	S. wells and waters Sta. Col.	Quaternary	9.5	-5.6	-36.5					-38.2	-5.8
SC0151	S. wells and waters Sta. Col.	Neogene	20							-35.5	-5.5
SCRA	S. wells and waters Sta. Col.	Stream	0							-36.5	-5.9
SCRB	S. wells and waters Sta. Col.	Stream	0							-35.3	-5.4
BE0077	Volcanic or with vol. materials	Volcanic+eogene	80	-5.4	-36.3	-5.6	-36.0	-5.8	-36.4	-35.6	-5.4
CM0151	Volcanic or with vol. materials	Volcanic	75							-32.0	-4.5
MS0060	Volcanic or with vol. materials	Volcanic	60	-4.5	-31.4	-5.1	-29.8	-4.9	-32.0	-30.5	-4.9

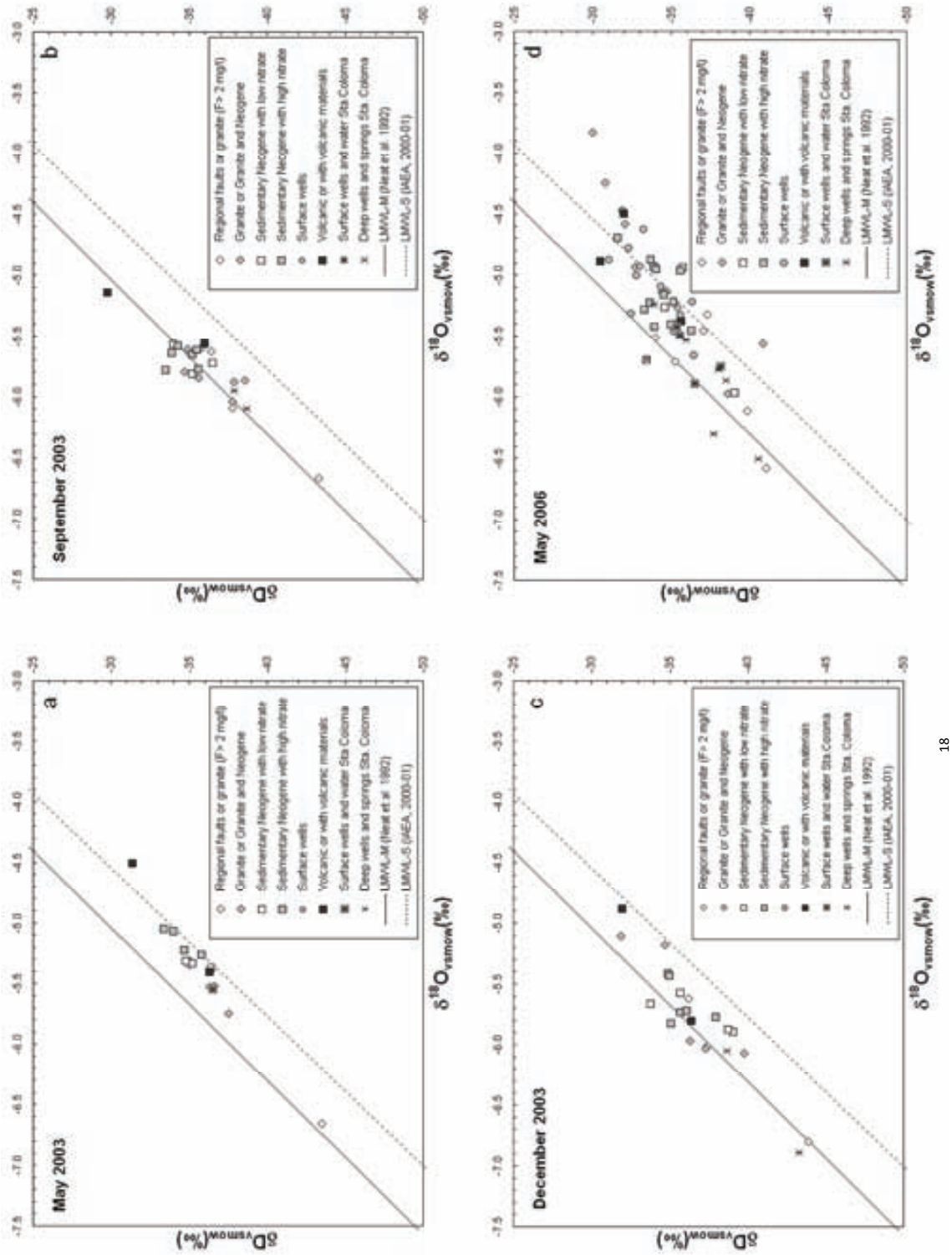

Figure 3.8. Environmental isotope distribution (δD, $\delta^{18}O$) in the different field surveys.

Conversely, most of the samples from wells in the Neogene sedimentary formations show enriched values of $\delta^{18}O$ and δD, denoting a lower altitude of recharge. Those samples with low nitrate content present lower isotopic values than those with evident nitrate pollution. In this way, isotopic data support nitrate as a tracer for the recharge pole located in the rainfall from the central, less elevated areas of the basin.

Isotopic content that varies within a similar geological environment in the same survey reflects the presence of different recharge flow systems, controlled by the hydraulic conductivity and storage capacity of distinct hydrogeological units, especially in the fault zones and in the coarse sediment layers of the Neogene infilling of the basin.

Seasonal variability is also encountered, as samples tend to lie along the LMWL-M in the September and December surveys, and then shift to the LMWL-S in both May surveys, with some evidence of evaporation processes in the bigger dataset of May 2006. The most obvious displacements affect samples from deep wells, and from the Neogene sedimentary layers.

As previously mentioned, wells located in the regional fault zones present lighter values, and therefore the highest altitudes of recharge (Table 3.4). However, sampling point FS0066, located in the central part of the ORB, showed light values in 2003, although its isotopic content was enriched in May 2006, suggesting that mixing processes of different flow systems may occur within the fault zones, probably induced by water withdrawal pressures. Despite this, its values are some of the lightest in the dataset, indicating that fault zones do act as interceptors of regional, large-scale flow systems. In addition, sample SG0200, placed at the northern limit of the Selva basin, presents isotopic values similar to those of FS0066, which indicates a common recharge origin for both groundwater samples regardless of their hydrochemical differences. In the same geochemical group as FS0066 (i.e. samples from regional fault zones and granitic aquifers) there are samples with higher isotopic values (e.g., LG0190 and LG0246). Such values denote a gradation of regional flow systems from distinct recharge areas at different altitudes in the surrounding ranges. In particular, isotopic values in wells located downstream along the flow line in the Neogene sediments and granite basement (CS0105 and CS0203) are interpreted as the result of mixing processes from different screened intervals in the borehole.

In the western SCRB, samples with light isotopic values are also indicative of high altitude recharge from the surrounding range areas, namely the Montseny-Guilleries range (SCFP,

RD0201). While some samples exhibit steady isotopic content in all surveys (SC0113) and show a recharge from a steady flow system, other samples, like SC117, vary through the seasons. Considering that this well is cased in the upper 20 m, a shifting isotopic content suggests that sampled water originated from distinct flow systems, whose contributions vary through the year depending on natural rainfall recharge and the effect of withdrawal regimes.

Light isotopic values coincide with a nitrate decrease and a fluoride increase during the summer season, when rainfall recharge is almost nil (Menció, 2006). Isotopic values reverse in fall and winter when rainfall events are intense, with hydrochemical data showing a similar seasonal trend. This series of results confirms that distinct, independent flow systems concur in a single aquifer, and alternate as a consequence of groundwater withdrawal regimes.

Carbon dioxide of thermal origin affects some samples in the SCRB (for instance, SCFP and RD201; Figure 3.8d). These samples show a decrease in $\delta^{18}O$, which is displaced to the left of the LMWL-M.

Isotopic values in samples from the Neogene sedimentary aquifers move closer to the LMWL-S in the spring surveys (May 2003 and 2006; Figures 3.8a,d; Table 3.4), while in surveys conducted in fall and winter (Figures 3.8b,c) they are placed on the LMWL-M and show lighter isotopic values. Some samples from wells in granite terrains also show a similar seasonal displacement.

Additionally, samples from the May surveys, notably May 2006 (Figure .38d), follow a line with a slope of ≈4.0 that is consistent with the occurrence of evaporation processes (Clark and Fritz, 1999). Evaporated samples are found in granitic areas in the southeastern corner of the Selva basin, where there are weathered or partially weathered granite outcrops and the unsaturated zone depth is up to 25 m.

The occurrence of partially evaporated samples allows seasonal hydrodynamics to be identified. Water withdrawn at the end of the summer season, that is in September or October, shows higher recharge altitudes and isotopic values aligned according to the LMWL-M. During May surveys, following the wet season that lasts from October to May, groundwater samples exhibit enriched isotopic values that have shifted to the LMWL-S. Moreover, specific samples located in the ORB are distinctively aligned along an evaporation line. Such seasonal differences are attributable to local recharge pulses during the wet season, i.e. rainfall in the

basin area infiltrating into the Neogene layers after being affected by evaporation processes. Such recharge is thus the main resource that is captured by pumping wells after the end of the wet season. Evaporated groundwater samples also exhibit a wide range of nitrate concentration (Table 3.2), as would be expected from the local recharge pole.

By September, intensive water withdrawal has exhausted such local resources, and the isotopic content reveals the dominant influence of groundwater flow from regional systems on the captured water. That is to say, the lateral and vertical upward recharge from the surrounding ranges and the basement provides water for the sedimentary aquifers of the basin, fulfilling major water needs as most of the wells can therefore maintain their exploitation rates. Such seasonal conduct emphasizes the effect of the groundwater withdrawal regime on the hydrogeological dynamics of this system, with the origin of captured water being modified from local to regional recharge sources. It also reveals the role of fault zones as preferential flow paths that recharge the overlying sedimentary layers from the basement.

In the December 2003 survey, isotopic data show a transitional distribution between the end of the dry season (mainly summer) and the beginning of the recharge period in October and November. In particular, those months had more rainfall than the average (i.e., 220 mm in October 2003; Figure 3.4), providing support for the behavior described.

3.5. Conclusions

The major features and findings of this hydrogeological research are as follows:

1. Potentiometric, hydrochemical and isotopic data have been used to describe the hydrogeological system of the Selva basin (NE Spain), located in a range-and-basin environment. Structural elements, i.e., fault zones, play an important role in the recharge from the ranges towards the basin's infill aquifers.
2. Water withdrawal, mainly from the basin sediments, exerts a significant influence upon the hydrogeology of the system, producing a modification of regional and local scale flow paths in accordance with natural recharge periods and seasonal exploitation regimes.

3. Potentiometric data measured over a six-year period reveal distinct flow dynamics within the sedimentary infilling of the basin. They indicate the degree of vertical connectivity in this multilayered leaky aquifer system, as well as the existence of a lateral inflow from the range-front and, more importantly, a vertical upward flow from the granitic basement. They also indicate that fault zones act as specific recharge spots, controlling the hydraulic efficiency of wells and, overall, the recharge flows.
4. Hydrochemical facies support the observations derived from potentiometric data. The occurrence of sodium and chloride-rich facies points to the contribution of groundwater flow from the basement to the basin sedimentary infill.
5. Fluoride and nitrate concentrations are taken as tracer components of, respectively, a regional end-member, defined by large-scale, long residence time flows from the range areas to the basin, and a local end-member, caused by rainfall infiltration in the basin surface. Variations in the content of both components are attributable to the capture of distinct flow paths, as stored resources decline during intensive pumping (irrigation) periods.
6. Using two local meteoric water lines, representing the range areas surrounding the basin and the basin itself, show different recharge flow systems. In this sense, the Selva basin recharge takes place from the basin surface, creating a local flow system, and from the surrounding ranges as regional flow systems originated at higher altitude and with a long residence time.
7. Seasonal isotopic data shift between both local meteoric water lines and the fact that fractionation processes related to evaporation are identified during the spring (May) surveys also indicate that the amount of captured water resources from the two flow systems may vary along the year.
8. Meeting water demand in the Selva basin does in fact depend on the seasonal exploitation of regional and local flow systems. In particular, regional flow systems related to fractures and major fault zones supply the necessary amount of resources that could not be satisfied by only the local rainfall recharge.

These conclusions demonstrate that hydrogeological systems are greatly disturbed by groundwater withdrawal regimes, which modify natural flow paths. Such modifications, which rule the water balance within the basin and, therefore, the amount of available water resource, can be identified with the aid of potentiometric, hydrochemical and isotopic data. Furthermore, structural elements, such as fault zones, represent a significant, preferential flow path whose contribution is fundamental to completely meeting water demand and, more

importantly, the recovery of the resources stored in periods of low demand. Data from surveys covering several years provide a crucial contribution to the depiction of spatial heterogeneity in groundwater dynamics under human pressures.

Such a regional, large-scale geological approach permits an understanding of the hydrogeological dynamics in a range-and-basin environment of this type, and an evaluation of the current extent of water resources in the system. Quality issues are also better understood if regional perspectives are used, by providing helpful explanations for the occurrence of natural or human introduced pollutants, such as fluoride and nitrate, respectively. They also contribute to the appropriate management of groundwater bodies in the context of the Water Framework Directive (Directive 2000/60/EC).

3.6. References

ACA, 2002. Model de Gestió del sistema hidrològic de naturalesa granítica del sistema Montseny-Guilleries. Agència Catalana de l'Aigua, Generalitat de Catalunya, Spain, 460 pp.

Aji, K., Tang, C., Song, X., Kondoh, A., Sakura, Y., Yu, J., Kaneko1, S., 2008. Characteristics of chemistry and stable isotopes in groundwater of Chaobai and Yongding River basin, North China Plain. Hydrological Processes 22, 63–72.

Albert, J.F., 1980. Estudio geotérmico preliminar de Cataluña. PhD dissertation, Universitat Autònoma de Barcelona, Spain.

Beaucaire, N., Gassama, N., Tresonne, N., Louvat, N., 1999. Saline groundwaters in the hercynian granites (Chardon Mine, France): geochemical evidence for the salinity origin. Applied Geochemistry 14, 67–84.

Carrillo-Rivera, J.J., Irén Varsányi, I., Kovács L.O., Cardona, A., 2007. Tracing Groundwater Flow Systems with Hydrogeochemistry in Contrasting Geological Environments. Water Air and Soil Pollution 184, 77–103.

Chen, J., Tang, C., Sakura, Y., Kondoh, A., Yu, J., Shimada, J., Tanaka, T., 2004. Spatial geochemical and isotopic characteristics associated with groundwater flow in the North China Plain. Hydrological Processes 18, 3133–3146.

Clark, I.D., Fritz, P., 1997. Environmental Isotopes in Hydrogeology. Lewis Publishers, New York, 329 pp.

Craig, H., 1961. Isotopic variations in meteoric waters. Science 133**,** 1702–1703.

Cunningham, E.E.B., Long, A., Eastoe, C., Basset, R. L., 1998. Migration of recharge waters downgradient from the Santa Catalina Mountains into the Tucson basin aquifer, Arizona, USA. Hydrogeology Journal 6, 94–103.

Demlie, M., Wohnlich, S., Gizaw, B., Stichler, W., 2007. Groundwater recharge in the Akaki catchment, central Ethiopia: evidence from environmental isotopes (d18O, d2H and 3H) and chloride mass balance. Hydrological Processes 21, 807–818.

Devlin, J.F, Sophocleos, M., 2005. The persistence of the water budget myth and its relationship to sustainability. Hydrogeology Journal 13, 549–554.

Folch, A., Mas-Pla. J., 2008. Hydrogeological interactions between fault zones and alluvial aquifers in regional flow systems. Hydrological Processes 22, 3476-3487.

Gascoyne, M., Davison, C.C., Ross, J.D., Pearson, R., 1987. Saline groundwaters and brines in plutons in the Canadian Shield. In: Fritz, P., and Frape, S.K. (eds.) Saline Water and Gases in Crystalline Rocks. Geological Association of Canada Special Paper 33, 53-68.

IAEA/WMO, 2006. Global Network of Isotopes in Precipitation. The GNIP Database. Accessible at: http://isohis.iaea.org**.**

IGME, 1993. Estudio hidrogeológico de la Selva. Tomo I, Memoria y Anexo 1. Intituto Geològico y Minero de España. Ministerio de Ciencia e Innovación, Spain.

Li, X., Zhang, L., Hou, X., 2008. Use of hydrogeochemistry and environmental isotopes for evaluation of groundwater in Qingshuihe Basin, northwestern China. Hydrogeology Journal 16, 335–348.

Mahlknecht, J., Gárfias-Solis, J., Aravena, R., Tesch, R., 2006. Geochemical and isotopic investigations on groundwater residence time and flow in the Independence Basin, Mexico. Journal of Hydrology 324, 283–300.

Menció, A., 2006. Anàlisi multidisciplinària de l'estat de l'aigua a la depressió de la Selva. PhD dissertation, Universitat Autònoma de Barcelona. http://www.tdx.cesca.es/TDX-0718106-140651/

MOPU, 1971b. Estudio de los recursos hidráulicos totales del Pirineo Oriental (zona norte). Estudio de los recursos subterráneos de la zona de la Selva (Gerona). Ministerio de Obras Públicas y Urbanismo, Dirección General de Obras Hidráulicas, Spain.

MOPU, 1985. Plan Hidrológico del Pirineo Oriental. EE2 Estudio complementario sobre aguas subterráneas. Zona5- La Selva. Síntesis Hidrogeológica. Ministerio de Obras Públicas y Urbanismo, Dirección General de Obras Hidráulicas, Spain.

Neal, C., Neal, M., Warrington, A., Avila, A., Pinol, J., Roda, F., 1992. Stable hydrogen and oxygen isotope studies of rainfall and streamwaters for two contrasting holm oak areas of Catalonia, northeastern Spain. Journal of Hydrology 140**,** 163–178.

Palmer, P.C., Gannett, M.W., Stephen R. Hinkle, S.R., 2007. Isotopic characterization of three groundwater recharge sources and inferences for selected aquifers in the upper Klamath Basin of Oregon and California, USA. Journal of Hydrology 336, 17-29.

Pous, J., Solé Sugrañes, L.,Badiella, P., 1990. Estudio geoeléctrico de la depresión de La Selva (Girona). Acta Geológica Hispánica 25, 261-269.

Cunningham, E.E.B, Long, A., Eastoe, C., Bassett R.L., 1998. Migration of recharge waters downgradient from the Santa Catalina Mountains into the Tucson basin aquifer, Arizona, USA. Hydrogeology Journal 6, 94–103.

Sukhija, B.S., Reddy, D.V., Nagabhushanam, P., Nagabhushanam, P., Bhattacharya, S. K., Jani, R.A., Kumar, D., 2006. Characterization of recharge processes and groundwater flow mechanisms in weathered-fractured granites of Hyderabad (India) using isotopes. Hydrogeology Journal 14, 663–674.

Tóth, J., 1995. Hydraulic continuity in large sedimentary basins. Hydrogeology Journal 3, 4–16.

Tóth, J., 2000. Las aguas subterráneas como agente geológico: Causas, procesos y manifestaciones. Boletín Geológico y Minero 111, 9–26.

Vilanova, E., 2004. Anàlisi dels sistemes de flux a l'àrea Gavarres-Selva-Baix Empordà. Proposta de model hidrodinàmic regional. PhD dissertation, Universitat Autònoma de Barcelona. http://www.tesisenxarxa.net/TDX-1217104-145328/

Vilanova, E., Menció, A., Mas-Pla, J., 2008. Determinación de sistemas de flujo regionales y locales en las depresiones tectónicas del Baix Empordà y la Selva (NE de España) en base a datos hidroquímicos e isotópicos. Boletín Geológico y Minero 119, 51-62. Instituto Geológico y Minero de España, Spain.

Chapter IV

Exploring different hydrochemical and isotopic data to define recharge patterns and groundwater quality: the Selva basin (NE Spain)

4.1. Introduction

In complex geological areas, as range-and-basin regions, hydrogeological flow systems adapt to the subsurface structures that determine groundwater paths. This involves a single flow system flowing through different geological formations that leave their own footprint as a hydrochemical pattern. This geological setting enables the occurrence of different scale flow systems that may interfere by mixing creating new hydrochemical features.

In this context, groundwater exploitation regimes influence the natural flow system by generating significant capture zones. That means that groundwater withdrawal may drain various geological units as the pumping of water resources becomes more intense. Water availability, and therefore a sustainable yield from the area, will depend on the response of the complex hydrogeological system to such pressures, and on its capacity to recharge the exploited aquifers.

Hydrogeological characterization of such specific areas therefore entails investigation of two distinct aspects. The first is the setup of the entire hydrogeological system in order to build up a conceptual model of its dynamics. The second is the effect of human pressures on the system and, more importantly, its capacity to safely supply the amount of water required by withdrawal regimes based on human needs, while considering the environmental functions of both surface water and groundwater.

Hydrochemical and isotopical data provide a useful approach for outlining the geochemical processes that indicate the groundwater flow path. This knowledge is fundamental in determining the recharge areas and the paths that groundwater has followed to the sampling point. They contribute to defining the main hydrogeological features of the system as recharge areas, the most productive hydrogeological formations, the role of aquitards or low permeability units and that of structural elements as fault zones, and the effect of pumping on the flow field. All this information is therefore valuable in assessing the availability and quality of water in the different sectors of a basin according to its subsurface constitution.

In the previous chapters, the hydrogeological dynamics of the Selva basin have been described based on its geological features. Hydraulic head data, as well as hydrochemical and isotopical information, have been used to distinguish flow systems within this range-and-basin area and

to show how the system responds to intense groundwater withdrawal during the dry season. Furthermore, the role of fracture zones as a geological frontier between range (recharge) and basin (discharge) areas has been investigated using numerical modeling, which shows their relevance in regional flow distribution. In particular, simulations indicate the occurrence of an effective upward vertical recharge through the fault zone, and from the basement, towards the sedimentary infilling of the basin. These data enable a conceptual model to be created, in which regional flow fields are responsible for recharging some depleted local aquifers within the basin.

However, a complete snapshot of the hydrogeological dynamics of such a geological area cannot be accomplished without a detailed analysis of the geochemical processes that determine the hydrochemical and isotopical features of each sample. Such an examination is then necessary to recognize and verify the contribution of specific geological units (for instance, the basement of the basin) to the flow field as a whole. Hydrochemical facies using major elements provide a general portrait of the hydrogeological system and a spatial distribution of specific chemical features. Other compounds such as nitrate indicate recent surface recharge, while elements such as fluoride are a sign of deep contribution. Moreover, major elements also give an insight into the main geochemical processes that are responsible for the current chemical composition of the water and for the mixing processes where they occur.

Nevertheless, a more complete description of the hydrogeological system is obtained if minor elements (such as fluoride, bromide, lithium, TOC, and their ratios to some major elements) or specific isotopes ($\delta^{18}O_{H2O}$, δD, tritium, $\delta^{34}S$, $\delta^{18}O_{SO4}$). are used to corroborate previous observations and to enhance our knowledge of the system.

This chapter aims to provide a detailed description of the geochemical processes that determine the hydrochemical characteristics of groundwater across the Selva basin, based on the interpretation of major element, minor element and isotope data ($\delta^{18}O_{H2O}$, δD, tritium, $\delta^{34}S$, $\delta^{18}O_{SO4}$). Its objective is to provide a sound basis for the evidence from the various flow systems already described, and to use this specific data to corroborate the overall hydrogeological conceptual model for the Selva range-and-basin area.

From a methodological perspective, this chapter explores the use of minor elements and isotopes in the interpretation of regional scale system hydrodynamics. It also discusses their

use as tracers of the various groundwater flows originating in different recharge areas and influenced by an intricate tectonic setting.

4.2. Hydrogeological setting and previous work

The Selva basin is a tectonic basin surrounded by the Montseny-Guilleries (1202 m asl), Gavarres (535 m asl), Selva Marítima (519 m asl) and Transversal (998 m asl) mountain ranges in the province of Girona (NE Spain). There are two main watersheds in the study area, those of the Santa Coloma River and Onyar River basins (65-135 m asl). The Santa Coloma River Basin extends along the entire length of the south-western side of the Selva basin, with part of its headwaters in the Montseny-Guilleries mountains. The Onyar River basin occupies the north-eastern side of the basin, and its headwaters are in the Gavarres and Selva Marítima ranges (Figure 4.1).

The Selva basin constitutes a type of range-and-basin structural area with a Neogene and Quaternary sedimentary infilling, arising from the erosion of the surrounding mountains. Sediments consist of unconsolidated gravel, coarse and medium sand and layers of silt reaching a maxim thickness up to 200 m in some areas (MOPU, 1985; Pous et al., 1990; Vehí, 2000). The main fault directions are NW–SE, NE–SW and N–S, and are responsible for the tectonic and morphological evolution of the area.

The Montseny-Guilleries, Selva Marítima and Gavarres ranges consist of Paleozoic igneous and metamorphic rocks (mainly shale and schist). The most important outcropping materials, which are also located at the bedrock, are granodiorites and leucogranites. The main granodiorite forming minerals are quartz, plagioclase (oligoclase and andesine), K feldspar and biotite. The secondary and accessory minerals are chlorite, apatite, zircon, muscovite, tourmaline and hematite. The main Leucogranite forming minerals are quartz, plagioclase (oligoclase), K feldspar and biotite, and secondary and accessory minerals as chlorite, apatite, zircon, muscovite, magnetite, garnet, kaoline and sericite.

On the basin surface, the main hydrogeological units are the unconfined aquifers created by the alluvial quaternary formations and the upper levels of the Neogene sediments. At a depth of between 30 and up 200 m depth (MOPU, 1985; Pous et al., 1990; Vehí, 2000), there is a multilayer aquifer working under semiconfined/confined conditions. These

deeper levels are located above the basin bedrock consisting of by igneous rocks. The surrounding reliefs and the bedrock contain different fault systems recharging the sedimentary levels of the basin (Menció, 2006; Folch and Mas-Pla 2008).

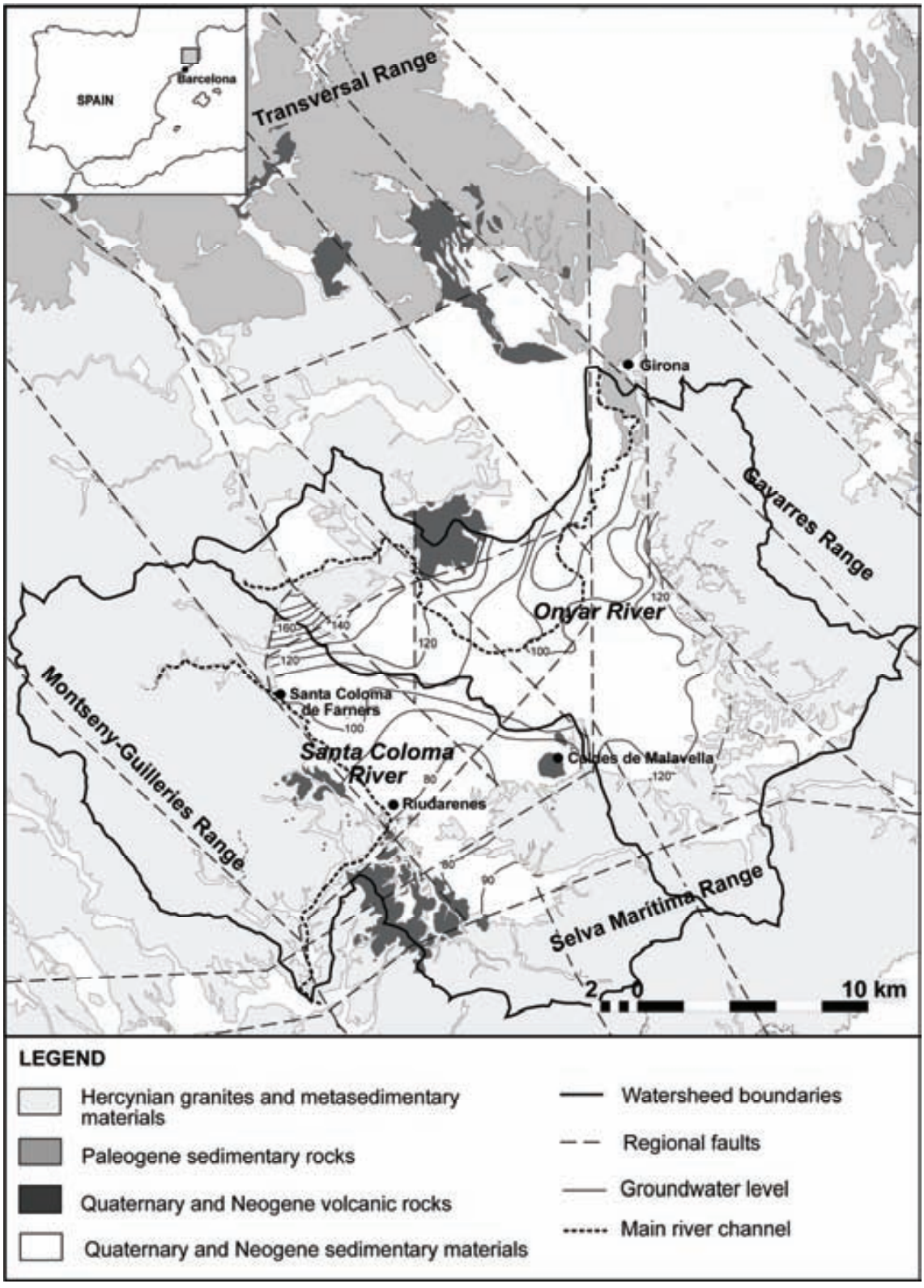

Figure 4.1. Geological and hydrogeological setting of the Selva basin.

The largest variations in hydraulic head in the basin wells, in both shallow and deep sedimentary aquifer levels, occur during the summer months because of the lack of recharge and heavy extractions. These are mainly for agricultural uses, with a loss of storage in the aquifer.

The deeper wells tend to have a large drawdown (up to 25-30 m) associated with intense exploitation regimes, despite the high hydraulic conductivity sand levels attributable to the Neogene formation. This suggests a limited storage capacity, offset by flow induced from the surrounding reliefs or the basin bedrock, such as regional flow systems, which balance the pumping rates. Most of these wells present good recovery of hydraulic head after rainy periods.

The Selva basin is made up of two smaller hydrological basins: the Santa Coloma River basin and the Onyar River basin. The drainage network interacts with the groundwater of the alluvial quaternary formations. There is a groundwater divide between both basins resulting in two different hydrogeological basins. The first one is located to the W, and is characterized by lower salinity waters on the western side and related geographically with the main river channel, the Santa Coloma River (Figure 4.1). The other side of the basin, considered to be the Onyar basin, usually has higher salinity levels and a more variable hydrochemical composition.

Both basins are characterized by two main types of flow systems: local and regional. Local flows recharge at the basin surface, and have an anthropogenic input with usually high nitrate concentrations and evaporation in some cases. Regional flows occur across the main faults recharging at the surrounding ranges. These present higher salinities, with high sodium and fluoride concentrations (until 15 mg/l) the most important attribute. Depending on the groundwater exploitation rates and the season, mixing between the two flow systems takes place (see chapter 3).

The different flow systems are also characterized by different hydrochemical facies (Figure 4.2). Local flow systems are represented by Ca-HCO_3 facies with high nitrate, sulphate and chloride concentrations related to pollution sources and founded in surface wells and some deep neogene wells. Regional flow systems are represented by Na-HCO_3 facies with high sodium content, low nitrate and sulphate content, and in some cases high chlorite and fluoride content (up to 15 mg/l). Wells with these facies are located in deep neogene and granite and

the Cl and F rich facies close to regional faults. In these groups, the first type of facies is found in deep neogene wells and in some granites. The second type consists of wells in granite related with regional faults. This flow system is characterized by high sodium concentrations and high fluoride (up to 15 mg/l) and chloride in some cases. There are intermediate flow systems characterized by Ca-HCO_3 and Na-Ca-HCO_3 in some wells located in neogene sediments and in weathered and unweathered granite.

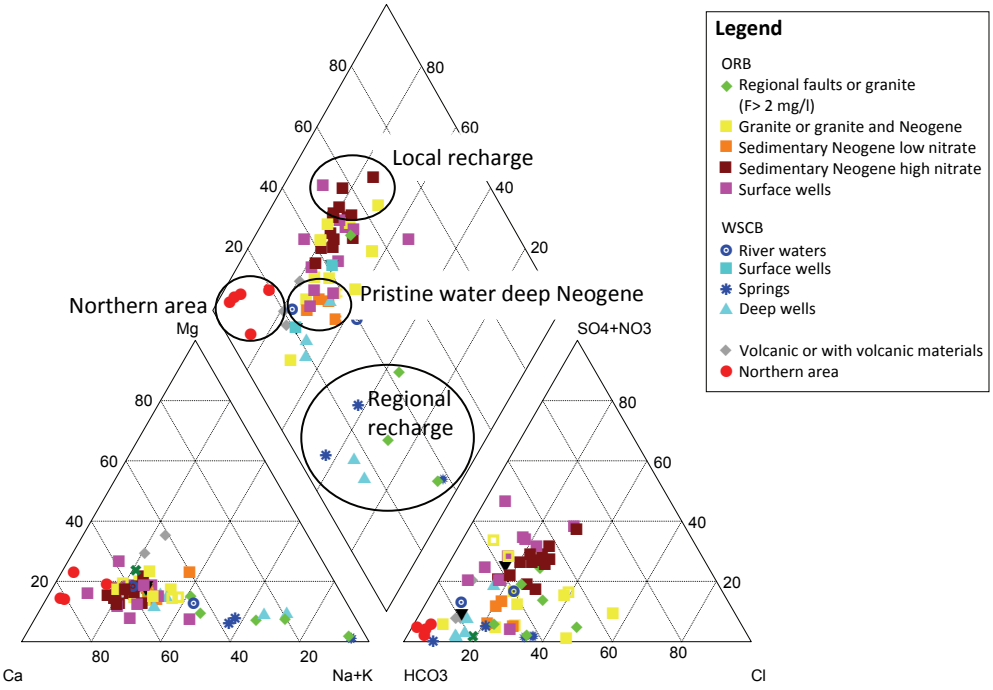

Figure 4.2. Piper diagram of each group of samples.

Water isotope data ($\delta^{18}O$ and δD) from various campaigns over several years and seasons show that during the December – May period, when pumping rates are lower, the isotope values indicate a recharge coming from local precipitation. Between June and September, a period of greater consumption, there is an influence by regional flows from the basin bedrock.

The hydrochemical and isotopic data, and the piezometrical data analyzed (see chapter 3) show seasonal trends in the water captured by wells. There are two different main flow systems: a regional, large-scale, long residence time system, originating in the surrounding ranges, and a local flow system caused by infiltration in the lower areas of the basin. These two systems contribute to the resources that are withdrawn in varying degrees, and their specific contributions define the potential for sustainable water exploitation in the basin.

4.3. Methodology

Due to the mixing processes and the modified natural hydrodynamics, the influences and the processes controlling the recharge are difficult to define. This study focuses on understanding the processes controlling the characteristics of each flow system and their distribution around the basin. To accomplish this goal, a complete field sampling was carried out in May 2006, with more chemical and isotopic parameters analyzed than in previous studies (Menció 2006, chapter 3). This season is when the most recharge occurs, with lower extractions rates, acting similarly to a natural flow system. This campaign enables easily differentiation between the end-member characteristics of each flow system and recharge area.

Groundwater samples for chemical and isotopic analysis were collected at 60 private wells (mainly pumped for domestic, agriculture and cattle raising uses), 3 springs and 2 sites from Santa Coloma River. Physicochemical parameters (pH, temperature, conductivity, Eh and dissolved O_2) were measured in situ, using a flow cell to avoid contact with the atmosphere. Eh was measured with a WTW SenTix® Plus electrode (consisting of a platinum measuring electrode and a silver/silver chloride reference electrode) connected to a WTW pH 330i pH/mV meter. All Eh measurements were corrected to the standard hydrogen electrode system (UH) by adding the reference electrode potential at the groundwater temperature to the measured potential. The concentration of dissolved oxygen was measured with a DO meter (Hach® LDO/HQ10). The samples were collected after the wells had been continuously pumped until the Eh values stabilized.

The samples were kept at 4 ºC and in a dark environment for subsequent chemical and isotopic analyses. In the laboratory, pH and conductivity at 25 ºC were measured again. Total organic carbon (TOC) was measured by organic matter combustion (TOC 500 SHIMADZU), alkalinity (HCO_3^-) by titration (METROHM 702SM Titrino) and F^- by ion selective electrode method (Orion 901 ion selective electrode). Afterwards a split of the sample was filtered through a 0.2 μm Millipore® filter. The anion (NO_3^-, SO_4^{2-} and Cl^-) content was measured by Capillary Electrophoresis (Agilent Technologies) using indirect UV detection, concentrations of Na, K, Ca, Mg, Sr, Fe, Zn, Si were measured by Inductively Coupled Plasma-Optical Emission Spectrometry (ICP-OES, Perkin Elmer 4300 DV), and concentrations of Mn, Ba, Cu, Cr, Al, Se, Cd, Pb, Li, U by Inductively Coupled Plasma-Mass Spectrometry (ICP-MS, Perkin Elmer Elan 6000). Br concentration was measured by Inductively Coupled Plasma-Mass Spectrometry (ICP-

MS, Thermo Elemental, PQEXcell), using the collision cell technique (CCT) and He as the collision gas. The quality of the chemical analysis was checked by performing an ionic mass balance, with an error lower than 5% accepted.

For the SO_4^{2-} isotopic analysis ($\delta^{34}S_{SO4}$ and $\delta^{18}O_{SO4}$), dissolved SO_4^{2-} was precipitated as $BaSO_4$ by adding $BaCl_2 \cdot 2H_2O$ after acidifying the sample with HCl and boiling it to prevent $BaCO_3$ precipitation following standard methods (e.g. Dogramaci et al., 2001). Deuterium and O isotopes of water were analyzed in a Finnigan Matt Delta S Isotope Ratio Mass Spectrometer (IRMS) coupled to an automated line based on the equilibration between H-water and H_2 gas with a Pt catalyst, and between O-water and CO_2 gas following standard methods (Epstein and Mayeda, 1953). The $\delta^{34}S_{SO4}$ was analyzed in a Carlo Erba Elemental Analyzer (EA) coupled in continuous flow to a Finnigan Delta C IRMS. The $\delta^{18}O_{SO4}$ was analyzed in duplicate with a ThermoQuest TC/EA (high Temperature Conversion/Elemental Analyzer) unit coupled with a Finnigan Matt Delta C IRMS. Notation is expressed in terms of δ ‰ relative to the international standards V-SMOW (Vienna Standard Mean Oceanic Water) for δD and δ^{18}O and V-CDT (Vienna Canyon Diablo Troilite) for δ^{34}S. The precision ($\equiv 1\sigma$) of the samples calculated from international and internal standards systematically interspersed in the analytical batches was ±1.5‰, ±0.2‰, ±0.4‰ and ±0.5‰ for δD, $\delta^{18}O_{H2O}$, $\delta^{34}S_{SO4}$ and $\delta^{18}O_{SO4}$, respectively. Tritium was analyzed by Electrolytic Enrichment and Liquid Scintillation Counting Method using a Ultra Low Level Liquid Scintillation Spectrometer (Quantulus 1220, LKB Wallac).

All chemical and isotopic analyses were prepared in the Mineralogia Aplicada i Medi Ambient Research Group laboratory. Major ions were analyzed at the Servei d'Anàlisi Química (SAQ) of the Autonomous University of Barcelona. Br was analyzed at the Grup de Tècniques de Separació (GTS) of Chemical Science Department of the Autonomous University of Barcelona. Tritium was analyzed at the Servei de Datació per Triti i ^{14}C. The other chemical and the isotopic compounds were analyzed at the Scientific Services of the University of Barcelona.

4.4. Results

The samples obtained from the field campaign were divided into different hydrogeological groups based on geology, well depth, basin and further nitrate and fluoride concentrations (see chapter 3). This provided two main groups of samples: wells and springs in the western Santa Coloma river basin (WSCB) and wells located in the south of the Santa Coloma basin and the Onyar river basin (ORB).

A few samples from the northern area, between the basin and the Transversal range were also considered (Table 1,2 and Figure 4.2). These samples are located in Neogene on Paleogene materials, without any interaction with granites in the Selva basement. In this area, there is one sample called SG0200, located over one of the regional faults oriented in the Transversal range-Selva basin direction (Figure 3.7, chapter 3). This is a spring with high salinity and no evidence of pollution being considered in the "Regional faults and/or granite" group. A sample from a thermal water (the Termes Orion sample) close to the Santa Coloma town area (Figure 4.1) was also considered (http://www.balneari-termas-orion.com/eng/lesaigues.html).

The saturation indexes were calculated using PHREEQC code (Parkhurst and and Appelo, 1999).

4.5. Interpretation of the hydrochemical and isotopical data

4.5.1. Origin of the hydrochemical facies

As shown in previous studies (Vilanova 2004, Menció 2006, chapter 3), the waters in the different flow systems in the Selva basin are characterized by different hydrochemical facies. Those facies are determined by the different flow paths of the groundwater recharging the basin. As a result, the Ca-HCO_3 facies are representative of shorter transit times and/or flow paths while the Na-HCO_3 and Na-HCO_3-Cl facies indicate longer transit times in different geological environments (Tóth, 1995, 2000; Beucaire, 1999; and Carrillo et al., 2007).

In the ORB and the WSCB, there are wells and/or springs representing regional flows presenting different hydrochemical facies, indicating diverse flow paths and/or processes during the transit time in the aquifer (Figure 4.3). Wells representative of regional flow

Table 4.1. Sample group, basin (western Santa Coloma basin or Onyar River basin), sample name, well geology, well depth, field parameters and major element and fluoride.

Group	Basin	Sample	Geology	Depth (m)	Cond. µS/cm	T ºC	pH	Eh mV	O_2 mg/L	Alk. as mg/l HCO3	Cl mg/l	SO4 mg/l	NO3 mg/l	F mg/l	Ca mg/l	Mg mg/l	Na mg/l	K mg/l	Si mg/l
Regional faults or granite	ORB	CS0105	Neogene+granite	100?	767	16.8	7.3	403.7	0.92	274.3	73.0	58.1	30.0	6.21	50.8	8.0	125.0	3.6	9.3
Regional faults or granite	ORB	CS0203	Neogene +granite	150	751	17.2	7.0	-	-	205.0	70.7	62.8	34.8	2.01	76.0	16.0	76.2	7.6	13.9
Regional faults or granite	ORB	FS0066	Neogene+granite	102	1533	19.7	7.8	243.8	0.15	653.9	221.1	21.0	< 0,5	15.40	18.7	5.3	397.8	1.8	9.3
Regional faults or granite	ORB	LG0190	Granite	120	963	17.4	7.3	18.1	0.14	314.8	196.1	29.6	0.5	2.32	133.7	24.8	71.8	1.4	13.0
Regional faults or granite	ORB	LG0246	Granite	>100	786	17.7	7.3	22.2	-	263.5	103.0	50.3	13.4	3.03	81.5	10.7	94.7	4.3	11.2
Regional faults or granite	ORB	SG0200	Spring not determined	0	4790	17.2	6.5	-	-	3220.8	651.9	238.4	< 0,5	0.00	319.5	74.1	1249.8	30	20.3
Granite or granite and Neo.	ORB	AG0113	Neogene+granite	70	556	18.2	7.2	343.4	2.31	329.4	19.7	17.1	4.5	0.72	77.7	11.6	47.8	1.5	19.3
Granite or granite and Neo.	ORB	BR0092	Quaternari+granite	80	361	17	6.3	456.8	4.25	122.0	29.8	11.3	24.4	0.17	36.1	8.1	29.0	0.0	24.6
Granite or granite and Neo.	ORB	BR0106	Granite	83	974	16.8	7.0	-	-	478.2	136.2	30.0	9.0	0.51	143.7	32.3	68.3	2.1	9.9
Granite or granite and Neo.	ORB	CM0049	Granite	121	681	17.2	7.2	-	-	270.8	73.9	28.1	26.9	0.51	89.9	15.8	50.8	1.2	14.3
Granite or granite and Neo.	ORB	CS0183	Granite	60	825	-	6.9	-	-	251.3	133.1	49.8	30.7	1.27	117.6	17.6	55.2	1.2	15.6
Granite or granite and Neo.	ORB	CS0304	Neogene+granite	116	1046	17.7	7.0	-	6.33	344.0	115.6	77.7	120	2.79	156.8	20.9	84.6	1.1	15.2
Granite or granite and Neo.	ORB	LG0029	Weath. granit+granite	110	970	17.3	7.4	-76.5	0.09	541.7	114.9	33.7	< 0,5	0.51	135.8	38.3	74.0	2.4	15.7
Granite or granite and Neo.	ORB	SI0052	Weathered granite	50	1217	16.3	6.9	343.6	5.51	385.5	213.6	64.7	79	0.51	159.3	29.4	129.5	1.4	20.6
Granite or granite and Neo.	ORB	VD0172	Weath. granit+granite	50	921	19.3	7.2	-	-	329.4	184.1	7.5	0.5	0.35	153.0	25.7	50.6	0.0	17.0
Granite or granite and Neo.	ORB	VD0173	Weathered granite	20	1136	17.0?	7.2	-	-	275.7	277.7	62.1	7.1	0.24	162.4	27.6	101.0	1.4	14.1
Granite or granite and Neo.	ORB	VD0177	Granite	80	612	16.5	7.0	351.0	0.11	214.7	37.9	44.2	67	0.18	66.9	12.8	60.2	0.0	11.4
Granite or granite and Neo.	ORB	VO0100	Quaternary+granite	80	783	16.9	7.1	464.9	3.83	317.2	29.6	42.0	156	0.26	126.8	25.0	44.4	1.5	11.8
S. Neogene with low nitrate	ORB	CM0272	Neogene	90	682	18	6.8	-	-	322.1	62.2	24.3	32.6	0.28	94.0	15.6	54.9	0.0	19.1
S. Neogene with low nitrate	ORB	RS0191	Neogene	90	765	18.6	6.9	423.6	6.05	370.9	67.0	13.1	20.5	0.32	99.8	20.2	55.3	1.9	26.2
S. Neogene with low nitrate	ORB	RS0270	Neogene	100	803	16.9	6.9	-	-	361.1	75.3	37.8	37.3	0.89	109.7	18.4	73.3	1.2	23.9
S. Neogene with low nitrate	ORB	VD0176	Neogene+volcanic	69	710	17.9	7.4	348.9	0.06	256.2	71.0	17.9	< 0,5	0.70	67.7	23.9	70.4	1.8	21.5
S. Neogene with high nitrate	ORB	BR0110	Quaternary+Neogene	70	894	17.0	6.9	-	-	319.6	94.8	30.9	87	0.65	118.0	28.7	58.6	1.4	15.1
S. Neogene with high nitrate	ORB	CL0259	Neogene	75	891	17.2	6.9	-	-	244.0	85.7	54.8	104	0.40	130.0	24.4	57.5	0.0	15.2
S. Neogene with high nitrate	ORB	CM0272B	Neogene	40	1004	16.9	6.9	344.1	5.05	380.6	131.8	49.3	78	0.19	154.2	24.9	66.3	0.0	15.6
S. Neogene with high nitrate	ORB	CS0271	Neogene	80	1049	16.3	6.8	337.1	5.15	334.3	134.6	94.5	114	0.22	163.1	28.2	74.8	0.0	9.9
S. Neogene with high nitrate	ORB	CS0284	Neogene	70	856	16.2	6.6	326.8	3.95	178.6	110.7	115.7	88	0.46	122.3	23.7	55.5	3.2	14.8
S. Neogene with high nitrate	ORB	LL0115	Neogene	80	763	17.2	7.0	371.3	7.01	319.6	53.6	41.4	67	0.15	125.1	14.9	46.7	0.0	14.1
S. Neogene with high nitrate	ORB	RS0263	Neogene	50	887	16.5	6.8	325.5	0.92	329.4	79.5	89.4	70	0.20	151.9	18.4	54.4	1.1	12.5
S. Neogene with high nitrate	ORB	RS0266	Neogene	120	1171	-	6.9	-	-	368.4	143.0	135.4	138	0.20	221.2	31.1	62.8	0.0	16.8
S. Neogene with high nitrate	ORB	RS0268	Neogene	65	1045	16	6.8	-	-	341.6	129.3	91.1	97	0.22	183.5	24.7	59.4	2.7	17.0
S. Neogene with high nitrate	ORB	RS0271	Neogene	65	948	15.9	6.9	-	-	327.0	91.6	96.0	95	0.15	156.6	27.2	52.3	0.0	17.6
S. Neogene with high nitrate	ORB	SA0167	Neogene	80	895	-	6.9	-	-	329.4	98.9	62.5	115	0.14	154.9	22.7	51.1	1.1	18.3
S. Neogene with high nitrate	ORB	VO0105	Neogene	150	916	16.5	6.8	396.1	6.18	366.0	77.1	48.5	94	0.23	147.7	26.5	56.5	0.0	17.6
Surface wells	ORB	BR0077	Quaternary	11.3	999	16.4?	6.8	-	-	373.3	66.0	90.0	100	0.21	128.9	28.1	53.6	39	9.4

Group	Basin	Sample	Geology	Depth (m)	Cond. µS/cm	T ºC	pH	Eh mV	O_2 mg/L	Alk. as mg/l HCO3	Cl mg/l	SO4 mg/l	NO3 mg/l	F mg/l	Ca mg/l	Mg mg/l	Na mg/l	K mg/l	Si mg/l
Surface wells	ORB	CM0147	Neogene	7	1011	14.7	6.8	352.0	3.55	336.7	78.6	111.2	128	0.22	151.8	24.6	50.0	35	12.1
Surface wells	ORB	CM0285	Neogene	14.7	835	15.4	7.8	440.9	6.58	402.6	43.0	66.8	88	0.41	133.7	25.8	52.0	2.8	16.6
Surface wells	ORB	CM0401	Neogene	14.6	1124	14.8	6.8	348.3	6.04	248.9	147.5	130.3	170	0.15	132.3	12.8	122.5	31	15.1
Surface wells	ORB	CS0400	Neogene	12	1078	15.3	6.9	341.4	3.22	339.2	104.0	96.8	139	0.15	170.8	21.7	86.5	1.5	14.6
Surface wells	ORB	LL0116	Neogene	11.8	1148	15	7.4	-	6.77	424.6	93.9	110.4	201	0.17	206.5	23.0	75.4	1.0	13.5
Surface wells	ORB	MS0115	Quaternary+volcanic	21.9	735	16.7	6.8	324.4	2.41	312.3	55.9	55.1	47	0.24	106.9	30.0	30.2	0.0	27.9
Surface wells	ORB	RS0253	Neogene	17.1	864	17.0	6.9	482.7	8.11	278.2	21.0	70.1	217	0.16	160.8	21.6	27.2	0.0	15.4
Surface wells	ORB	SI0180	Weathered Granite	12	612	15	7.2	329.2	2.64	261.1	18.6	51.9	18.4	0.38	91.5	7.1	42.0	3.3	13.5
Surface wells	ORB	VD0171	Quaternary	80	909	16.4	7.1	377.9	4.71	385.5	67.5	64.0	60	0.42	125.4	21.7	84.8	0.0	17.8
Surface wells	ORB	VO0280	Neogene	8	805	17.0	7.0	357.7	6.82	366.0	98.4	9.3	14.7	0.51	111.5	22.6	58.0	1.4	21.4
River water	WSCB	SCRA	River	0	358	19.2	8.1	-	-	164.5	13.3	18.7	7.7	0.35	47.4	9.2	19.8	1.1	11.6
River water	WSCB	SCRB	River	0	524	22.3	8.8	-	-	183.0	45.5	36.8	10.7	0.55	51.3	9.3	55.4	3.1	11.1
Surface wells	WSCB	SC0073	Quaternary	9.5	502	15.6	6.6	-	-	175.7	31.2	60.9	8.5	0.22	61.3	12.8	33.2	1.1	8.1
Surface wells	WSCB	SC0151	Neogene	20	466	-	6.9	-	-	234.2	22.1	9.5	20.1	0.47	59.8	12.3	33.1	0.0	19.5
Spring	WSCB	Termes O.	Graite	-	-	-	-	-	-	228.1	66.7	11.9	0.5	8.50	7	0.2	128.0	3.5	-
Spring	WSCB	SCFP	Granite	-	1471	17.1	6.4	-	-	1207.8	66.2	5.8	< 0,5	3.42	161.4	17.4	273.9	4.2	26.4
Spring	WSCB	SCFSS	Granite	-	131	17	6.1	-	-	51.2	9.1	2.9	< 0,5	0.79	8.9	1.3	16.9	0.0	26.9
Deep wells	WSCB	RD0201	Neogene	75	1093	18.2	6.8	270.7	0.74	675.9	70.2	16.3	< 0,5	3.23	51.7	16.5	221.9	3.7	32.1
Deep wells	WSCB	RD0202	Neogene	65	839	17.2	7.2	-	-	550.2	50.3	12.1	4.3	1.00	48.0	11.3	138.4	2.5	30.3
Deep wells	WSCB	SC0113	Neogene	73	440	16	7.1	496.7	5.00	226.9	27.6	5.1	5.7	0.34	51.3	9.3	38.8	0.0	20.2
Deep wells	WSCB	SC0117	Neogene	65	533	17.4	6.7	391.4	3.72	214.7	33.8	28.7	35.5	2.63	69.3	9.4	45.4	0.0	16.2
Deep wells	WSCB	SC0150	Neogene	80	447	16.9	6.9	-	-	212.3	24.0	7.1	16.3	0.54	52.3	10.2	35.7	0.0	20.9
Volcanic or with vol. materials	ORB	BE0077	Volcanic+Neogene	80	588	17.9	7.2	409.1	1.31	307.4	29.3	18.3	11.3	0.33	71.6	25.7	30.6	3.8	12.0
Volcanic or with vol. materials	ORB	CM0151	Volcanic	75	764	18.7	7.2	-	-	390.4	31.9	46.9	68	1.15	127.4	20.2	42.7	3.3	18.4
Volcanic or with vol. materials	ORB	MS0060	Volcanic	60	693	18.3	7.0	263.8	1.12	412.4	34.1	34.6	0.7	0.21	75.8	40.4	44.8	6.6	30.5
Northern area	-	SG0123	Neogene	75	530	-	7.3	-	-	336.7	9.9	3.2	6.1	0.19	89.3	15.9	20.6	2.0	9.6
Northern area	-	SG0134	Neogene	80	597	15.9	7.4	363.5	7.15	334.3	17.6	18.5	37.2	0.29	91.1	24.6	17.4	7.5	19.0
Northern area	-	SG0138	Neogene	67	750	-	6.8	-	-	536.8	16.6	20.4	15.5	0.23	175.6	19.1	11.8	0.0	8.4
Northern area	-	SMLL001	Paleogene	0	521	15.9	7.1	-	-	419.7	10.6	17.9	0.5	-	137.8	14.6	6.6	0.0	4.5

Table 4.2. Sample group, basin (western Santa Coloma basin or Onyar River basin), Saturation index, environmental water isotopes, tritium, sulphate isotopes, Total Organic Carbon, trace elements and Cl/Br mass ratio.

Group	Basin	Sample	Geology	SI Calcite	SI Quartz	SI Fluoride	δD_{vsmow} (‰)	$\delta^{18}O_{vsmow}$ (‰)	Tritium (U.T)	$\delta^{34}S\text{-}SO_4$ (‰)	$\delta^{18}O\text{-}SO_4$ (‰)	TOC mg/l	Br mg/l	Cl/Br ratio	Li mg/l	B mg/ l
Regional faults or granite	ORB	CS0105	Neogene+granite	-0.13	0.29	0.51	-37.3	-5.33	3.3	6.8	6.3	0.065	0.364	201	0.201	0.070
Regional faults or granite	ORB	CS0203	Neogene +granite	-0.39	0.46	-0.31	-37.0	-5.45	1.6	-	-	0.247	0.302	234	0.234	0.082
Regional faults or granite	ORB	FS0066	Neogene+granite	0.22	0.25	0.75	-39.9	-6.12	1.6	28.7	14.4	3.539	1.203	184	0.184	1.25
Regional faults or granite	ORB	LG0190	Granite	0.23	0.43	0.01	-34.0	-5.51	1.5	-	-	0.565	0.897	219	0.219	< 0.05
Regional faults or granite	ORB	LG0246	Granite	-0.02	0.36	0.07	-35.2	-5.71	-	5.6	7.2	2.75	0.486	212	0.212	0.061
Regional faults or granite	ORB	SG0200	Spring not determined	0.54	0.64	-2.51	-41.0	-6.58	1.9	22.0	5.2	48.184	3.454	189	0.189	1.94
Granite or granite and Neo.	ORB	AG0113	Neogene+granite	0.04	0.58	-1.17	-35.5	-5.37	-	14.4	7.1	0	0.116	170	0.170	< 0.05
Granite or granite and Neo.	ORB	BR0092	Quaternari+granite	-1.61	0.71	-2.66	-38.6	-5.97	2.4	10.0	7.6	0.584	0.099	301	0.301	< 0.05
Granite or granite and Neo.	ORB	BR0106	Granite	0.18	0.32	-1.30	-35.4	-5.26	1.3	-	-	0	0.66	206	0.206	< 0.05
Granite or granite and Neo.	ORB	CM0049	Granite	-0.03	0.48	-1.42	-30.0	-3.83	2.7	-	-	3.144	0.364	203	0.203	< 0.05
Granite or granite and Neo.	ORB	CS0183	Granite	-0.22	0.47	-0.59	-34.7	-5.13	3.8	5.7	4.8	0.444	0.543	245	0.245	< 0.05
Granite or granite and Neo.	ORB	CS0304	Neogene+granite	0.01	0.50	0.19	-33.0	-4.93	3.5	7.2	5.8	2.992	0.436	265	0.265	< 0.05
Granite or granite and Neo.	ORB	LG0029	Weath. granit+granite	0.62	0.51	-1.34	-32.7	-4.94	0.7	-	-	0	0.433	265	0.265	0.057
Granite or granite and Neo.	ORB	SI0052	Weath. granite	-0.05	0.65	-1.28	-34.4	-5.14	2.7	7.5	5.4	1.897	0.765	279	0.279	0.061
Granite or granite and Neo.	ORB	VD0172	Weath. granit+granite	0.30	0.52	-1.60	-35.4	-5.47	0.1	-	-	1.809	0.947	194	0.194	< 0.05
Granite or granite and Neo.	ORB	VD0173	Weathered granite	0.25	0.43	-1.95	-30.8	-4.24	1.9	-	-	3.162	1.333	208	0.208	< 0.05
Granite or granite and Neo.	ORB	VD0177	Granite	-0.42	0.39	-2.46	-32.1	-4.58	3.3	3.8	7.1	0.996	0.108	351	0.351	< 0.05
Granite or granite and Neo.	ORB	VO0100	Quaternary+granite	0.00	0.40	-1.94	-40.8	-5.57	4.7	5.2	5.5	0	0.141	210	0.210	< 0.05
S. Neogene with low nitrate	ORB	CM0272	Neogene	-0.36	0.59	-1.93	-35.7	-4.93	3.5	-	-	1.2	0.204	305	0.305	< 0.05
S. Neogene with low nitrate	ORB	RS0191	Neogene	-0.16	0.72	-1.81	-33.4	-5.69	0.5	11.2	6.7	0.421	0.399	168	0.168	< 0.05
S. Neogene with low nitrate	ORB	RS0270	Neogene	-0.11	0.70	-0.88	-39.0	-5.96	1.5	-	-	0.789	0.332	227	0.227	0.080
S. Neogene with low nitrate	ORB	VD0176	Neogene+volcanic	0.02	0.64	-1.27	-34.6	-5.26	1	-	-	0.911	0.281	253	0.253	0.052
S. Neogene with high nitrate	ORB	BR0110	Quaternary+Neogene	-0.15	0.50	-1.16	-33.9	-4.93	0.9	9.0	6.1	3.446	0.59	161	0.161	< 0.05
S. Neogene with high nitrate	ORB	CL0259	Neogene	-0.24	0.50	-1.53	-35.2	-5.22	-	7.2	5.0	2.248	0.256	335	0.335	< 0.05
S. Neogene with high nitrate	ORB	CM0272B	Neogene	-0.05	0.52	-2.15	-35.6	-4.96	4.6	7.3	6.8	1.571	0.532	248	0.248	< 0.05
S. Neogene with high nitrate	ORB	CS0271	Neogene	-0.21	0.33	-1.98	-33.7	-4.87	4.2	9.0	7.3	4.569	0.24	561	0.561	< 0.05
S. Neogene with high nitrate	ORB	CS0284	Neogene	-0.79	0.51	-1.43	-35.0	-5.40	-	2.2	3.2	1.298	0.29	382	0.382	< 0.05
S. Neogene with high nitrate	ORB	LL0115	Neogene	-0.08	0.47	-2.35	-34.5	-5.16	5.2	7.6	4.2	0.572	0.27	199	0.199	< 0.05
S. Neogene with high nitrate	ORB	RS0263	Neogene	-0.19	0.43	-2.06	-36.3	-5.45	-	5.9	8.9	0.58	0.246	323	0.323	< 0.05
S. Neogene with high nitrate	ORB	RS0266	Neogene	0.10	0.50	-2.06	-33.6	-5.22	5.5	-	-	1.962	0.3	477	0.477	< 0.05
S. Neogene with high nitrate	ORB	RS0268	Neogene	-0.12	0.57	-1.92	-33.3	-5.28	3.6	-	-	2.474	0.241	537	0.537	< 0.05
S. Neogene with high nitrate	ORB	RS0271	Neogene	-0.10	0.59	-2.30	-33.9	-5.42	-	-	-	1.134	0.193	475	0.475	< 0.05
S. Neogene with high nitrate	ORB	SA0167	Neogene	-0.04	0.54	-2.42	-31.6	-4.69	-	-	-	6.628	0.229	432	0.432	< 0.05
S. Neogene with high nitrate	ORB	VO0105	Neogene	-0.15	0.58	-1.96	-34.1	-4.95	4.2	7.1	6.7	2.709	0.235	328	0.328	< 0.05
Surface wells	ORB	BR0077	Quaternary	-0.12	0.25	-2.16	-36.4	-5.66	3	-	-	1.098	0.264	250	0.250	0.130

Group	Basin	Sample	Geology	SI Calcite	SI Quartz	SI Fluoride	δD_{vsmow} (‰)	$\delta^{18}O_{vsmow}$ (‰)	Tritium (U.T)	$\delta^{34}S\text{-}SO_4$ (‰)	$\delta^{18}O\text{-}SO_4$ (‰)	TOC mg/l	Br mg/l	Cl/B ratio	Li mg/l	B mg/ l
Surface wells	ORB	CM0147	Neogene	-0.23	0.44	-1.98	-34.3	-5.09	-	6.9	6.7	6.793	0.268	293	0.293	< 0.05
Surface wells	ORB	CM0285	Neogene	0.88	0.57	-1.51	-33.2	-4.62	-	7.2	4.8	0	0.165	261	0.261	< 0.05
Surface wells	ORB	CM0401	Neogene	-0.39	0.54	-2.37	-36.3	-5.22	3.5	7.4	5.6	4.6	0.505	292	0.292	0.121
Surface wells	ORB	CS0400	Neogene	-0.10	0.52	-2.29	-32.5	-5.31	3	7.1	4.7	0.951	0.226	460	0.460	< 0.05
Surface wells	ORB	LL0116	Neogene	0.60	0.49	-2.14	-32.8	-5.00	5.6	8.1	4.8	1.44	0.324	290	0.290	0.051
Surface wells	ORB	MS0115	Quaternary+volcanic	-0.28	0.77	-2.03	-31.0	-4.87	-	7.2	8.8	1.023	0.371	151	0.151	< 0.05
Surface wells	ORB	RS0253	Neogene	-0.14	0.51	-2.28	-32.3	-4.77	-	5.1	6.7	1.921	0.165	127	0.127	< 0.05
Surface wells	ORB	SI0180	Weathered Granite	-0.11	0.49	-1.61	-35.2	-5.46	-	7.3	6.5	9.245	0.155	120	0.120	< 0.05
Surface wells	ORB	VD0171	Quaternary	0.12	0.58	-1.51	-31.9	-4.47	-	6.4	7.6	2.184	0.337	200	0.200	< 0.05
Surface wells	ORB	VO0280	Neogene	0.01	0.65	-1.36	-35.6	-5.32	-	12.2	5.8	0.985	0.293	336	0.336	0.055
River water	WSCB	SCRA	River	0.43	0.35	-1.97	-36.5	-5.89	-	-	-	1.131	0.043	310	0.310	< 0.05
River water	WSCB	SCRB	River	1.17	0.25	-1.64	-35.3	-5.43	-	-	-	1.079	0.291	156	0.156	0.094
Surface wells	WSCB	SC0073	Quaternary	-0.98	0.25	-2.24	-38.2	-5.75	4.2	-	-	1.285	0.1	312	0.312	< 0.05
Surface wells	WSCB	SC0151	Neogene	-0.45	0.57	-1.65	-35.5	-5.49	-	-	-	0.149	0.071	312	0.312	< 0.05
Spring	WSCB	Temres O.	Granite	-1.28	-	-0.04	-	-	-	-	-	-	1	66	-	-
Springs	WSCB	SCFP	Granite	-0.03	0.75	0.34	-40.6	-6.50	0.6	-	-	0	0.539	123	0.123	< 0.05
Springs	WSCB	SCFSS	Granite	-2.71	0.75	-1.83	-38.5	-5.87	4.6	-	-	0	0.063	144	0.144	< 0.05
Deep wells	WSCB	RD0201	Neogene	-0.30	0.81	-0.12	-37.7	-6.30	1.2	-	-	0	0.499	141	0.141	0.089
Deep wells	WSCB	RD0202	Neogene	-0.05	0.80	-1.12	-33.4	-5.70	1.1	-	-	1.507	0.296	170	0.170	0.074
Deep wells	WSCB	SC0113	Neogene	-0.40	0.64	-1.93	-38.0	-5.77	0.7	-	-	0.786	0.127	217	0.217	< 0.05
Deep wells	WSCB	SC0117	Neogene	-0.71	0.53	-0.08	-33.9	-5.24	4.1	10.1	7.5	1.543	0.146	231	0.231	< 0.05
Deep wells	WSCB	SC0150	Neogene	-0.59	0.65	-1.54	-35.9	-5.53	1.8	-	-	0.202	0.111	217	0.217	< 0.05
Volcanic or with vol. materials	ORB	BE0077	Volcanic+Neogene	-0.09	0.39	-1.91	-35.6	-5.37	-	7.6	9.5	1.088	0.101	290	0.290	< 0.05
Volcanic or with vol. materials	ORB	CM0151	Volcanic	0.21	0.56	-0.64	-32.0	-4.49	-	-	-	0.529	0.109	292	0.292	< 0.05
Volcanic or with vol. materials	ORB	MS0060	Volcanic	-0.16	0.79	-2.31	-30.5	-4.89	-	-	-	0.479	0.158	216	0.216	< 0.05
Northern area	-	SG0123	Neogene	0.24	0.26	-2.32	-34.5	-5.15	-	-	-	0.15	0.087	114	0.114	< 0.05
Northern area	-	SG0134	Neogene	0.21	0.62	-1.89	-33.5	-5.04	-	5.6	8.3	0	0.074	238	0.238	< 0.05
Northern area	-	SG0138	Neogene	0.20	0.20	-1.91	-35.0	-5.60	-	-	-	0.657	0.077	215	0.215	< 0.05
Northern area	-	SMLL001	Paleogene?	0.22	-0.01	-	-37.5	-5.62	-	-	-	-	0.059	180	0.180	< 0.05

systems in the Onyar basin tend to have higher concentrations of Cl and Na and the Na/Cl ratio is lower than in the Santa Coloma basin.

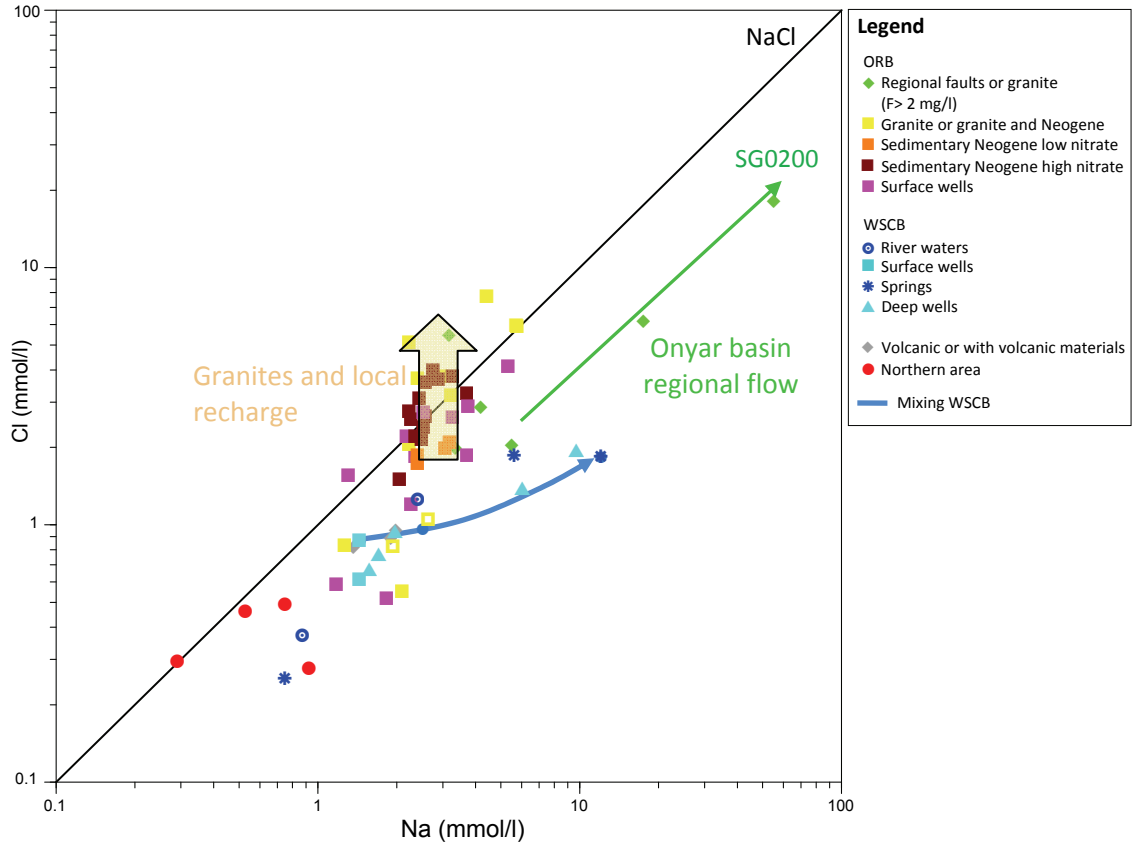

Figure 4.3. Cl-Na relation. The WSCB mixing line shows the concentrations of the mixing between the sample SC0073 (surface well) and the sample SCFP (higher salinity spring) in the western Santa Coloma basin.

These differences between regional flow paths are also observed in the Ca-Na relation (Figure 4.4). While in the Santa Coloma basin the Ca content remains approximately constant with the increase of Na in some samples, in the Onyar basin the Ca content tends to decrease as Na increases. Only the SG0200 sample does not behave in this manner. Furthermore, some samples in the WSCB the Ca content increase as Na does, if compared with the less saline samples from the same basin. No relation was found between Ca content and the Saturation Index of calcite, indicating that calcite dissolution does not determine Ca content. However, the processes that may be determining the hydrochemistry of these waters could be the weathering of silicates such as the plagioclases, as shown in the deep wells and springs of the WSCB (Figure 4.5). These tend to present the highest concentrations of silica, and have the most saline waters saturated in quartz.

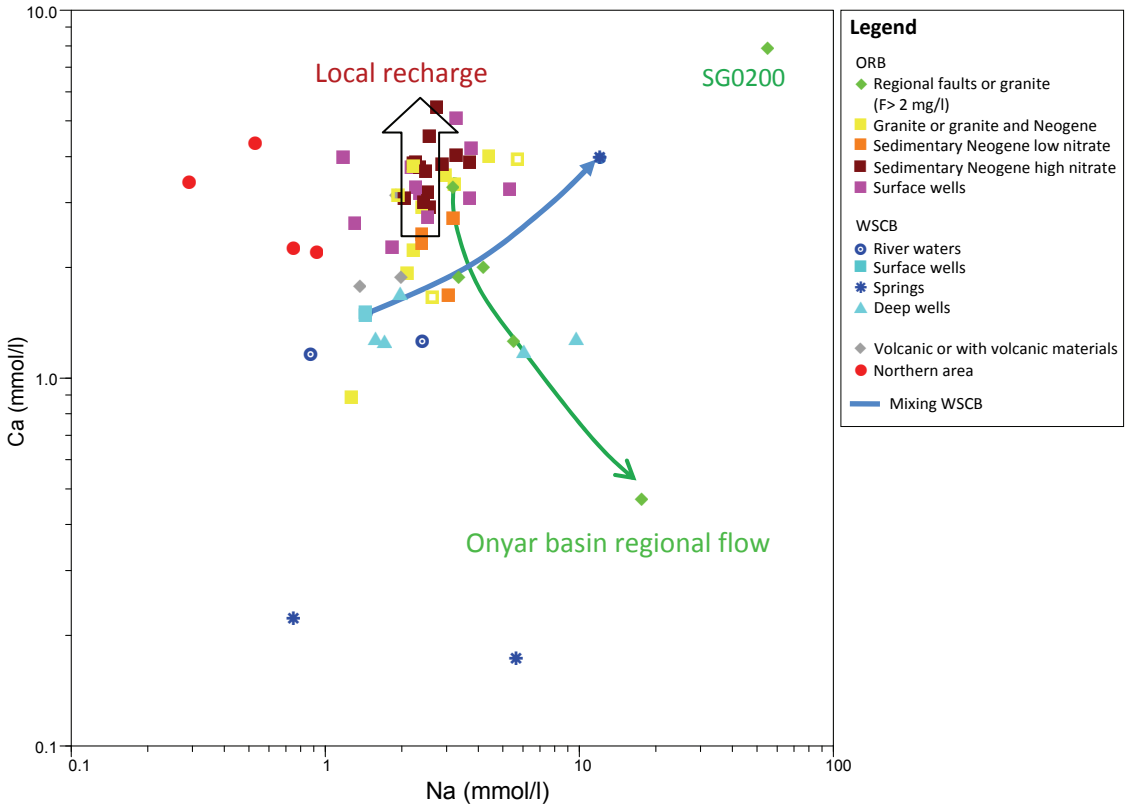

Figure 4.4. Ca-Na relation. **The** WSCB mixing line shows the concentrations of the mixing between the sample SC0073 (surface well) and the sample SCFP (higher salinity spring) in the western Santa Coloma basin.

The samples related to regional flows in the ORB tend to present a decrease in Ca concentration when Na increases, except for the sample SG0200 (Figure 4.4). In addition, there is no relation between quartz saturation and Na or even a tendency for Na to decrease as SI increases (Figure 4.5). Furthermore, with the exception of SG0200, the samples from this basin tend to be undersaturated indicating the existence of other processes controlling the groundwater hydrochemistry, such as the Na-Ca exchange and the influence of F rich waters (Piqué 2008).

In the WSCB, a low saturation index of fluorite Ca concentration remains constant (Figure 4.6a). The amount of Ca tends to increase at higher SI values. On the other hand, in samples related with regional flow in the ORB, Ca tends to decrease as fluoride increases, leading to higher saturation indexes of fluorite. However, in both basins the amount of Na tend to increases with fluoride, except in sample SG0200 (Figure 4.6b). Along the flow path, there is therefore an influence of F rich waters (Pique et al. 2008) apart from alteration of silicates. Furthermore, in the Onyar basin there is an Na-Ca exchange, leading to higher Na and lower Ca

concentrations. The sample SG0200, from close to the Onyar basin, presents the same reactions along the flow path but with no mixing with F rich water, since this spring is not in the Selva basin.

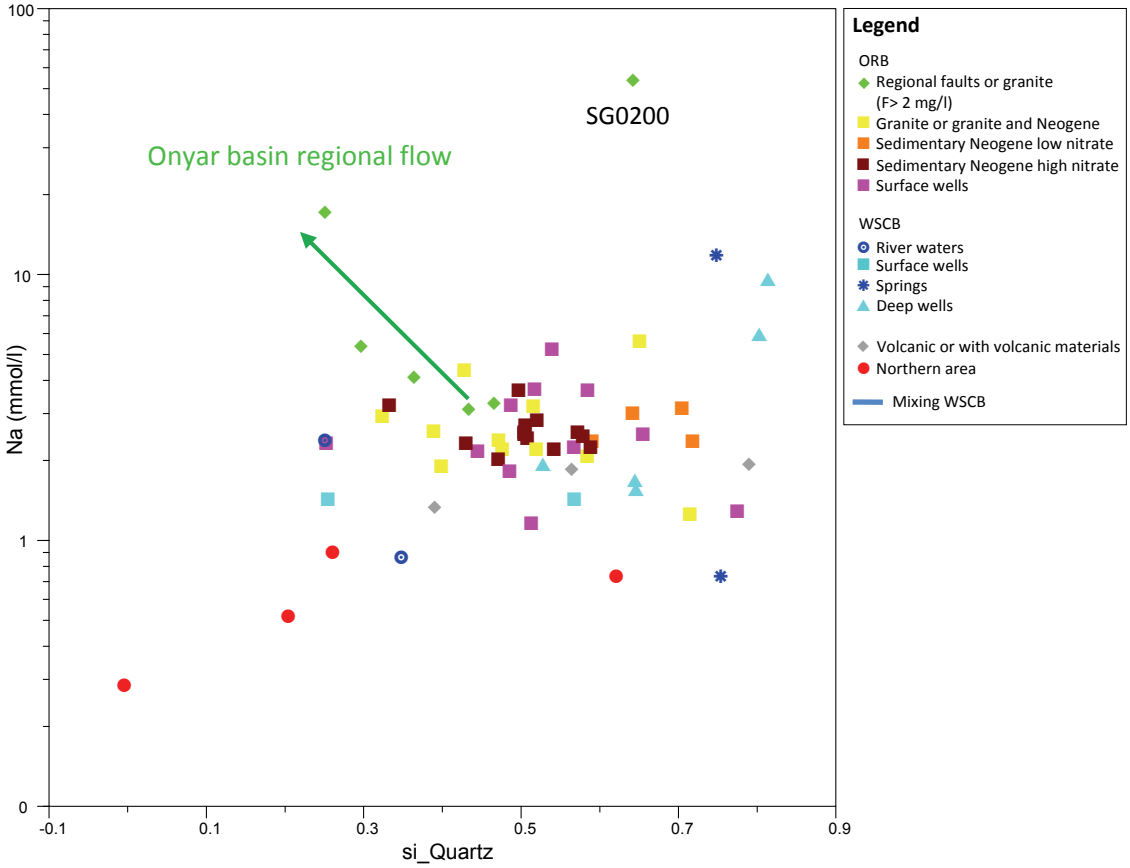

Figure 4.5. Na vs Si Quarz

Samples from local flow systems mainly show Ca-HCO_3 facies, as well as high nitrate, sulphate and Ca concentrations (Figure 4.4). The source of Ca in these samples is attributed to pollution and/or reactions in the soil and non-saturated zones related with carbonates or secondary calcite, since these samples with much less transit time are also saturated in calcite (Table 1). Non-polluted samples show the same range of Na content with a higher quartz SI (Figure 4.5) than the polluted samples, indicating that the silicate weathering cannot be the source of the higher Ca concentrations.

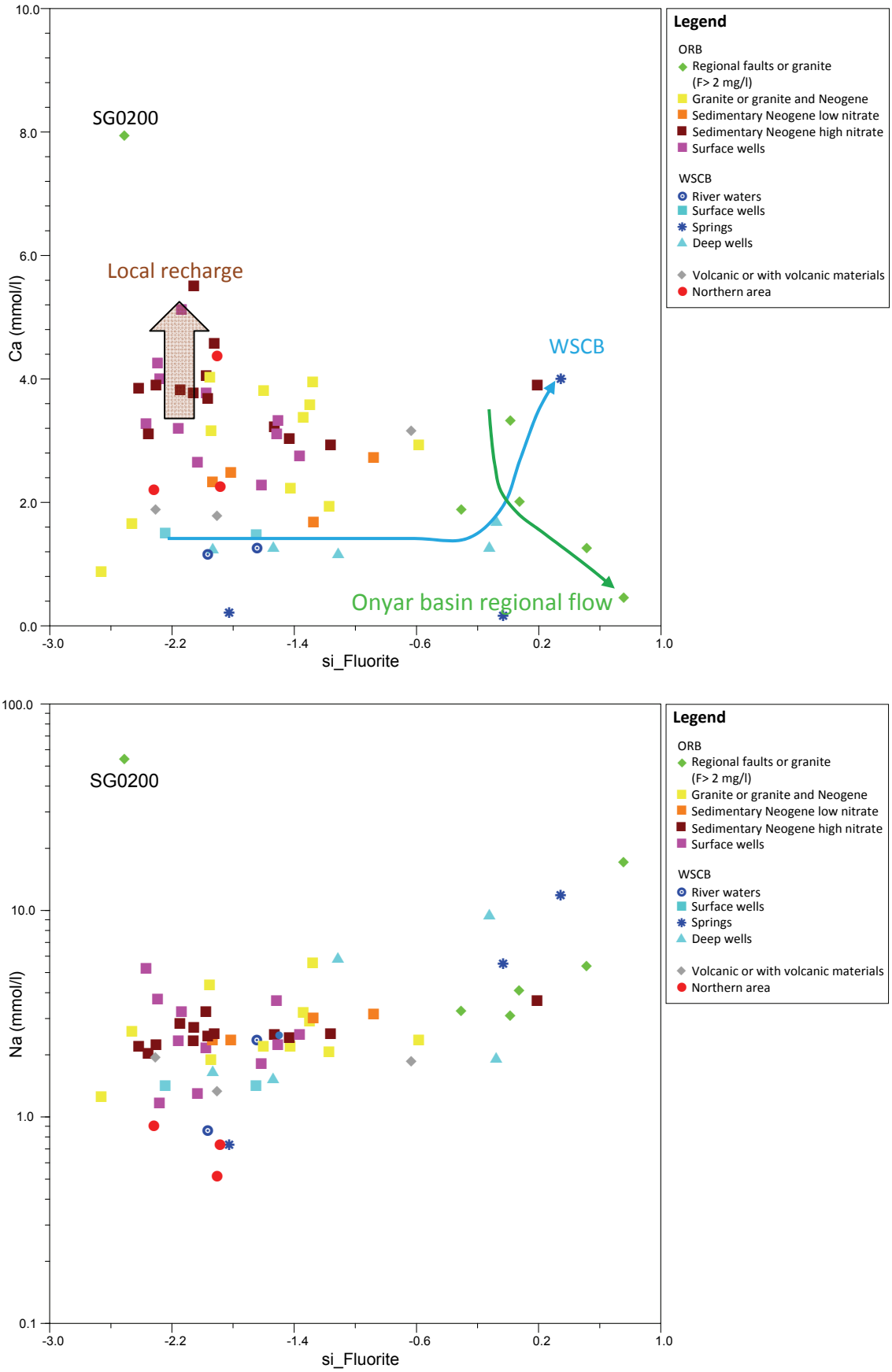

Figure 4.6 a) Ca vs SI of Fluorite b) Na vs SI of fluorite.

The other groups of samples are from wells in granites with low fluoride concentrations and wells in neogene sediments with low nitrate concentrationss, showing Ca-HCO_3 and/or Ca-Na-HCO_3 facies. Samples in granites in general have lower concentrations of Si than the deep neogene wells. However, samples in granites tend to have higher concentrations of F and in some cases more Ca and/or Na content than non-polluted sedimentary wells. High calcium is indicative of more local flows, as explained above, while high Na is indicative of a shorter transit time but the same geochemical processes as occur in regional flow systems. These groups of samples therefore represent intermediate flow systems characterized by higher water rock interaction than in local flow systems and/or a mixing between local and regional flows. This mixing process is also observed from Cl, Na and Ca contents in deep neogene wells in the WSCB (Figure 4.3 and 4.4).

Different flow paths modify groundwater hydrochemistry and also groundwater temperature (Figure 4.7). Warmer waters are mainly located close to regional faults and/or in places where the thickness of the neogene sediments is greatest, indicating a longer transit time. Deep wells with a relatively lower temperature similar to surface wells (Table 1) can be interpreted as a local flow at depth due to pumping or faster intermediate flow systems in the areas close to the edge of the basin.

In the NW of the basin, the neogene sediment thickness is relatively low and there is a waterdivide between both basins (Figure 4.1). Most deep wells in this area show similar temperatures, indicating that the recharge of this side of the basin could be by means of the same flow system coming from the surrounding area.

In the Selva basin, there are therefore different flow systems represented by different hydrochemical facies. Regional flows are represented by Na-HCO3 facies with high water-rock interaction. In the WSCB, these facies are the result of silicate weathering, while in the ORB more reactions take place, such as the Na-Ca exchange and the influence of F-rich fluids. Local flows are characterized by Ca-HCO3 facies, with pollution and water input across the basin's surface being important. The Na-Ca-HCO3 facies are the result of intermediate flow systems with less water-rock interaction and/or mixing between different flow systems. The distribution of the different facies in the Selva basin is determined by the tectonic context and the Neogene sediment thickness.

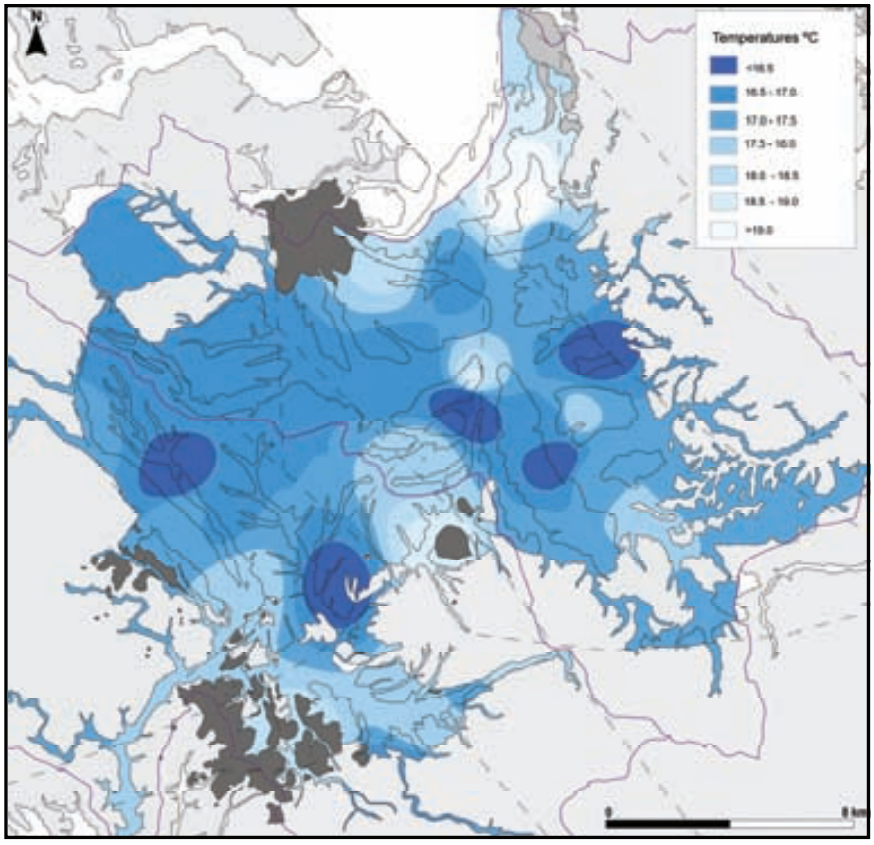

Figure 4.7. Groundwater temperatures of springs and deep wells (>30 m depth)

4.5.2. Environmental isotopes and tritium

Environmental isotopes (δD, δ^{18}O) were analyzed to define the potential recharge areas of the Selva basin.Tritium concentrations were simultaneously studied to determine the transit time characterizing each flow system. Deuterium and Oxigen-18 data was interpreted using two meteoric water lines: one in the Monteny-Guilleries range (Neat et al. 1992) located in the west of the study area representing the range areas surrounding the basin (LMWL-M, δD = 7.9 δ^{18}O + 9.8) and a second using isotopic data from the IAEA-GNIP database (IAEA/WMO 2006) for the *Girona airport* station in the central part of the Selva basin (LMWL-S, δD = 8.13 δ^{18}O + 6.95). Both meteoric lines have similar slopes and diverge at the deuterium enrichment, which can be explained by differences in precipitation regimes and processes in each area studied (chapter 3).

The results obtained from the field campaign in this range and basin area show various isotopic signatures for the different flow systems (Figure 4.8). Regional flow systems show low isotopic content near LMWL-M, indicating recharge of the surrounding basin from higher altitudes. The wells and areas related with recharge of regional flow systems are located in the west and the north of the study area (Figure 4.8b). In view of the different local relations

between δD and δ^{18}O content and recharge altitudes (Carmona et al. 2000, Grup de Recerca en Geologia i Cartografia Ambiental 2009) the lightest samples have to be infiltrated at altitudes between 500-800 m a.s.l. Because of the geological and tectonic context and the location, the recharge on the west side is attributed to the Guilleries range while the recharge in the north comes at least partially from the transversal range.

Local recharge is well represented by the isotopic signature of the surface wells (Table 1). However, some wells in deep neogene have a similar signature to surface wells indicating local recharge. There are some areas where this signature is well defined in the NE, E and central part of the Selva basin (Figure 4.8 b). A part of the local recharge is an evaporated signature (Figure 4.8 a) in the wells located in the SE of the basin (Figure 4.8 b). This location has some of the highest temperatures in the basin (Figure 4.7) with a significant non-saturated zone thickness.

Wells with an intermediate isotopic signal are located in the west, the north and the south-east of the Selva basin (Figure 4.8 b). The samples in the western part are mainly aligned along a supposed line between the two local meteoric lines described (Figure 4.8 a). Considering that this area is geographically situated between Girona airport and the Montseny Guillerires range, the recharge of this area can be attributed to the middle and lower elevations of the Guilleries range as presented previously by Folch and Mas-Pla (2008). The area to the SE, because of its range content and geological context can be explained by the recharge originating the Gavarres range (Figure 4.8 a and b). The intermediate isotopic content in the north can be attributed to a recharge from the Gavarres ranges and/or a mixing between water from the transversal range and the basin.

The other parts of the basin may be representative of water recharged in the nearby areas of the basin and a mixing between the different flow systems in different proportions.

Like the environmental isotopes, Cl and tritium are indicators of groundwater residence time. Chloride is one of the most conservative ions in groundwater, and its concentrations tends to increase along the flow paths. Tritium is present in most modern groundwaters around the world. Its appearance in groundwater depends on the concentration in the atmosphere, and was modified by nuclear weapons testing during the 1950s and 1960s. In different flow models (piston flow, mixing, etc.) tritium can be used as an indicator of residence time in the aquifer.

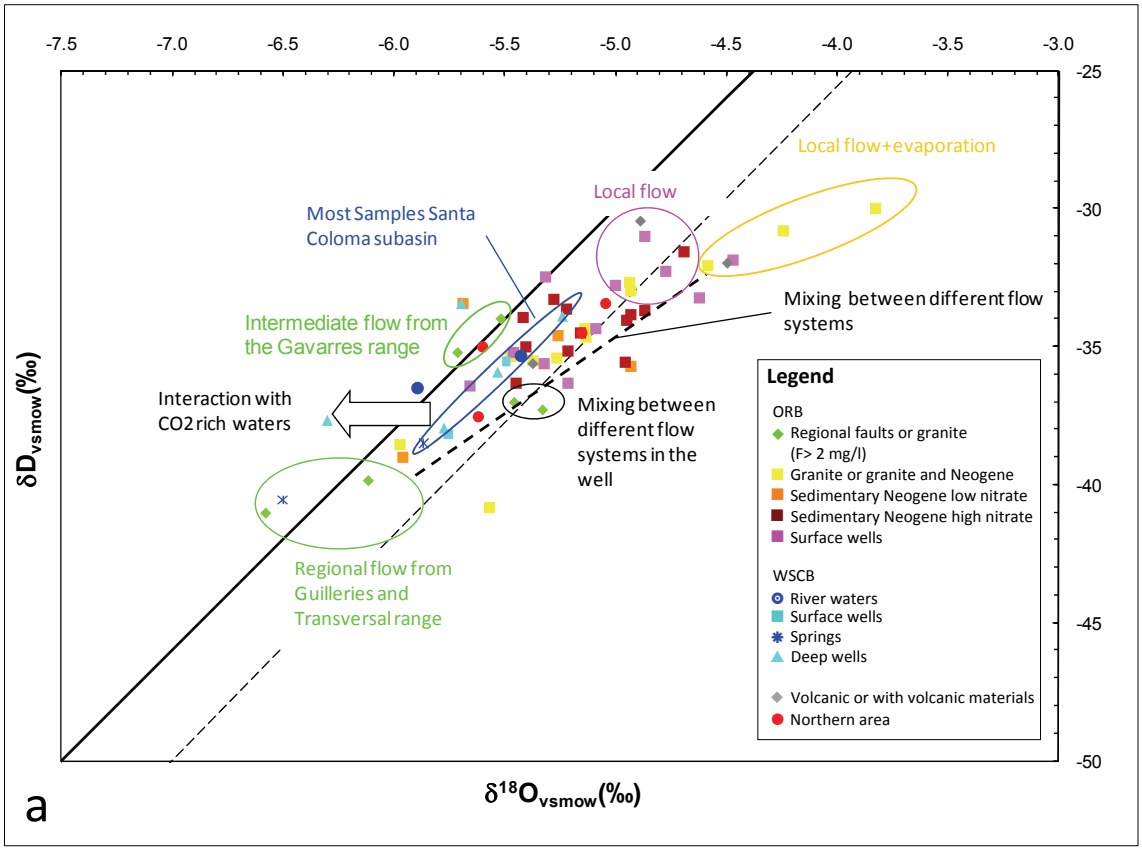

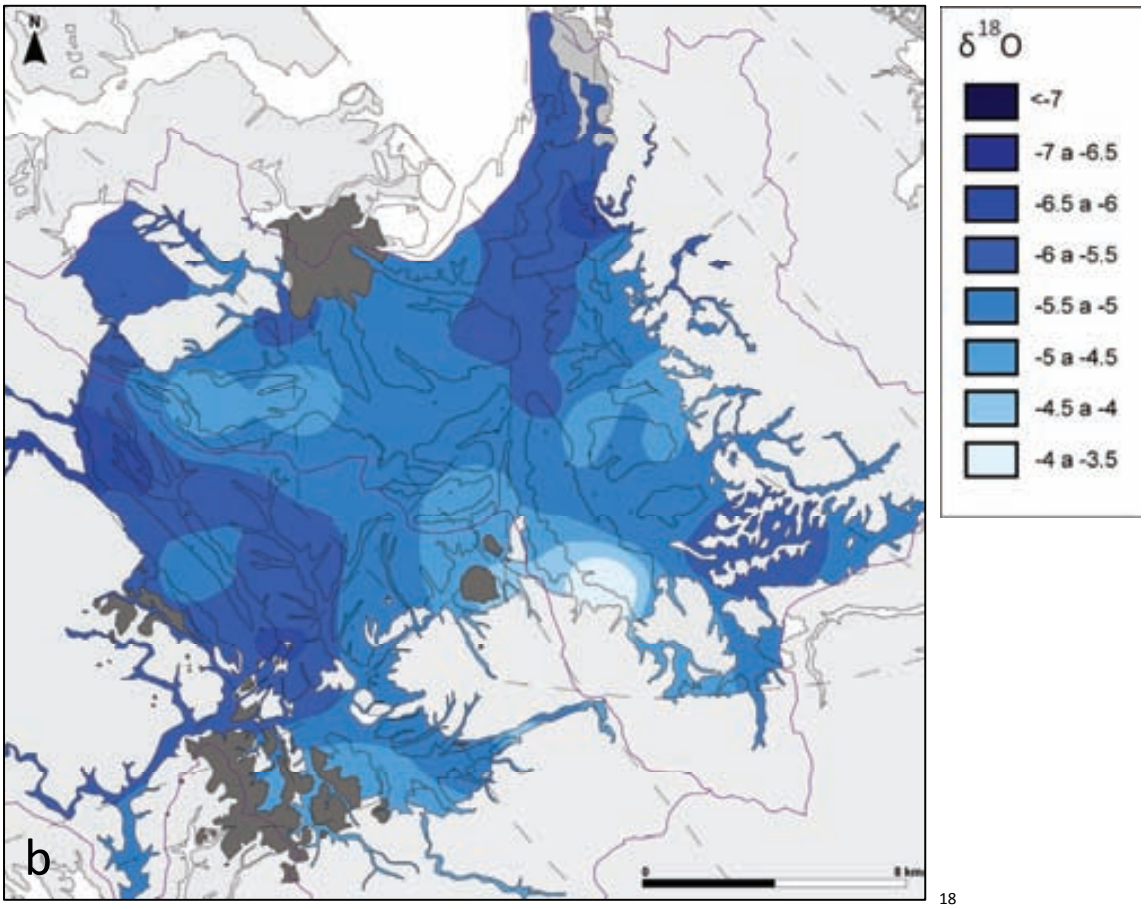

Figure 4.8 a) Environmental isotope (δD,) from the various groups of samples. b) $\delta^{18}O$ distribution in deep wells (>30 m) in the Selva basin.

Due to the complex hydrogeology in the Selva basin, these different flow models have not been applied. However, based on tritium data in precipitation since the 60s (Menció 2006) it is possible to say that groundwater with less than 3 U.T must at least partially have water that was infiltrated prior to bomb testing period.

All the samples from surface wells and deep neogene wells with high nitrate have a specific range of ^{18}O and tritium values (Figure 4.9). This shows the range of ^{18}O values in the water recharged in the Selva basin and the surrounding areas. Simultaneously, groundwater infiltrating the basin surface has a relatively low transit time in the aquifer. It is possible to see that concentrations of Cl in the neogene polluted wells is higher than in wells in neogene with low nitrate and below that of the samples representing regional flows (Figure 4.10), indicating the level of Cl input in the system because of pollution. Furthermore, samples in neogene with low nitrate in the Onyar basin have longer transit times (Figure 4.9). This shows that a large proportion of modern groundwater of the local flow regimes, recharged by runoff at the basin surface, is contaminated with nitrates. In the WSCB, most samples from the deep neogene sediments have low tritium content and isotopic values found in areas with a higher elevation than the basin. The water recharging this part of the Neogene materials is therefore infiltrating more elevated areas with a longer transit time.

Samples related to regional flow systems have lighter isotopes and tritium under 3 U.T, showing that the recharge areas of most of this groundwater are topographically more elevated, and have longer transit times. However, there are some samples that are infiltrated in the surrounding basins but this is relatively modern groundwater. There is also groundwater in the range area with preferential flow paths to the basin, such as fractures or weathering granite.

Some wells in granites, located in the basin or practically in it, show high chlorite concentrations with ^{18}O values in the basin's range or lower. This enrichment can be partially explained because evaporation processes in the vadose zone. However, there some samples non-evaporated with high Cl content (Figure 4.10). This shows that there are some waters being recharged on the basin's surface, presenting relatively high transit times with significant water-rock interaction modifying their hydrochemistry. This can also be seen in some wells in granites that pump waters with high salinities but with a very low yield.

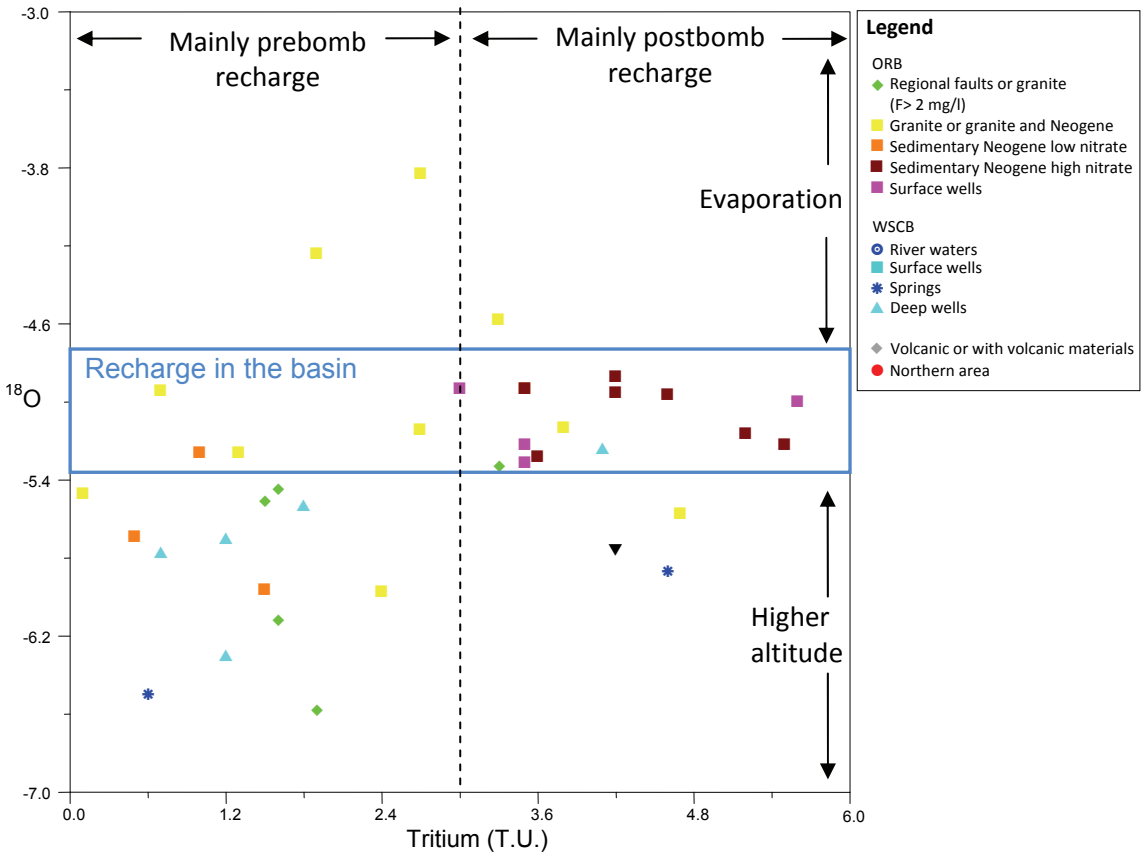

Figure 4.9 Relation between tritium and ^{18}O.

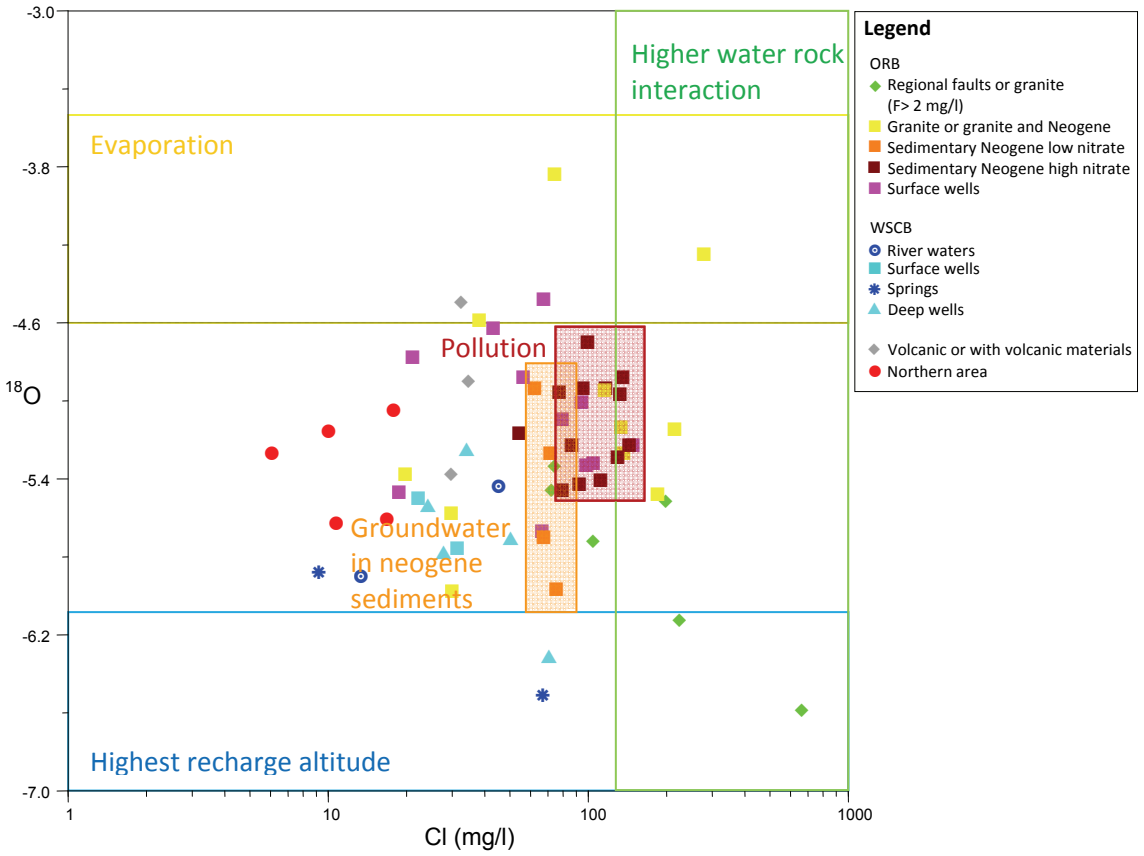

Figure 4.10. Relation between ^{18}O and Cl.

In the Selva basin different flow systems therefore coexist with various transit times and characteristics. There is the groundwater infiltrated at high altitude in the surrounding ranges with a longer transit time and high water-rock interaction. In the lower parts of the range areas there is also a flow recharging the basin at relatively high velocities.The water that currently recharges the basin surface is polluted and has a short transit time. Some parts of the basin sediments, mainly in the parts with greater thickness, were recharged by old waters infiltrated in the basin surface some time ago (before the 1960s). The last group consists of waters recharged in some of the granite outcrops on the basin's surface and its edges, and is old water with low flow velocities and relatively high water-rock interaction. Groundwater with an isotopic value between the defined groups is groundwater arising from the mixing between the different flow systems.

4.5.3. Sulphate isotopes

The dual isotope approach ($\delta^{34}S$ and $\delta^{18}O_{SO4}$) of dissolved SO_4 has been extensively used for examining SO_4 sources and pathways in the sulfur cycle in recent decades. The coupled use of S and O isotopic composition is a useful tool for improved constraint of the origin and the fate of sulfate, and to evaluate the transformations undergone by this solute (Kendall, 1998). A stable isotope study of sulfate was carried out on 33 groundwater samples in order to: (a) trace the sources of dissolved sulfate and (2) investigate possible relationships between the isotope and hydrogeochemical data in the Selva basin groundwater system.

The isotopic composition of SO_4 is controlled by: (a) the isotopic composition of the primary – and secondary – sulfate sources, (b) isotope exchange reactions, and (c) kinetic isotope effects during sulfur and oxygen transformations. Variations in the isotopic ratio of groundwater sulfate during the flow in aquifers depend on recharge, flow systems, mixing processes and chemical and microbial reactions (Krouse and Mayer, 2000).

$\delta^{34}S$ of the sampled groundwater range between +2.2 and +28.7‰, with a median value of +7.2‰ (n = 33), and $\delta^{18}O_{SO4}$ range between +3.2 and +14.4‰, with a median value of +6.7‰ (n = 33). The concentration of dissolved sulfate varies from 5 to 238 mg/l, with a median value of 49.3 mg/l (n = 39).

4.5.3.1. Natural and anthropogenic inputs of sulphate in groundwater

The dissolved sulfate in Selva basin groundwater can have various origins: a) Natural sources linked to hydrogeological conditions (oxidation of reduced S compounds, dissolution of evaporites, soil-derived sulfate, CO_2-rich thermal waters or rainwater), and b) anthropogenic non-point sources related to land use and human pressure (sulfate from livestock manure, synthetic fertilizers or sewage leaking). The contribution of rainwater sulfate is negligible, since the measured sulfate concentration in rainwater samples collected near the basin is around 0.7 mg/l (Avila et al., 2009) and the mean annual precipitation is 706 mm. The resulting sulfate flux of 0.5 g m^{-2}/year can be considered a low sulfate input in terms of mass balance.

SO_4 contribution by oxidation of either sulfides from the Paleozoic rocks or magmatic sulfides would be characterized by $\delta^{34}S$ between 0 and +5‰. The dissolution of outcropping marine evaporites in the massifs in the north of the basin (Beuda formation), with $\delta^{34}S$ between +20.2 and +21.8‰, and $\delta^{18}O_{SO4}$ between +11.1 and +14.7‰ (Utrilla et al., 1992; Carrillo and Rossell, personal communication), would lead to similar isotopic signatures of dissolved sulfate. Furthermore, there is no evidence of Tertiary gypsum layers and/or evaporite sulfates in the Selva basin. The influence of soil-derived sulfates would lead to groundwater with $\delta^{34}S$ ranging between 0‰ and 6‰, and $\delta^{18}O_{SO4}$ between 0‰ and 6‰ (Krouse and Mayer, 2000).

Agrochemical products and pig manure are considered the main anthropogenic sources of sulfate in the area studied, since they are spread as fertilizers onto fields. The isotopic composition of fertilizers covers a wide range of values, with a mean isotopic composition of $\delta^{34}S$ = +5‰ and $\delta^{18}O_{SO4}$ = +12‰ (Vitòria et al., 2004b). Moreover, fertilizers are not a negligible source, since their mean sulfur concentration ranges between 6 and 12%, similar to the concentration of primary nutrients (N, P and K) (Otero et al., 2005a). Cravotta (1997) reported sulfur isotopic values of pig manure ranging from -0.9‰ to +5.8‰, with a mean value of +3.7‰; and Otero et al. (2007) obtained values of $\delta^{34}S$ = 0‰ and 5‰ for pig manure. The oxygen isotopic composition of pig manure dissolved sulfate is not reported in the literature, and is therefore estimated based on previous studies at between +3.8‰ and +6‰ (Otero et al., 2007). Sewage, with a mean $\delta^{34}S$ = +9.6‰ and $\delta^{18}O_{SO4}$ = +10‰ (Otero et al., 2007), is another potential anthropogenic source, since the seven water treatment plants in the Selva basin (Quart d'Onyar, Riudellots de la Selva, Vilobí d'Onyar, Cassà de la Selva, Santa Coloma de Farners, Caldes de Malavella and Riudarenes) usually discharge into the rivers. The outflow

water can have a significant sulfate content (Otero et al., 2007) as the area has an important surface-groundwater interaction in the alluvial formations. The influence of seepage from the drain net or septic systems can be considered negligible in terms of non-point pollution.

4.5.3.2. The role of redox processes

Sulfates originated through sulfide oxidation must show a relationship between $\delta^{18}O_{SO4}$ and $\delta^{18}O_{H2O}$, as 60-100% of SO_4 oxygen comes from water and the rest from atmospheric oxygen (Van Stempvoort and Krouse, 1994). 30% of the samples studied fall within the experimental area of sulfates derived from sulfide oxidation as defined by Van Stempvoort and Krouse (1994) (Figure 4.11). If sulfide oxidation was a major process in the Selva basin, the $\delta^{34}S$ values of the affected samples should approximate that of the parent sulfide (from 0‰ to 5‰). Nonetheless, only two samples (CS0284 and VD0177) present $\delta^{34}S$ values below 5‰.Other sulfate sources, other processes involving fractionation processes, or a combination of both, are therefore needed to explain the isotopic values analyzed. Meanwhile, the absence of pyrites in the Selva basin makes sulfide oxidation an unlikely process in the area studied. Only the sample CS0284, with the lowest $\delta^{34}S$ and $\delta^{18}O_{SO4}$ values, might be linked to a ^{34}S-depleted source of reduced sulfur associated with volcanic rocks.

In anaerobic environments, bacteriogenic sulfate reduction can give rise to a substantial enhancement of the isotopic signature of both S and O in the residual sulfate, combined with a lowering of SO_4 concentration (Mizutani and Rafter, 1973). Dissolved O_2 values in the Selva wells sampled ranged between 0.1 and 8.1 mg/l, with a median value of 3.9 mg/l (n = 34), almost all of which were below the atmospheric oxygen concentration (8 mg/l). Eh values ranged between -76 and 497 mV, with a median value of 349 mV (n = 33). These physico-chemical parameters related to redox conditions mainly indicate oxic conditions for most of the studied samples. It is remarkable that several samples (LG0029, LG0190, LG0246 and FS0066) presented the lowest values of dissolved O_2 (0-1 mg/l), together with the lowest values of Eh (<300 mV), the lowest concentrations of SO_4, coupled with the absence of NO_3 and the highest values of Fe and Mn. The redox conditions suggested by these parameters are quite favorable for achieving denitrification processes, andSO_4 reduction mechanisms in some cases. Only the sulfate from the sample FS0066 can be clearly explained as a residual sulfate of the bacteriogenic sulfate reduction, since it presents the highest $\delta^{34}S$ and $\delta^{18}O_{SO4}$ values and plots in the area defined by the extreme enrichment ratios of that process. The $\varepsilon\delta^{34}S/\varepsilon\delta^{18}O_{SO4}$

enrichment ratios in sulfate reduction reactions are between 2.5 and 4 (Mizutani and Rafter, 1973) (Figure 4.14). Moreover, sample FS0066 is linked to regional flows and as Einsiedl and Mayer (2005) observed in groundwaters with mean residence times of more than 60 years, a trend of increasing $\delta^{34}S$ and $\delta^{18}O_{SO4}$ values along with decreasing SO_4 concentrations can be explained by the occurrence of bacterial (dissimilatory) sulfate reduction. This interpretation is also suggested by plotting the SO_4/Cl ratio (sulfate concentration normalized by respective and conservative chloride concentration) versus the $\delta^{34}S$ data: as shown in Figure 4.12, the samples with F concentration >1 mg/l present a slightly negative correlation, which indicates the occurrence of bacterial reduction processes (Marimon et al., 2007).

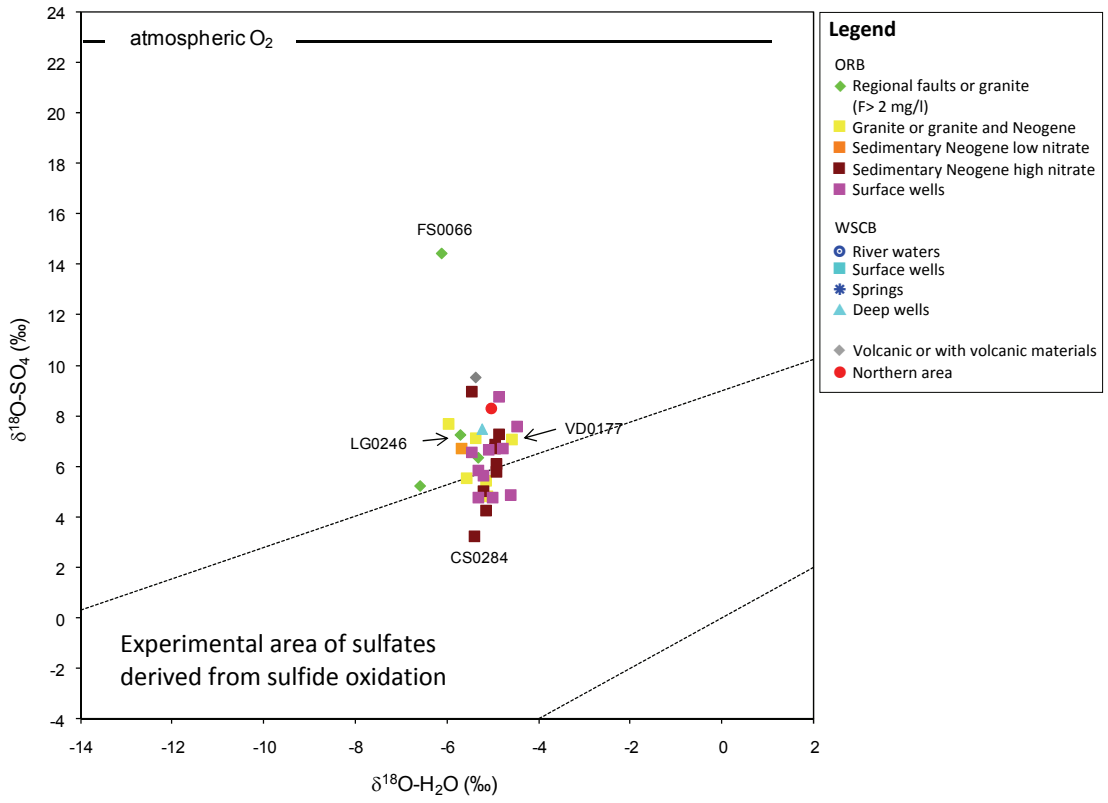

Figure 4.11. $\delta^{18}O_{SO4}$-$\delta^{18}O_{H2O}$ diagram. Although 30% of the studied samples fall within the experimental area of sulfates derived from sulfide oxidation, only the sample CS0284 might be linked to a ^{34}S-depleted source of reduced sulfur.

The other samples with dissolved O_2 concentrations between 0 and 1 mg/l might be accounted for by mixing processes with CO_2-rich thermal waters.

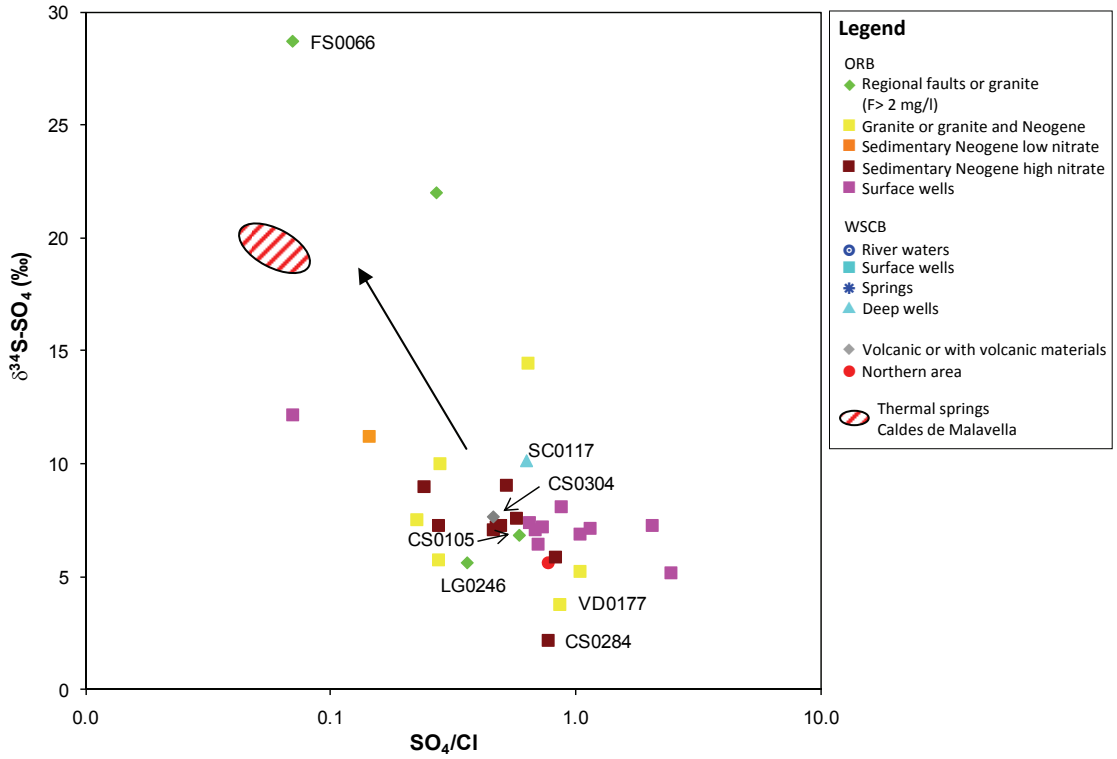

Figure 4.12. δ^{34}S-(SO_4/Cl) diagram, where the samples with F concentration >1 mg/l (with sample code) show a slightly negative correlation, which indicates the occurrence of bacterial reduction processes. The shaded circle shows the isotopic value found in the thermal springs in Caldes de Malavella (Piqué 2008).

4.5.3.3. Sources of sulphate in groundwater

Most of the Selva samples with a sulfate concentration of between 50 and 150 mg/l show δ^{34}S between +5.0‰ and +9.0‰, consistent with anthropogenic source values (pig manure, fertilizers and sewage). It is worth noting that most of these samples are from shallow wells or deep Neogene wells with high NO_3 concentrations, consistent with sulfate due to human contamination. The samples with sulfate concentration below 50 mg/l presented a higher isotopic variability, with δ^{34}S ranging from +3.8‰ to +28.7‰ (Figure 4.18). As stated previously, this increase in δ^{34}S with lower SO_4 concentration values could be linked either to bacteriogenic sulfate reduction processes or to mixing with CO_2-rich thermal waters.

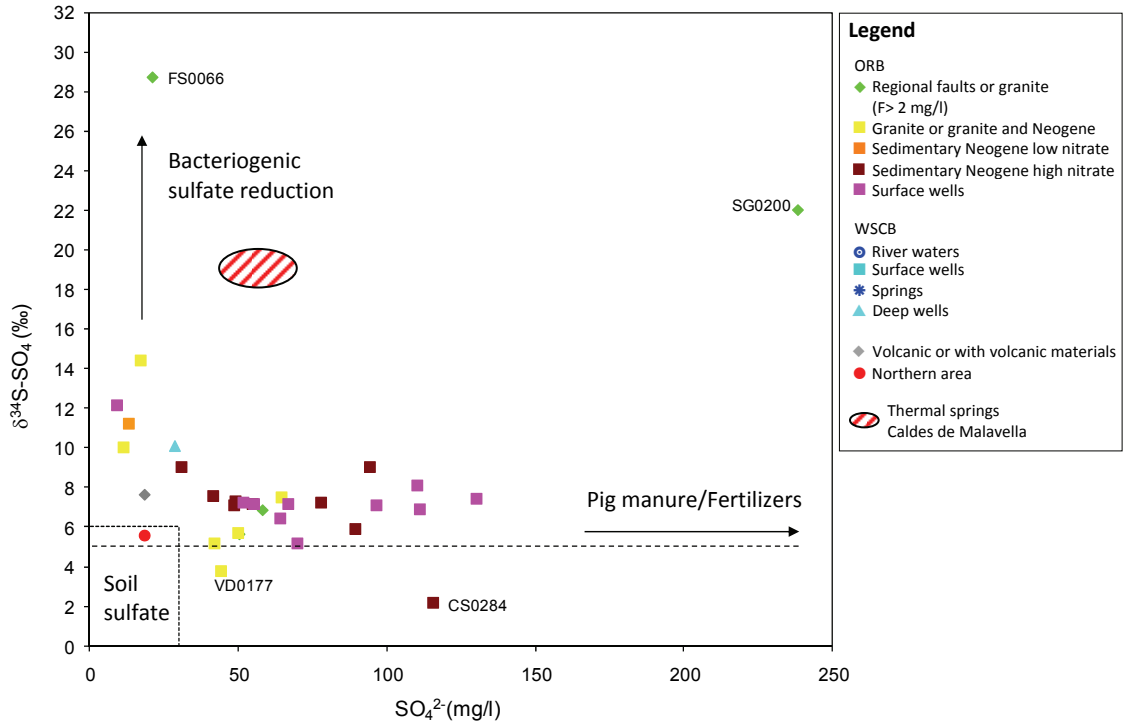

Figure 4.13. δ^{34}S-SO_4 diagram showing that most of the samples with SO_4 concentration between 50 and 150 mg/l present δ^{34}S values consistent with an anthropogenic influence. The shaded circle shows the isotopic value found in the thermal springs in Caldes de Malavella (Piqué 2008).

The lack of correlation between S and O isotopic compositions of groundwater dissolved sulfate (Figure 4.14) confirms that the sulfate reduction process does not generally occur (it probably only affects sample FS0066), thus indicating that other sources are controlling groundwater sulfate. The δ^{34}S and $\delta^{18}O_{SO4}$ values found in groundwater samples are plotted in Figure 4.14 together with those of the main sulfate end-members, indicating the contribution by these different sources. As can be seen, most of the samples lie in the mixing area defined by the isotopic ranges of fertilizers, pig manure and sewage.

Natural sources like sulfate derived from magmatic sulfide oxidation or CO_2-rich thermal waters could exert some influence, but only for few samples and to a limited extent. If groundwater sulfate was partly derived from soil sulfate, samples with low SO_4 concentrations and δ^{34}S between 0‰ and +6‰ would have been obtained (Figure 4.13), as reported by Rock and Mayer (2002). Moreover, the substantial nitrate concentrations registered, as well as a slight correlation between SO_4 and NO_3, suggest the influence of an anthropogenic source, rather than an organic soil contribution.

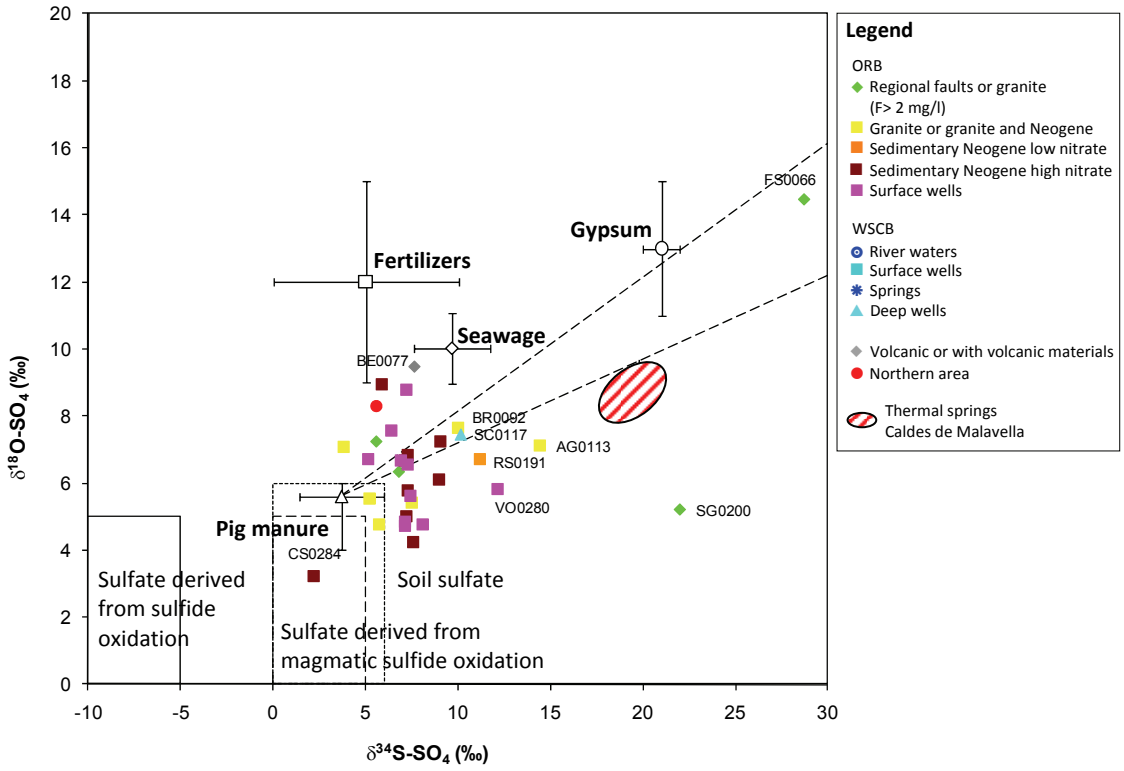

Figure 4.14. Results of $\delta^{34}S$ vs. $\delta^{18}O_{SO4}$. The natural and anthropogenic sources values are shown. The two broken lines define the enrichment ratios range from Mizutani and Rafter (1973) for sulfate reduction reactions. The shaded circle shows the isotopic value found in the thermal springs in Caldes de Malavella (Piqué 2008).

In an attempt to track any fertilizer contribution, Ca/SO_4 ratios have been plotted versus $\delta^{34}S$ (Figuere 4.15). Groundwater samples with $\delta^{34}S$ values in the range of fertilizers show Ca/SO_4 >1. As the Ca/SO_4 ratio for fertilizers is <<1 (Otero et al., 2005a), this result suggests that fertilizers are not a notable source of sulfate in the Selva basin, although some sampled wells are near agriculture areas and plant nurseries. Furthermore, plotting the Ca/SO_4 ratio versus $\delta^{34}S$ values also yields information about other potential sulfate sources. If the sulfate in the Selva basin originated from the dissolution of marine gypsum, the sulfate concentrations would be significantly higher - Ca/SO_4 should be around 1 and $\delta^{34}S$, between +20 and 23‰. The only sample that comes close to these characteristics is SG0200, but its $\delta^{18}O_{SO4}$ value (+5.2‰) differs enough from those of gypsum to rule out the dissolution of this mineral as a feasible origin. The Ca/SO_4 ratio of pig manure is around 2.4 (Vitòria, 2004, 2004a) and that of thermal waters in the Selva basin is around 2.5-3.0 (Piqué, 2008). As shown in Figure 4.15, whereas thermal waters also do not seem to participate with a substantial sulfate contribution, an origin of groundwater sulfate related to pig manure and/or treated sewage seems likely. Taking into account that the influence of sewage in the area studied is occasionally possible (e.g. sample BE0077 in Figure 4.14), the isotope analyses of sulfate

therefore presumably support the interpretation that the application of pig manure onto the fields is the basic control of sulfate in the area.

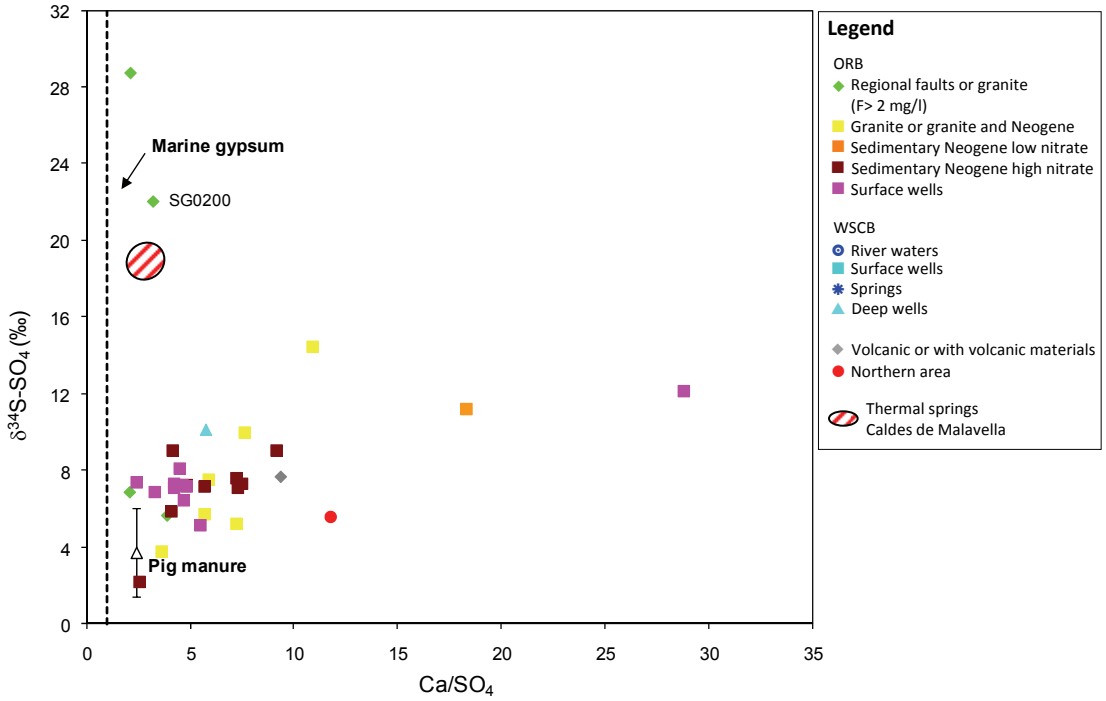

Figure 4.15. $\delta^{34}S$ vs. (Ca/SO_4). Most of the samples plot near the pig manure area, whereas marine gypsum and CO_2-rich thermal are not significant sulfate sources. The shaded circle shows the isotopic and hydrochemical value found in the thermal springs in Caldes de Malavella (Piqué 2008).

As mentioned previously, the sulfate content of sample CS0284 ($\delta^{34}S$= 2.2 ‰, $\delta^{18}O_{SO4}$= 3.2 ‰) appears to be derived from sulfide oxidation. The sulfate in sample FS0066 might have originated from the same process, but the subsequent effects of bacteriogenic sulfate reduction would have caused the isotopic difference between both samples. Sample SG0200 ($\delta^{34}S$= 22 ‰, $\delta^{18}O_{SO4}$= 5.2 ‰), a highly mineralized spring (238 mg/l of SO_4) located outside the Selva basin, shows a $\delta^{34}S$ value close to thermal waters and marine gypsum. However, its $\delta^{18}O_{SO4}$ value is lower than those end-members, indicating a different source. One possible origin is sulfate reduction from a previous sulfate originating in dissolutions of disseminated pyrite from granites (Figure 4.14). This groundwater linked to a regional flow can therefore be equilibrated with a particular lithology, with a sulfate isotopic composition for further study. Apart from the samples clustered near the isotopic range of pig manure (mainly shallow wells and deep Neogene wells with high NO_3), there are 5 samples (AG0113, BR0092, RS0191, SC0117 and VO0280) presenting higher values of $\delta^{34}S$ and lower sulfate concentrations. These samples are all located close to the edge of the basin. When $\delta^{18}O$-H_2O versus $\delta^{34}S$ is plotted on

a diagram (Figure 4.16), they can be interpreted either as an intermediate flow or as a mixing between the local recharge affected by human contamination and a ^{34}S-enriched source. Figure 4.16, shows that shallow wells and deep Neogene wells with high NO_3 are controlled by an anthropogenic isotopic signature, whereas these 5 samples follow a trend towards CO_2-rich thermal and/or regional groundwaters.

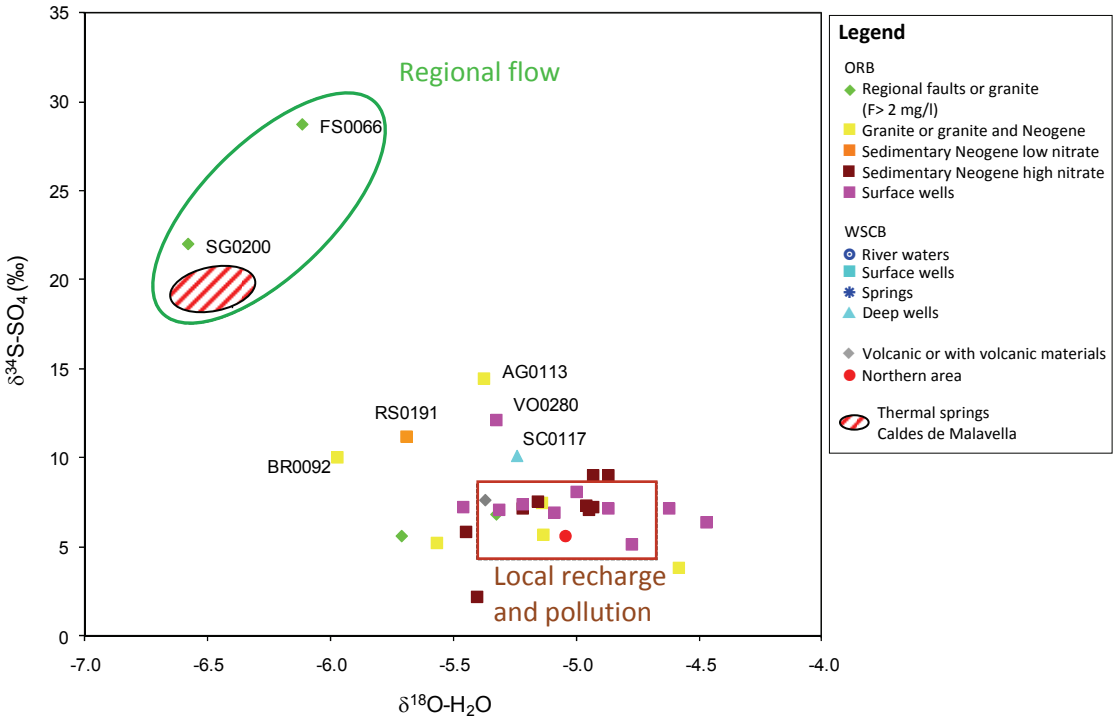

Figure 4.16. $\delta^{34}S$-$\delta^{18}O_{H2O}$ diagram, showing the distinction between local recharge samples affected by human contamination and regional flows. The shaded circle shows the isotopic and hydrochemical value found in the thermal springs in Caldes de Malavella (Piqué 2008).

The possible contribution of CO_2-rich thermal waters to the groundwaters studied could be argued by considering the slight correlation between groundwater temperature and the SO_4 concentration: the higher the temperature, the lower the SO_4 content (Figure 4.17). Except for for sample SG0200, for instance, samples with temperatures higher than 17ºC present sulfate concentrations of below 50 mg/l.

Based on the coupled use of $\delta^{34}S$ and $\delta^{18}O_{SO4}$ values, the main source that controls groundwater sulfate is pig manure dissolved sulfate. In this case, the S and O isotopic composition of dissolved sulfate can be used as a tracer of local recharge and anthropogenic contributions.

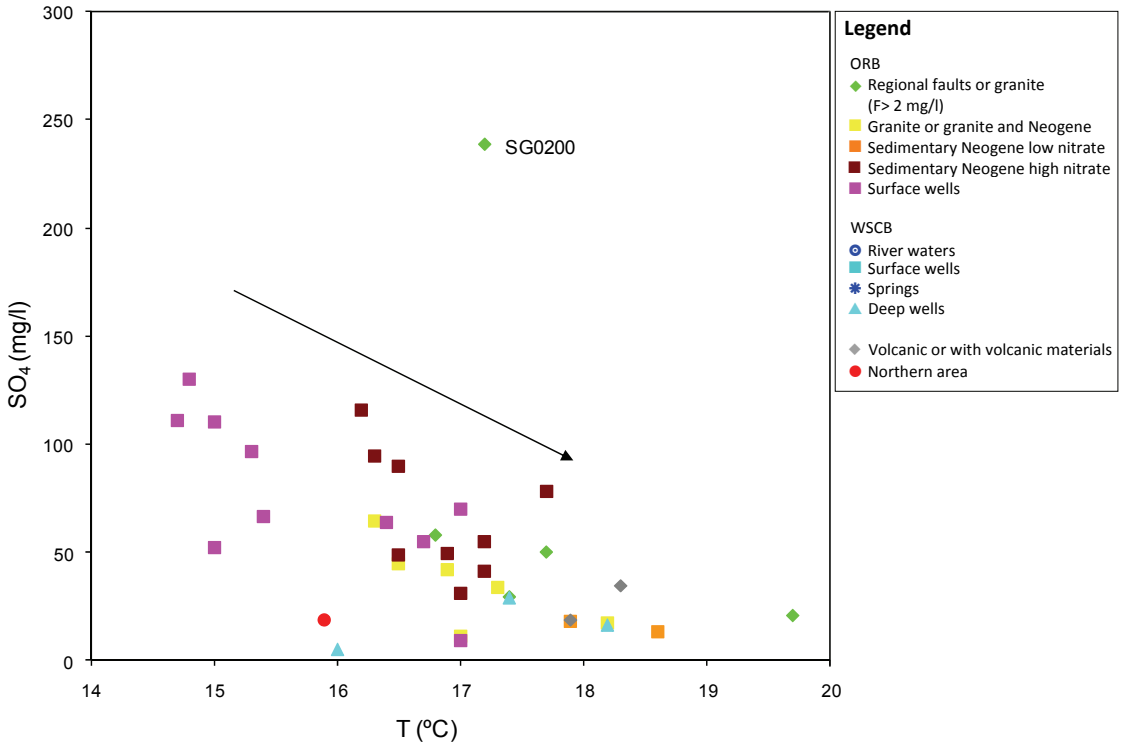

Figure 4.17. SO_4 vs. Tª diagram showing the slight correlation between groundwater temperature and the SO_4 concentration.

4.5.4. Using NO_3, F and TOC to define mixing processes and regional flow systems.

As has been explained with regard to the hydrochemistry and more extensively for the isotopic data for different seasons (see chapter 3), there is a mixing of different flow systems throughout the year that is partially influenced by pumping. A good indicator of this mixing process is the concentration of fluoride and nitrate (Figure 4.18).Three wells and one spring of the northern area (close to the transversal range) with no presence of granite, the main source of fluorite (Piqué 2008) were plotted to define the background concentration of fluoride in the Selva basin. Wells with a fluoride concentration of under 0.3 mg/l (Figure 4.18) indicate no (or negligible) influence of regional flows in the granitic basement.

One one side of this relationship are the wells with a high fluoride concentration and an almost negligible concentration of nitrate indicative of regional/longer transit time flow systems. On the opposite side, with high nitrate and very low fluoride levels, are samples represented by the local polluted recharge. This group mainly consists of surface wells and some wells in

neogene sediments. These wells indicate the deep groundwater affected by local pollution caused by pumping. This group also includes some wells in granite, indicating that in these materials it may have preferential flow paths through weathered granite (where it has high hydraulic conductivity) and/or fractures. As a consequence, in granite wells with high nitrate and low fluoride levels, the groundwater quality will be determined by the pollution input of the system (agriculture fertilizers, pig manure or treated urban waters).

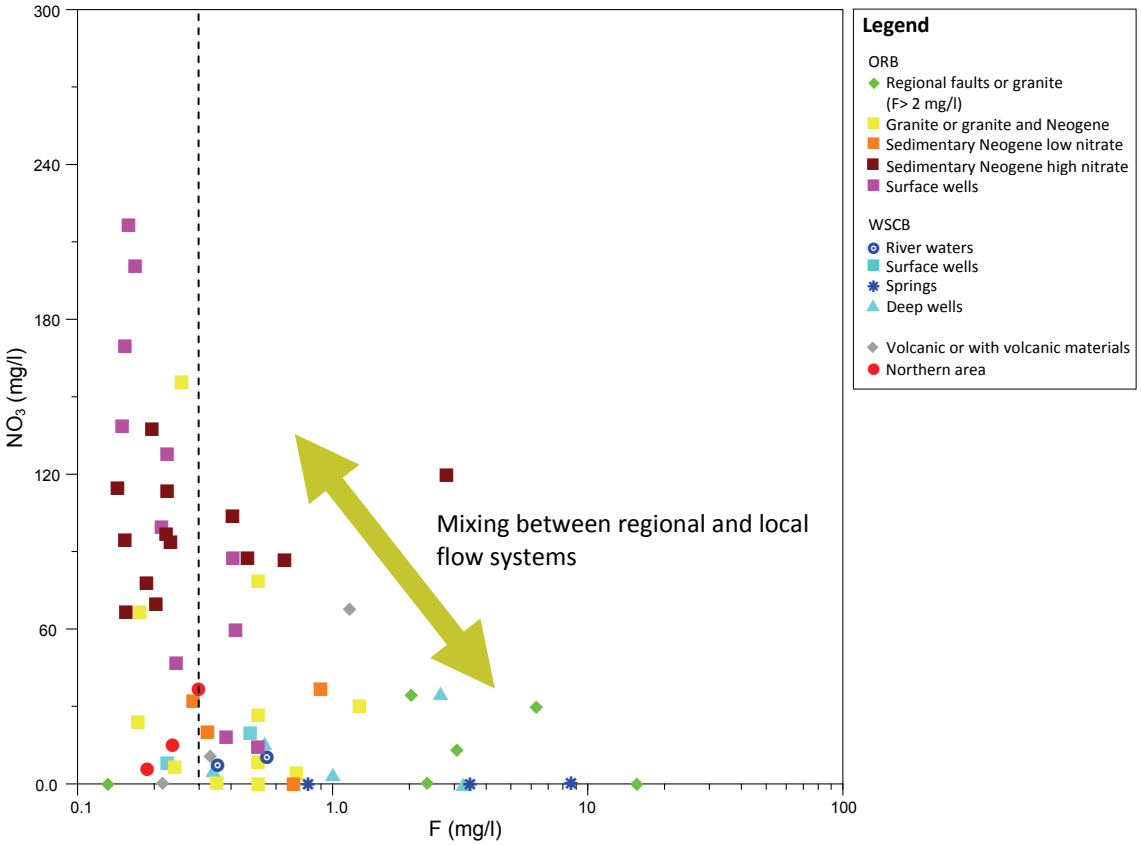

Figure 4.18. Concentrations of nitrate vs fluoride. The dotted line indicates the fluoride concentration unrelated to granites.

At lower nitrate and fluoride concentration levels, there are some wells located in the neogene sediments in the WSCB and ORB. These wells have little influence on the direct recharge at the basin's surface, and are also unrelated with the deepest flow systems. Although, these samples can be representative of the intermediate flow systems. Nevertheless, they may also be wells with a relatively low transit time with no pollution.

Some samples also show a relatively high concentration of nitrate and fluoride. These samples are representative of waters mixing between regional and local flow systems. As some of these wells have several screen intervals, the mixing may occur in the well during pumping, or

because of vertical flows caused during water extractions. Furthermore, different F content may indicate variable F content in the regional flow.

In various geological environments, the organic matter in the groundwater is related with pollution (Hem 1985). In the Selva basin Total Organic Carbon (TOC) tends to increase as NO3 increases (Figure 4.19). However, there are some samples with low NO3 content that show significant concentrations of TOC, indicating that this compound is of geological origin. In this context, the organic matter is not a good indicator for differentiating between local flow systems.

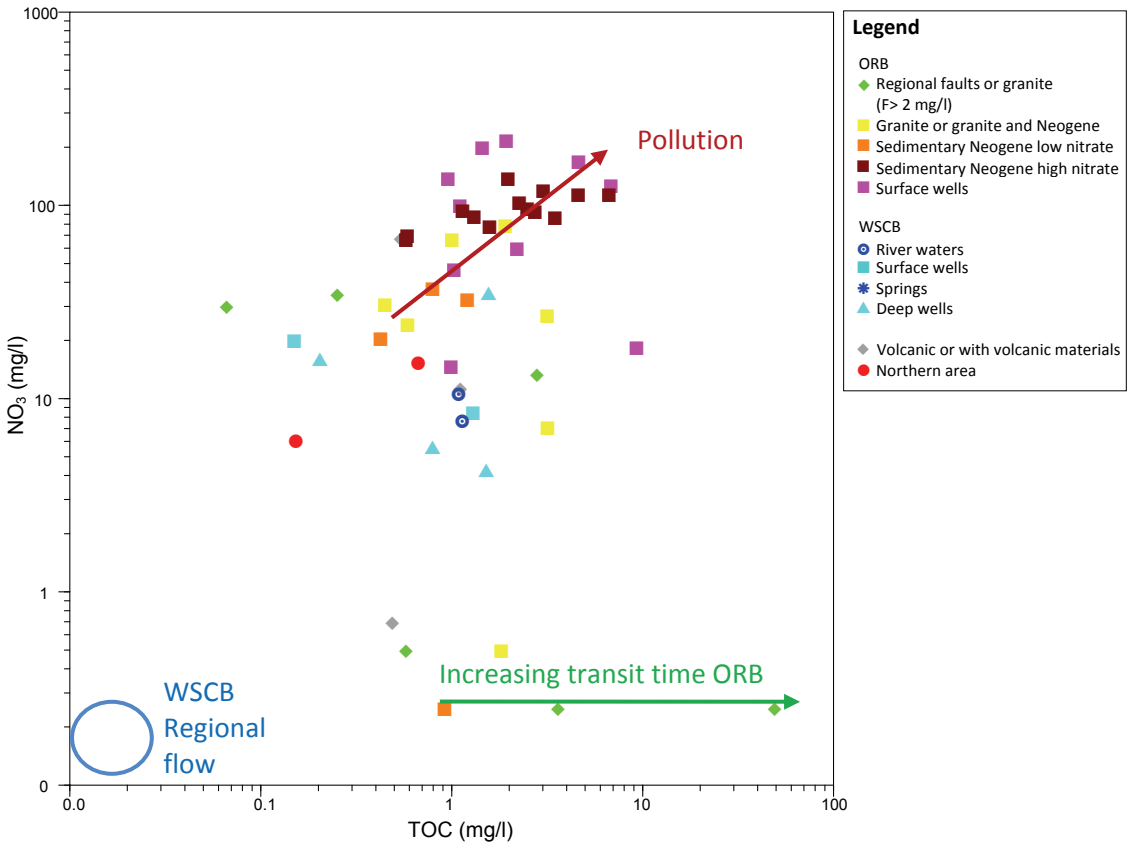

Figure 4.19. Nitrate vs Total Organic Carbon.

In the WSCB, the most representative samples of regional flows have no TOC content. Oppositely, wells related with deep flow systems in the ORB have relatively high concentrations, which increase as the salt contents increases. Considering that these samples are not related to anthropogenic pollution, the total organic carbon origin may be attributed to the geological context. In the Girona area, there is a complex tectonic setting, involving several geological units with very different lithologies. However, the Santa Coloma basin area

is characterized by igneous and metamorphic rocks with no TOC sources. TOC concentration is therefore a good indicator for differentiating between regional flow systems.

Fluorite and nitrate concentrations are good indicators of the end members of the system. At the same time, these two tracers enable a distinction to be made between intermediate flow systems and samples arising from mixing between regional and local flow systems. As complementary information, TOC is useful for distinguishing between recharge sources, and more importantly, for discriminating between different regional flow systems: one coming from the west in the Guilleries range, and another coming from the north.

4.5.5. Cl/Br, F and trace elements

Chloride and bromide are found as monovalent anions in natural groundwater systems. These anions tend to be conservative, and have different concentrations and ratios depending on their origin and some processes that can modify their concentrations, being a powerful tracer (Edmunds 1987, Davis et al. 1998, Beucaire et al 1999, Stober and Bucher 1999, Davis et al. 2004, Hudek 2003, Alcalà and Custodia 2008a and others).

Different end-members can be defined from previous studies. Rainwater in the Iberian peninsula was studied by Alcalá and Custodio (2008a), who defined the Cl/Br ratio of recharge water depending on different atmospheric and hydrological conditions. Thermal springs in the area have been studied by Pique (2008) giving a Cl/Br ratio for this type of water of between 210-240. Lastly, the end-member characterized by pollution has not been studied specifically in this region. However, there are several studies of groundwater pollution, and in most cases polluted water presents different Cl/Br ratios to natural groundwater. The Cl/Br ratio has been studied for the different groups of samples, adding new information to the previous results and helping to describe the different processes defined as mixing, water-rock interaction and pollution. The results obtained have been complemented with the information given by F and some trace elements such as Li and B.

In Spain, the Cl/Br ratio in rain water has been defined as similar to sea water or less, at between approximately 220-310 in coastal areas unaffected by atmospheric pollution. Only a few of the samples collected have been considered representative of the rain recharge end-

member, showing chloride content (< 15 mg/l). This concentration is common for rain water sampled close to the study area (Vilanova 2006), as these samples are less affected by other processes in the aquifer that can modify Cl and Br content. However, rain water can show higher Cl content and a different Cl/Br ratio depending on atmospheric pollution, the inland effect (the area is affected by Mediterranean and Atlantic fronts), type of precipitation, etc. (Alcalá and Custodio 2008). Two of the samples considered, one from a surface well (SC0151) and one of river water (SCRA), are located in the WSCB and show a Cl/Br ratio close to that of sea water (Table 1 and 2) consistent with the recharge water data presented by Alcalá and Custodio (2008).

Another two samples showing that the source of Cl may be rain water are SMLL001 and SG0123, located in neogene sediments in the northern area. Although these samples show a Cl concentration in the range of precipitation or lower, their Cl/Br ratio (114-192) is below the typical level for rain water near coastal areas. There are other surface wells in the Selva basin that with slightly higher Cl content (≈20 mg/l) show similar Cl/Br ratios (Table 2). This lower ratio may indicate the inland effect (Alcalà and Custodio 2008a) affecting the Atlantic fronts that also recharge the area studied. Considering that all these wells have a non-saturated zone at least a few meters thick, another explanation could be the occurrence of some processes in the soil or in the non-saturated zone modifying the typical Cl/Br content of rain water.The recharge water in the Selva basin and surrounding areas may therefore show a Cl content of a few dozen mg/l of Cl and a Cl/Br ratio of between 114-310.

As shown by the hydrochemical and the isotopical data, the western Santa Coloma basin and the Onyar basin behave like two different hydrogeological basins. Samples in the ORB tend to show more variability (Cl/Br =161-537) and higher chloride concentrations, while those in the WSCB have lower Cl concentrations, and more importantly, specific Cl/Br ratios (66-310) (Figure 4.20).

In particular, the samples of deep neogene with low nitrate in the Onyar basin show a relative greater range in the Cl/Br ratio. Considering the different lithologies of the sediments fulfilling this part of the basin, this variability may be caused by interaction with different materials and mineralogies, the organic matter in the sediments or interaction with different flow systems (Figure 4.19). Taking into account that the Cl concentrations in the neogene non-polluted samples are almost constant, the most important processes controlling Cl/Br relation may be the decomposition of organic matter and/or the sorption of Br in clays (Gerritse and George

1988, Fabryka-Martin et al. 1991; Wittemore and Davis 1995, Boggs ans Adams 1992, Hite and Cheng 1996).

Samples in deep neogene with high nitrate concentrations show a higher Cl/Br ratio, of mainly between 300-540. Considering that the change of this ratio in these wells and some samples of the surface aquifer is due to an increase in Cl concentration, these changes are attributed to pollution by pig manure and/or wastewaters, and the values are similar to those in other studies of domestic sewage (Davis et al. 1987, Behl et al 1987, Davis et al. 1998, Vengosh and Pankratov 1998, Davis et al. 2004). However, the Cl/Br ratio described by Huak (2003) for leachate from farm-animal waste (cattle, horses and goats) is much lower. As the domestic water treatment plants are only located close to the main river channels, and the pollution is also distributed far from the alluvial aquifers, it is possible to state that pig manure has the same Cl/Br ratio as sewage waters and a different one from other farm animals. In this regard, Panno et al. (2006) found that other farm animals such as hogs and horses have much larger median ratios, ranging from 1245 to 1654.

The other groups of samples in the ORB to be considered are from wells in granites and regional faults, in general showing low nitrate (Figure 4.18). Most have higher Cl concentrations (> 80 mg/l) and some have high fluoride content, indicating a source of Cl other than pollution (Figure 4.20). These groups of samples have a Cl/Br ratio of between 185-220 keeping, with this relation remaining almost constant with the increase of Cl (Figure 4.21) indicating that the origin of Cl and Br is the same.

The Cl/Br of leachate of granitic rocks in the United States, Sweden, and France are mostly slightly higher than 100, and the range of this ratio is about 100 to 200 (Grigsby 1983, Nordstrom et al. 1989 and Pauwels et al 1992). In this regard, the leachate of granite is the most feasible source of Cl for the waters studied. Furthermore, this source of Cl is proposed by Pique (2008) for thermal springs (Figure 4.20) in the same study area, with similar Cl/Br ratio and consistent with strontium isotopes and Rare Earth Elements (REE). A sea water origin is ruled out because the Cl/Br ratio in sea water is higher (Cl/Br=288). Interaction with halites as a source of groundwater salinization reported in other studies of granites (Stober and Bucher 1999), does not seem a feasible source since halite deposits have not been reported in the study area and the source usually shows much greater concentrations of Cl and much larger values of the Cl/Br ratio (Cl/Br=2400). Sulphate isotopes also rule out this origin.

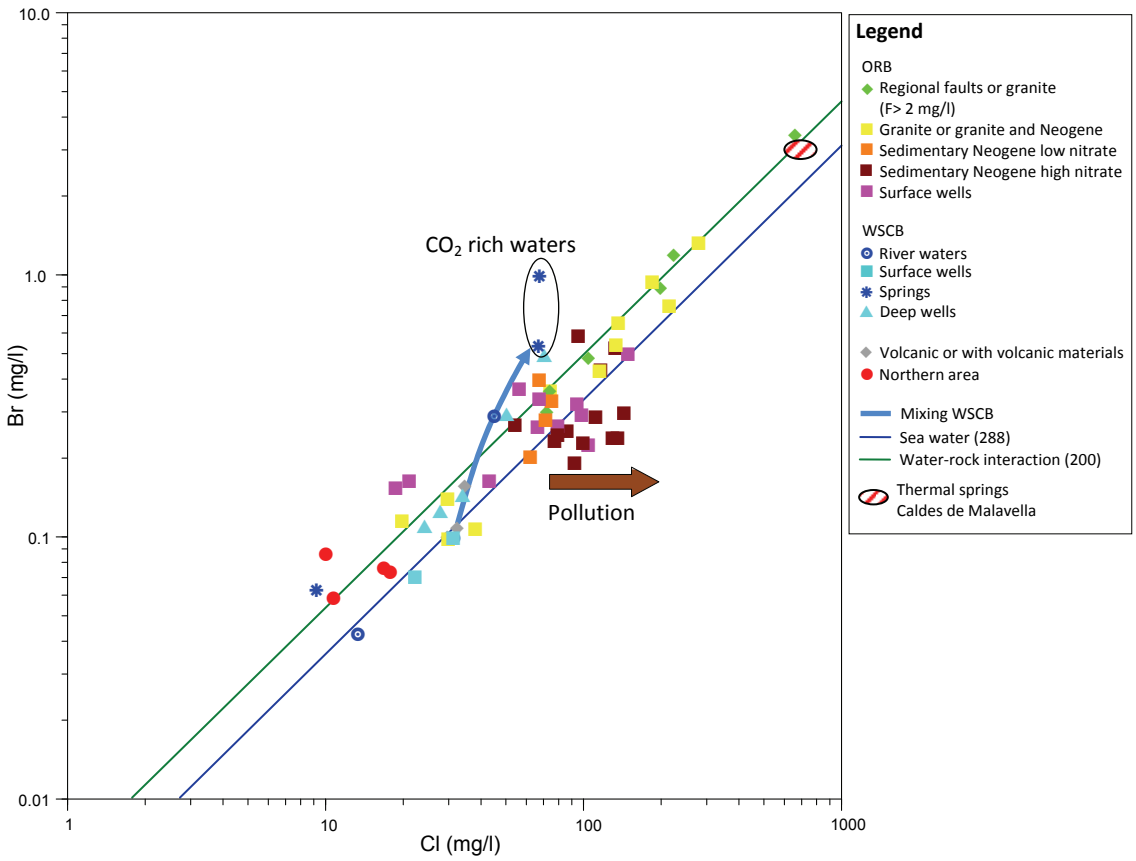

Figure 4.20. Cl vs Br ratio in the Selva basin. Mixing WSCB indicated the mixing line between the sample SC0073 and SCFP. The shaded cercle show the Cl/Br mass ratio found in the thermal springs in Caldes de Malavella (Piqué 2008).

The evaporation in the non saturated zone shown by some of the samples in granites (Figure 4.8a and 4.10) could also lead to an enrichment in Cl. However, considering that these samples keep the Cl/Br ratio around 200, which very different from the rain ratio, the main processes controlling the chloride in these samples is water-rock interaction. There are some wells in granites that show Cl/Br ratios of over 200 with high Cl content. One of the reasons for this may be the influence of pollution, as shown by the high NO3 content of some of these samples. Nevertheless, there is one sample with no or very low nitrate with significant amounts of Cl and a Cl/Br ratio of around 260. This well, like others with low pollution and a similar Cl/Br ratio, is weathered granite, and may indicate some geochemical differences between weathered granite on the basin's surface and granites at depth. This assumption is also consistent with the Na-Cl ratios (Figure 4.6) showing the enrichment of Cl of some samples in granites. Similar phenomena have been shown in other studies, in which the same granite, mineral samples at different depths and leaches give a result of different solute content (Edmunds et al. 1985). Furthermore, this ratio is similar to the ratio of close to 300 proposed in other studies of this type of rock (Fuge 1979, Edmunds et al 1987).

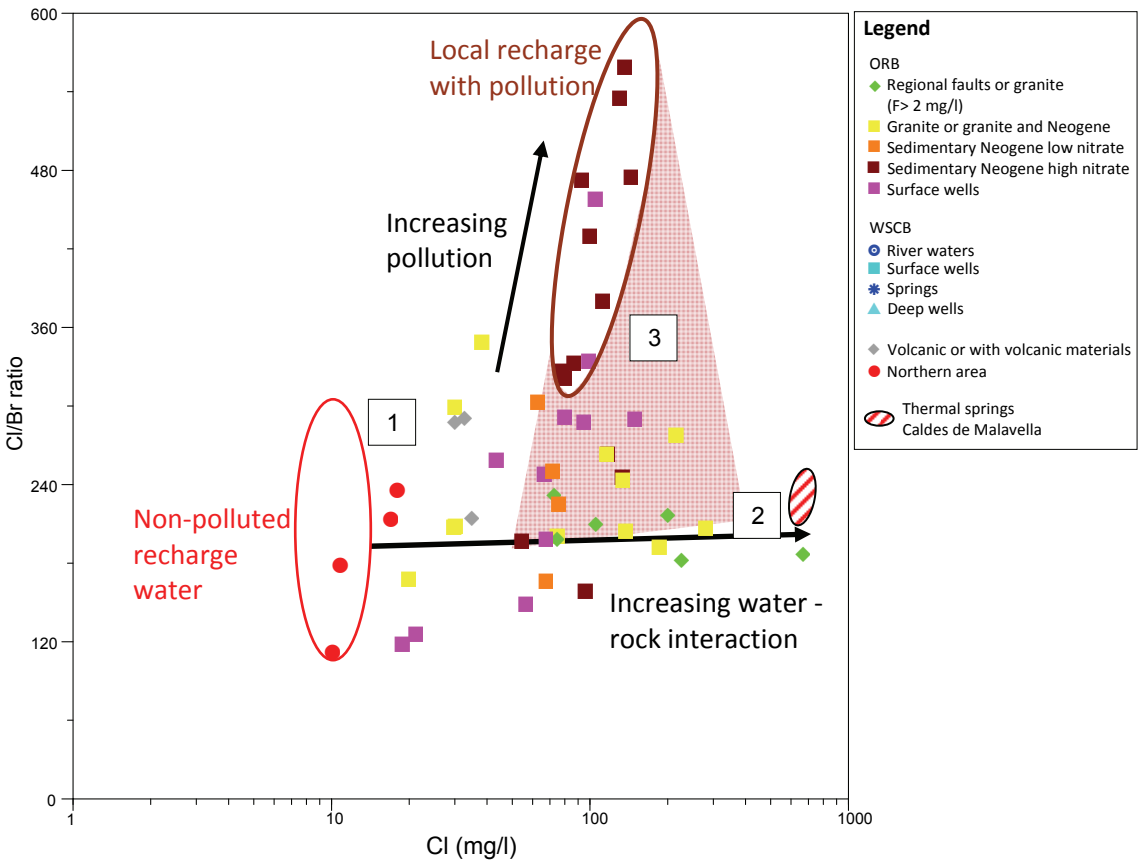

Figure 4.21. Cl/Br mass ratio vs Cl in the Onyar subasin. Evaporation processes have not been considered for some samples for reasons of simplicity. The coloured areas indicate: 1) Low water rock interaction with granites or/and neogene sediments or evaporation of recharge water; 2) High water-rock interaction with granites; 3) Mixing between different flow systems. The shaded circle shows the Cl/Br mass ratio found in the thermal springs in Caldes de Malavella (Piqué 2008).

In the Onyar basin the Cl/Br ratio therefore supports the coexistence of different flow systems, controlled by different processes and transit times and modified because of a mixing between them (Figure 4.21). The less mineralized end-member is the non-polluted recharge water coming from the direct infiltration of rain water. This water can interact with neogene sediments with non-polluted waters found in deep neogene wells. Along the faults, high water-rock interaction is possible, leading to the water found in some wells in granites or regional faults. Another end-member is the polluted water recharged mainly on the basin's surface. Finally, a mix between these different flow lines may be found in different wells and lithologies.

In the Santa Coloma basin, one river sample and two surface well samples show the same Cl/Br ratio with different Cl content (Figure 4.22). Considering than these samples show a thin non-saturated zone and the water isotopes indicate non-evaporation (Figure 4.8a), these

differences may attributed to infiltration of rain water at different altitudes and/or rainy episodes.The water recharged in the aquifer surface in this area is therefore shown by the rain water Cl/Br ratio.

Another end-member is the samples representing the regional flow system in the western Santa Coloma basin (Figure 4.20 and 4.22). These samples, with the highest Cl content in the basin, have a much lower Cl/Br ratio, of between 123 (SCFP) and 64 (Termes Orion, thermal waters). These ratios are representative of granites and are around 100 or less (Behne, W. 1953 and Correns 1956 and Davis at al. 1998). This could indicate that the Cl/Br ratio of these granites in this part of the basin have low Cl content. The sample of thermal water (Termes Orion), which has the lowest ratio, could be the result of the interaction of the same granites as in the other samples but with an input of CO_2 (Stober and Bacher 1999). However, there is no isotopical data for this sample, and this interpretation is consistent with isotopic values from other samples such as SCFP (Table 2), which shows regional flow interaction with CO_2 consistent with Pique (2008) (Figure 4.8) .

Samples of deep neogene in the WSCB vary widely in terms of their Cl/Br ratio, which are between 140 and 230. However, the samples located close to the town of Santa Coloma have a narrower Cl/Br ratio range of between 216 and 231 (Figure 4.20 and 4.22). The range of values in these three samples can be explained in two different ways:

1) different flow patterns along the neogene sediments with different processes controlling the Cl/Br ratio.
2) a mixing between different flow systems.

Most samples from wells located in deep neogene sediments show a recharge altitude above the basin's surface throughout the year (see chapter 3). Based on this assumption, the first option is consistent considering that the samples close to the town of Santa Coloma show a Cl/Br ratio similar to the samples from the ORB that show high water-rock interaction (Figure 4.21) while the samples close to the town of Riudarenes show a ratio similar to granites in the WSCB. The groundwater contour map (Figure 4.1) and other hydrochemical indicators (Figure 4.23) are consistent with the idea of the inflow coming from the north in the northern part of the basin. In terms of the tectonic context, with one important regional fault close to the sampled area in a NW-SE direction, this could act as a preferential flow path bringing water from the north, with different rock compositions to the granites of the Guilleries.

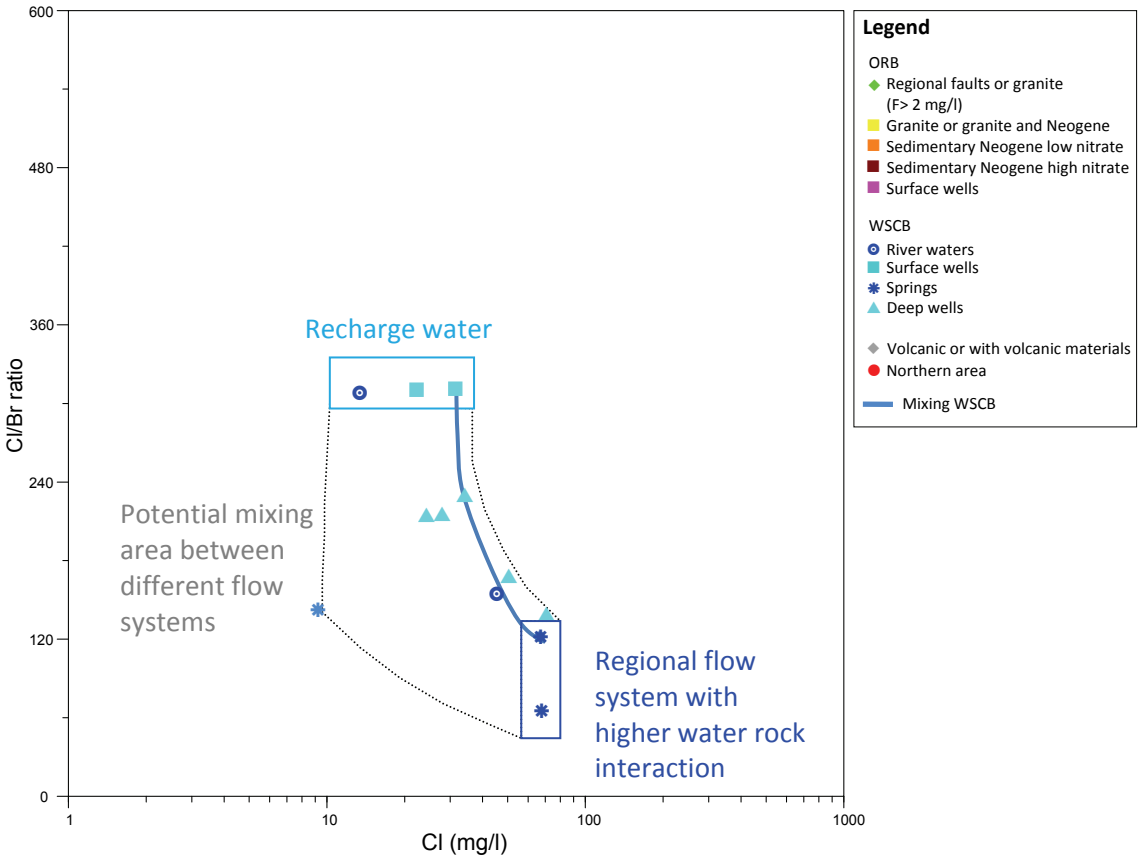

Figure 4.22. Cl/Br ratio vs Cl in the Santa Coloma basin.

The option of mixing between different flow systems have been previously shown in the conceptual models presented by Folch and Mas-Pla (2008). In this regard, there are several samples on the theoretical mixing line between sample SC0073 and the SCFP (Figure 4.22). The first sample is the most evolved water, with the same Cl/Br ratio as other surface water and groundwater samples. SCFP is the sample with the highest Cl content and the lightest ^{18}O value without being a thermal spring. There are three groundwater samples and one surface water sample that are higher than this ratio, indicating different mixing proportions. This hypothesis is consistent with the isotopic values, since the samples closest to SCFP tend to have lighter values, indicating a higher altitude or greater interaction with CO_2, as in the SCFP sample. Moreover, well SC0117, which is also in the mixing line, shows significant concentrations of NO_3 (35.5 mg/l) and F (2.63 mg/l). Furthermore, the water from this well has been described as mixing different flow systems due to its change in isotopic values during the year (see chapter 3). Finally, this mixing model is followed by other hydrochemical components (Figure 4.5). Considering that there are some less mineralized springs in the area (such as SCFSS) indicating another potential inflow into the neogene sediments from the Guilleries range (see also

isotopic values), the resulting water in the neogene geological formation may be a mix between three different end-members (Figure 4.22).

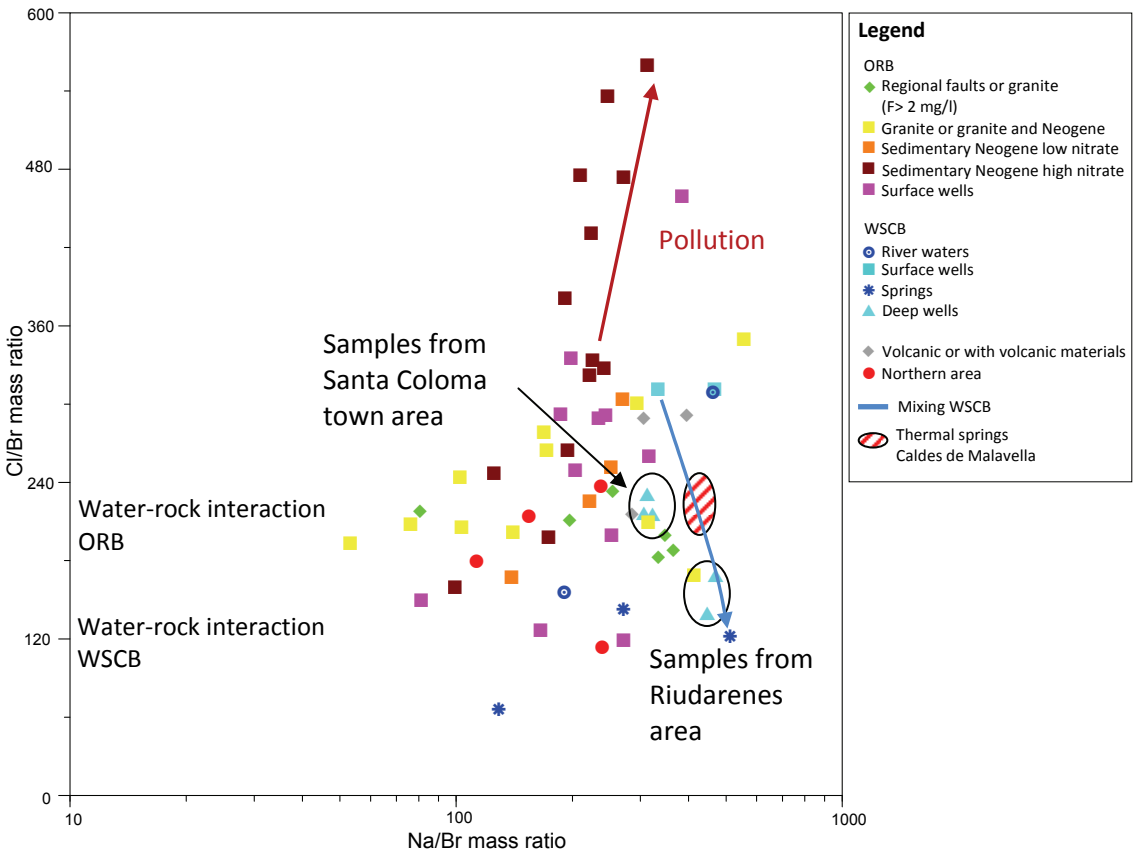

Figure 4.23. Cl/Br vs Na/Br mass ratio. Mixing WSCB indicates the mixing line between the sample SC0073 and SCFP. The shaded circle shows the Cl/Br mass ratio found in thermal springs in Caldes de Malavella (Piqué 2008).

In the Santa Coloma basin, the Santa Coloma fault could act in two different ways in recharging the deeper neogen sediments. On the northern side, close to the town of Santa Coloma, the fault and deep geological formations bring water from the N-NW with similar water-rock interaction to the faults in the Onyar basin. To the south, in the Neogene closer to the fault zone and the town of Riudarenes, there is a mix between water recharged in the Guilleries range and the surface water of the alluvial aquifer and the river. Water in the middle part of the river also could also be explained as a mixture of surface water (river or groundwater) and water from the regional flow systems. However, another end-member for the mixing and spillages into the river from industries using deep groundwater must be considered.

The waters in granites with the lowest concentrations of Cl (BR0092, VO100, VD0177 and AG0113) are all situated on the boundary of the Selva basin. They have a lower transit time

and a more variable Cl/Br ratio due to the different processes controlling it (rain content, pollution, water rock interaction, etc.).

4.5.5.1. The influence of F rich fluids

When considering the influence of fluoride rich fluids in the hydrochemistry, it is possible to appreciate that the sample SG0200 has a similar Cl/Br ratio to the other samples related with regional flow in the Onyar basin, but much lower F concentrations (Figure 4.24). As a result, considering that F tends to increase with transit time and that granite can have minerals leaching fluoride to groundwater (Edmunds et al. 1987), other minerals could be controlling its concentration. This may be because of changes in the granite facies (increase in mafic minerals) in the basin and the areas around it and/or due to preexisting fluorite mineralizations in the area (Pique, 2008 and Piqué et al., 2008) that could contribute to increasing the fluoride dissolved in water. This behavior is also different in the ORB and the WSCB, which both basins have groundwater with high F content (8 and 15 mg/l respectively) and different water-rock interaction.

It is important to consider that because of the higher F concentration in groundwater, the Cl/Br relation tends to decrease slightly (Figure 4.24). Considering that the amount of Cl tends to increase in these samples, it is possible that the source(s) of fluoride are associated with other minerals or compounds that can add bromide to groundwater. This could be one of the reasons why the Cl/Br ratio in granites characterized by water rock interaction vary significantly (Behne, W. 1953, Corens 1956, Edmunds et al. 1987, Davis at al. 1998, Stober and Bacher 1999 and others).

The amount of lithium, and other elements such as Na, is an indicator of long transit times (Tóth 2000, Carrillo-Rivera et al. 2007). Li is strongly correlated with Na (Figure 4.25a) for the water representing regional flows with higher recharge altitudes (Figure 4.8) or a long transit time (Figure 4.21). However, comparison of Li with Cl (Figure 4.25b) shows that the regional flows in the WSCB show different Cl/Li ratios to the ORB, as shown previously in other hidrochemical indicators.

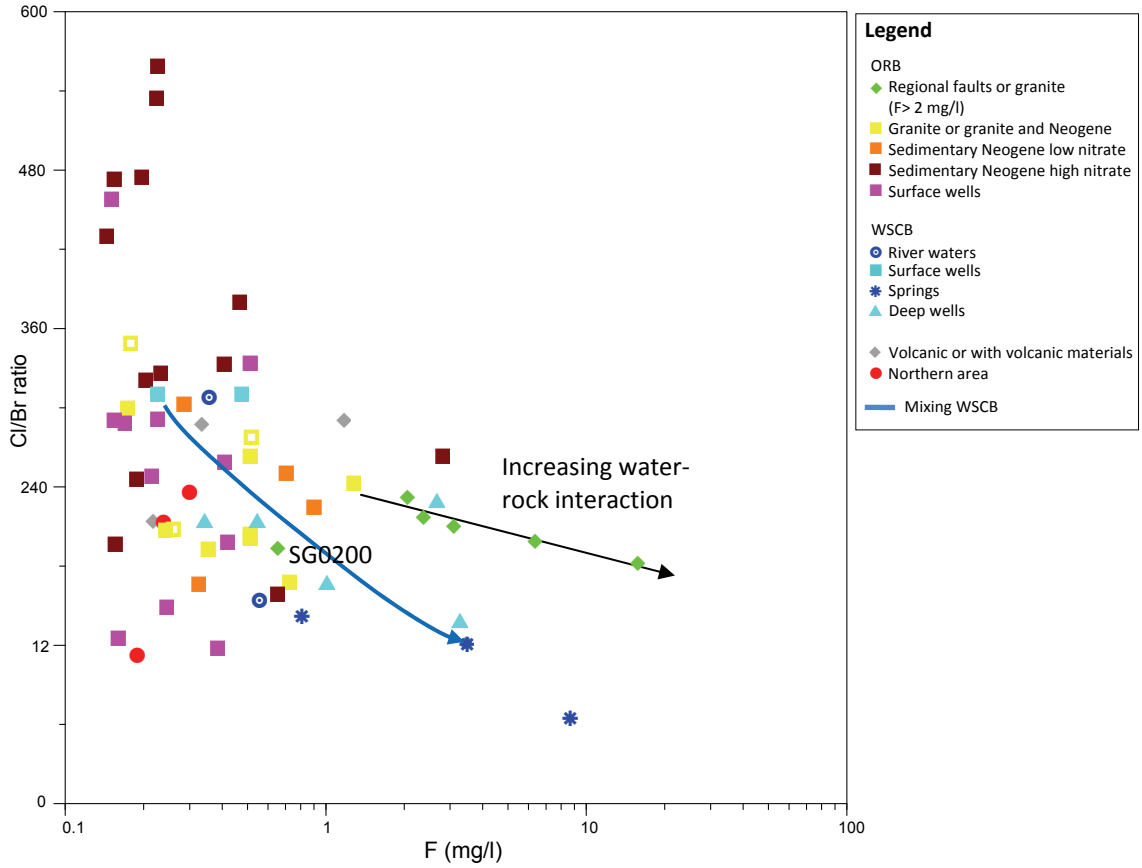

Figure 4.24. Cl/Br vs F. Mixing in the WSCB indicated the mixing line between the sample SC0073 and SCFP.

The sources of lithium in the two basins are different. In the WSCB, which has lower Cl levels, the main source of lithium could be the weathering of plagioclase or muscovite where Li is replacing Al sites (Huh at al 1998). This assumption is consistent with the higher SI of quartz shown in the samples of larger amounts of lithium in the WSCB (Figure 4.5). Groundwater in the ORB, with higher amounts of Li, may be the result of other processes, such as the weathering of phylosilicates, such as the biotite (Edmunds et al. 1987, Beucaire et al. 1999) which also leads to larger amounts of Cl.

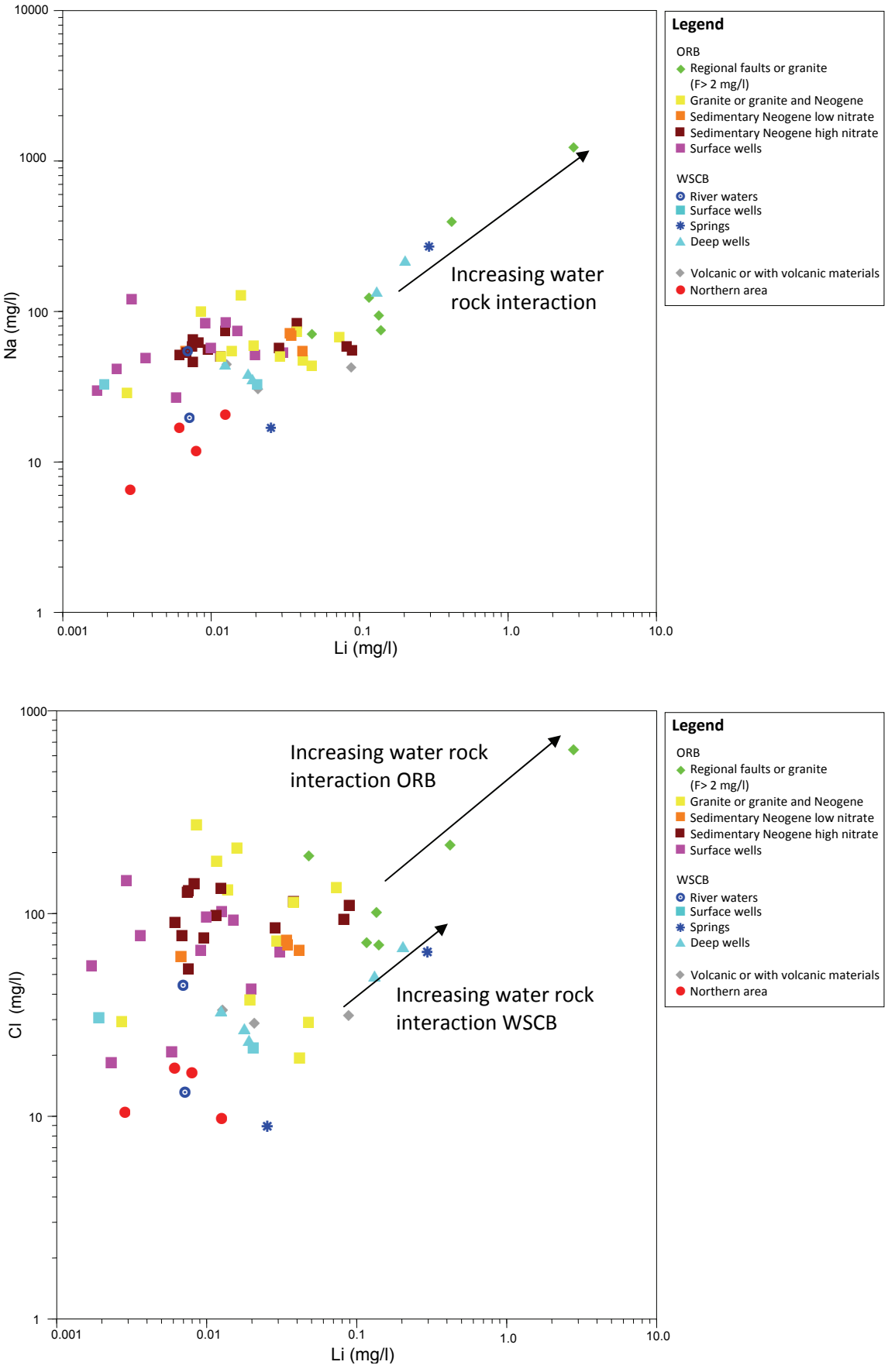

Figure 4.25. a) Na vs Li. b) Cl vs Li

The various groups of samples tend to show a relationship between Li and F, indicating an increase of the two compounds along the flow path (Figure 4.26a). However, there is no correlation in the WSCB, with some samples having high F at low Li concentrations (SC0117). Furthermore, sample SG0200, which has the highest Li content, has relatively low F concentrations with a similar Cl/Br ratio to the other samples from granites (Figure 4.26b). This shows that apart from the leachate of granite, one of the sources of F in groundwater may be fluorite dissolution. This assumption is particularly feasible in the WSCB, where there is high F (8 mg/l) with lower Cl values (66.7 mg/l).

Another indicator of long transit times is B. The two samples with the highest Cl concentration related to regional flows (FS0066 and SG0200) show B content of over 1 mg/l. In saline waters, one of the sources of B could be the dissolution of silicates (Moldovani et al. 1993 and Vengoh et al. 1994) occurring in different minerals of granites (Harder 1975, Edmunds et al. 1987 and Bottomley et al. 2003). Because of the Cl/Li and Cl/B ratios, a marine origin of the water related to regional flows can be discarded. However, the B and Li concentrations indicate that the samples from the Onyar basin show longer transit times than those from the Santa Coloma basin.

There are therefore different regional flow systems the Selva basin. One is located in the WSCB, with a lower concentration of Cl and Cl/Br values around 100. The other is located in the ORB, with a longer transit time and Cl/Br ratios of around 200, and larger amounts of F, Li and B. There are various mixing processes between these regional flow paths and other flow systems around the basin. In the ORB, this mixing mainly consists of a polluted local input with higher Cl/Br ratios (between 300 and 560) and the regional flow. In the WSCB, the local input does not have high nitrate concentrations, with a Cl/Br ratio similar to rain water (300). While in the ORB the mixing is more variable because of the end-members' characteristics, in the WSCB the mixing is mainly due to a two well defined end-members: recharge water and CO_2 rich groundwater. Around the Selva basin, there also intermediate flow systems originating in the surrounding areas, which being another end-meber of the flow system, may be part of the mixing processes assessed.

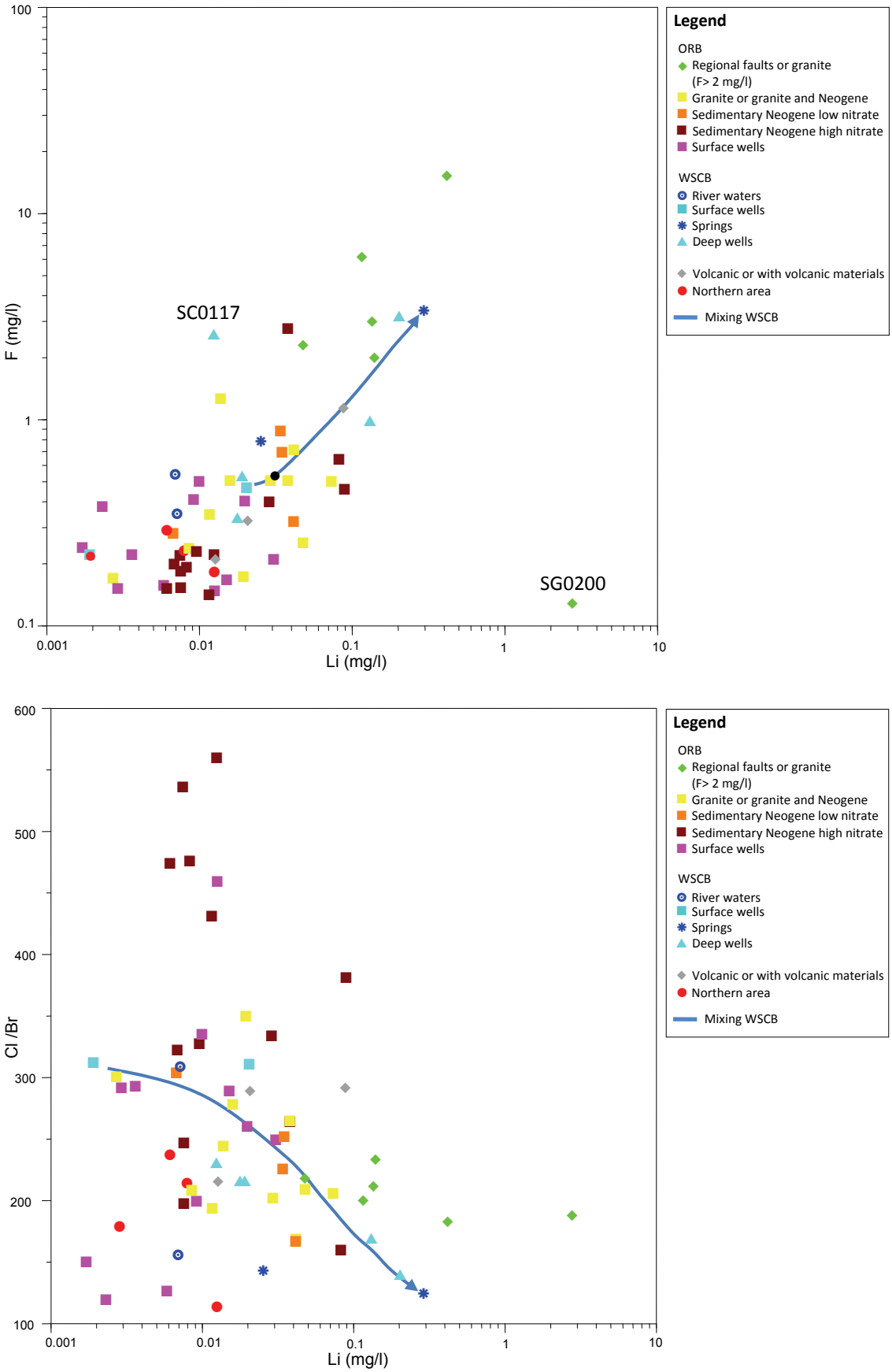

Figure 4.26. a) F vs Li b) Cl/Br mass ratio vs Li.

4.6. Conclusions

4.6.1. Hydrogeological conclusions

The processes controlling the water quality of the different flow systems have been described.

The water resources of the Selva basin are determined by different flow systems, on different spatial and time scales. There are mainly local and regional flows, with the second type different in the western Santa Coloma and the Onyar river basins. Their distribution is uneven over the basin and determined by geology, tectonics and the extraction rates. The quality of each flow system, and therefore the available water resources, is based on water-rock interaction and anthropogenic pressure.

The local flow recharged on the basin's surface can be classified in two different groups. First, there is the water recharged in the WSCB and older water with low nitrate, tritium and mineralization in the ORB with no water quality problems. The second group is modern waters characterized mainly by anthropogenic pollution (high NO_3, SO_4 and Cl) and high Ca. However most present recharge, unlike old waters, is characterized by pollution, leading to a progressive deterioration in the groundwater quality as older recharged water runs out. Furthermore, due to the intense pumping in some areas where the surface aquifer is well connected with deeper levels, this pollution is faster compared with the same flow system working under natural hydrological conditions and the same land use.

Regional flow systems are characterized by water-rock interaction with different characteristics in the ORB and the WSCB. Although both regional flows are recharged in the most elevated areas in the surrounding ranges (the Guilleries and Transversal ranges), they present particular water-rock interactions, leading to different water qualities. The regional flow recharging the Onyar basin shows greater mineralization, with higher levels of F, Cl and Li and some cases B.A potential upward flow due to pumping of deeper regional flow systems can therefore lead to limitations of groundwater use.

Although the bedrock and the surrounding range areas consist mainly of granite, groundwater interaction with this kind of rock is different in the ORB and the WSCB. There is therefore a change between the minerals forming the granite in the Selva basin and/or the groundwater of

the ORB, with a longer transit time interacting with less weathering minerals, leading to major concentrations of some solutes.

The intermediate flow systems are characterized by groundwater recharged around the Selva basin. Water inflow to the basin is by means of hydraulic continuity between the sedimentary materials of the Neogene and the granite and metamorphic formations of the Guilleries, Gavarres and the Selva marítima. Furthermore, flows can take place along the faults leading to deeper flow systems.

Groundwater in granites with major salt content may be the result of water-rock interaction in two different hydrogeological contexts. The first is when water is recharged in an elevated area with a long flow path that has been defined as the regional flow system. The second is when water is recharged in the granite outcrops in the basin or the surrounding areas, with relatively short flow paths but with low flow velocity. The first case is where the most productive wells are located, and is associated with higher F content, which is in most cases above safe drinking levels.

A last group and process involves water characterized by a mixing of different flow systems. This process take place between different aquifer levels, depending on the vertical hydraulic connectivity, or in the pumping well due to several screen intervals. The resulting groundwater can present quality problems related with each flow systems, (such as NO_3^- or F^-) or all of them.

The studies carried out enable the water quality problems associated with each flow system, it origin and its distribution in the basin to be defined. With this information, it is possible to define the appropriate exploitation management to maintain the water quality as long as possible. When a groundwater flow system is well defined, it is possible to ascertain which flow system is running with a few hydrochemical and isotopic indicators. It is therefore possible to define the most accurate management measures to retain the water quality, have the least impact on other flow systems and define the most appropriate water use for each well.

4.6.2. Methodological conclusions

In basins where drawing flow lines is difficult because of complex hydrogeology or mixing processes, it is difficult to define the available water resources from a quantative and qualitative point of view. However, if samples are classified and studied based on hydrogeological and hydrochemical criteria using various tools, it is possible to properly describe the hydrodynamic context of various types of basins.

The hydrochemistry of major ions allow the most important processes determining water quality to be ascertained. However, because concentration of major ions is determined by different hydrogeological factors, it is a limited tool in a hydrogeological context with different flow systems and mixing processes.

Environmental isotopes (δD, δ^{18}O) enable the relative recharge altitude of the groundwater and the recharge areas of a hydrogeological system to be defined. Furthermore, if it is not possible to distinguish between hydrochemically well defined end-members, differentiating different flow systems is feasible. Finally, they can help in defining processes that cannot always be characterized using hydrochemistry, such as CO_2 interaction or evaporation processes.

Using ions or compounds characteristic of a unique end-member, such as F and NO_3^- in this case, allows a clear distinction to be made between mixing processes. Futhermore, in areas where each flow system does not have a distinguished hydrochemistry, it is possible to distinguish between mixing of local and regional flow systems and intermediate flow systems.

TOC is a limited indicator of anthropogenic pollution in some geological contexts in which organic matter is related to geological formations. However, it may be a useful tool in defining natural end-members characterized by a very low or no presence of organic matter.

Sulphate isotopes are useful in defining the anthropogenic input in basins characterized by pig manure, sewage water and chemical fertilizers. In certain hydrogeological contexts, they are also useful in defining end-members of various different origins. Furthermore, the isotopic composition of sulfate can present a redox process such as the bacteriogenic sulfate reduction.

However, their application is limited in areas where natural sulphate concentrations are low, when the isotopic signature can be hidden by polluted waters with high sulfate contents.

Cl/Br ratios have been used on several occasions to study deep flows with high salinity, associated with a long transit time or by characterization of pollution from different sources. However, they have been shown to be a useful tool for any type of hydrogeological study, especially when is used with other hydrochemical and isotopic data.

The Cl/Br ratio in granites (>40 – 200) for any range of Cl content will be determined by different inputs and processes: granite composition, secondary mineralizations such as fluorite, CO_2 interaction, etc. If these processes are known, it is possible to define a tight range of Cl/Br ratios for each case study and/or geological context.

When using the Cl/Br ratio to identify the source of pollution, it is important to stress that sewage waters can have the same Cl/Br ratio as groundwater polluted by pig manure. However, as shown in previous studies, the Cl/Br ratio characteristic of farm animal pollution has a huge range, depending not only on the livestock concerned but the operation of the facility, the fee, the locations where the sample was collected and the animals' drinking water. In this regard, when using the Cl/Br ratio as an indicator of pollution, it is necessary to find out the Cl/Br ratio of the pollution input or use other hydrochemical and/or isotopic tools.

It is possible to define relatively accurate complex hydrogeological flow systems using different hydrochemical and isotopical tools. Depending on the aim and the characteristics of the area studied, various types and/or quantities of tools will be used in hydrogeological research.

4.7. References

Alcalá, F.J, Custodio, E., 2008a. Using Cl/Br ratio as a tracer to identify the origin of salinity in aquifers in Spain and Portugal. Journal of Hydrology 359, 189-207.

Alcalá, F.J, Custodio, E., 2008b. Atmospheric chloride deposition in continental Spain. Hydrological processes 22, 3636-3650.

Avila, A., Molowny-Horas, R., Gimeno, B.S., Peñuelas, J., 2009. Analysis of Decadal Time Series in Wet N Concentrations at Five Rural Sites in NE Spain. Water Air & Soil Pollution. DOI 10.1007/s11270-009-0124-7

Beaucaire, N., Gassama, N., Tresonne, N., Louvat, N., 1999. Saline groundwaters in the hercynian granites (Chardon Mine, France): geochemical evidence for the salinity origin. Applied Geochemistry 14, 67–84.

Behl, E., Davis, S.N., Goldwitz, J., 1987. Cl/Br ratios as an environmental tracer of anthropogenically altered waters. In Geological Society of America, Abstracts with Programs 19, 7:585.

Behne, W., 1953. Untersuchungen zur Geochemie des Chlor und Brom. Geochemica et Comsochimica Acta 3 (4), 186-214.

Boggs, J.M., Adams E.E., 1992. Field study of dispersion in heterogeneous aquifer 4: Investigations of adsorption and sampling biac. Water Resources Research 28, 3325-3338.

Bottomley, D.J., Chan, L.H., Katz, A., Starinsky, A., Clark, I.D., 2003. Lithium isotope geochemistry and origin of Canadian Shield brines, Ground water 41, 847-856.

Carmona, J.M. , Bitzer, K., López, E. And Bouazza, M., 2000. Isotopic composition and origin of geothermal waters at Caldetes (Maresme-Barcelona). Journal of Geochemical Exploration 69–70, 441–447.

Carrillo-Rivera, J.J., Irén Varsányi, I., Kovács L.O., Cardona, A., 2007. Tracing Groundwater Flow Systems with Hydrogeochemistry in Contrasting Geological Environments. Water Air and Soil Pollution 184, 77–103.

Correns, C.W., 1956. The geochemistry of the halogens. In: Physics and Chemistry of the Earth (L.F. Ahrens et al., eds), Vol. 1, pp. 181-233. McGraw-Hill, New York.

Cravotta, C.A., 1997. Use of Stable Isotopes of Carbon, Nitrogen, and Sulfur to Identify Sources of Nitrogen in Surface Waters in the Lower Susquehanna River Basin, Pennsylvania. U.S. Geological Survey Water-Supply Paper 2497.

Davis, S.N., Behl, E., Goldwitz, J., 1987. Hydrogeologic importance of bromide. In Geological Society of America, Abstracts with Programs 19, 637.

Davis, S.N., Whittemore, D.O., Fabryka-Martin, J., 1998. Uses of Chloride/Bromide Ratios in Studies of Potable Water. Groundwater 36, 338-350.

Davis, S. N., Fabryka-Martin, J., Wolfsberg, L.E., 2004. Variations of Bromide in potable groundwater in the United States. Ground Water 4, 902-909.

Dogramaci, S.S., Herczeg, A.L., Schiff, S.L., Bone, Y., 2001. Controls on $\delta^{34}S$ and $\delta^{18}O$ of dissolved SO_4 in aquifers of the Murray Basin, Australia and their use as indicators of flow processes. Applied Geochemistry 16, 475–488.

Edmund, W.M., Kay, R.L.F., McCartney, R.A., 1985. Origin of saline groundwater in the Carnellis Granite (Cornwall, England): Natural processes and reaction during hot dry rock reservoir circulation. Chemical Geology 49, 287-301.

Edmunds, W. M., Kay, R.L.F., Miles, D. L., Cook, J.M., 1987. The origin of saline groundwaters in the Carnellis granite, Cornwall (U.K): further evidence from minor and trace elements. In *Saline waters and gases in crystalline rocks*, (ed. P Fritz and S.K. Frape), pp. 127-43. Geological Association of Canada Special Paper No. 33.

Einsiedl, F., Mayer, B., 2005. Sources and Processes Affecting Sulfate in a Karstic Groundwater System of the Franconian Alb, Southern Germany. Environtal Science and Technology 39, 7118-7125.

Epstein, S., Mayeda, T.K., 1953. Variation of ^{18}O content of waters from natural sources. Geochimica e Cosmochimca Acta 4, 213–224.

Fabryka-Martin, J., Whittemore, D.O, Davis, S.N, Kubik, P.W., Sharma, P., 1991. Geochemistry of halogens in the Milk River aquifer, Alberta, Canada. Applied Geochemistry 6, 447-464.

Folch, A., Mas-Pla, J., 2008. Hydrogeological interactions between fault zones and alluvial aquifers in regional flow systems. Hydrological Processes 22, 3476-3487.

Fuge, R., 1979. Water-soluble chlorine in granitic rocks. Chemical Geology 25, 169-174.

Gerritse,R., George, R., 1988. The role of soil organic matter in the geochemical cycling of chloride and bromide. Journal of Hydrology 101, 83-95.

Grigsby, C.O., 1983. Personal communication, letter from Los Alamos National Laboratory, New Mexico.

Grup de Recerca en Geologia i Cartografia Ambiental, 2009. Diagnosi hidrogeològica de la conca alta de la Muga (Alt Empordà). Universitat de Girona. Finançat per Agència Catalana de l'Aigua i Associació de Municipis Salines – Bassegoda. Girona (Spain).

Harder, H., 1975. Boron in minerals and igneous rock: in Walker C.T., ed., Geochemistry of boron: Dowden, Hutchinson and Ross Inc. Stroudberg.

Hem, D. J., 1985. Study and Interpretation of the Chemical Characteristics of Natural Water. U.S. Geological Survey, Water Supply Paper 2254.

Hite, C.D., Cheng, S., 1996. Spatial characterization of hydrochemistry within constructed fen, Green County, Ohio. Groundwater 34, 415-424.

Husak, P.F., 2003. Chloride/Bromide ratios in leachate derived from farm-animal waste. Environmental Pollution 121, 23-25.

Huh, Y., Chan, L.H., Zhang, L., Edmond, J.M., 1998, Lithium and its isotopes in major world rivers: Implications for weathering and the oceanic budget. Geochimica and Cosmochimica Acta 62, 2039-2051.

IAEA/WMO, 2006. Global Network of Isotopes in Precipitation. The GNIP Database. Accessible at: http://isohis.iaea.org.

Kendall, C., 1998. Tracing nitrogen sources and cycling in catchments. In: Kendall, C. and Mc Donnell, J.J. (Eds.), *Isotope Tracers in Catchment Hydrology*. Elsevier, pp. 519-576.

Krouse, H.R., Mayer, B., 2000. Sulfur and oxygen isotopes in sulfate. In: Cook, P.G., Hercseg, A.L. (Eds.), Environmental Tracers in Subsurface Hydrology. Kluwer Academic Press, Boston, pp. 195–231.

Marimon, M.P.C., Knöller, K., Roisenberg, A., 2007. Anomalous fluoride concentration in groundwater – is it natural or pollution? A stable isotope approach. Isotopes in Environmental and Health Studies 43, 165-175.

Menció, A., 2006. Anàlisi multidisciplinària de l'estat de l'aigua a la depressió de la Selva. PhD dissertation, Universitat Autònoma de Barcelona.

Mizutani, Y., Rafter, T.A., 1973. Isotopic behaviour of sulfate oxygen in the bacterial reduction of sulfate. Geochemical Journal 6, 183-191

Moldovani, L.M. Walter and L.S. Land, Strontium, boron, oxygen and hydrogen isotope geochemistry of brines from basal strata of the Gulf Coast sedimentary basin, USA Geochimica et Cosmochimica Acta 57, 2083-2099.

MOPU, 1985. Plan Hidrológico del Pirineo Oriental. EE2 Estudio complementario sobre aguas subterráneas. Zona5 - La Selva. Síntesis Hidrogeológica. Ministerio de Obras Públicas y Urbanismo, Dirección General de Obras Hidráulicas, Spain.

Neal, C., Neal, M., Warrington, A., Avila, A., Pinol, J., Roda, F., 1992. Stable hydrogen and oxygen isotope studies of rainfall and streamwaters for two contrasting holm oak areas of Catalonia, northeastern Spain. Journal of Hydrology 140**,** 163–178.

Nordstrom, D.K., Lindblom, S., Donohoe, R.J. and Barton, C.C., 1989. Fluid inclusions in the Stripa granite and their possible influence on the groundwater chemistry. Geochemica et Cosmochimica Acta 53, 1741-1755.

Otero, N., Vitòria, L., Soler, A., Canals, A., 2005a. Fertilizer characterisation: Major, trace and rare earth elements. Applied Geochemistry 20, 1473-1488

Otero, N., Canals, A., Soler, A., 2007. Using dual-isotope data to trace the origin and processes of dissolved sulphate: a case study in Calders stream (Llobregat basin, Spain). Aquatic Geochemitry 13, 109–126.

Panno, S.V., Hackley, K.C., Hwang, H.H., Greenberg, S.E., Krapac, I.G., Landsberger, S. and D.J. O'Kelly., 2006. Characterization and Identification of Na-Cl Sources in Ground Water. Ground water 44, 176-187.

Parkhurst, D.L., Appelo, C.A.J., 1999. User's guide to PHREEQC (version 2) - a computer program for speciation, reaction-path, 1D-transport, and inverse geochemical calculations. US Geol. Surv. Water Resour. Inv. Rep. 99-4259, 312p

Pauwels, H., Fouilliac, C., Criaud, A., 1992. Water-rock interactions during the experimets within the geothermal hot dry rock borehole GPK 1, Soultz-sous-Forêts, Alsace, france. Applied Geochemistry 7, 243-255.

Piqué, A., 2008. Insights into the geochemistry of F, Ba and Zn-(Pb) hydrothermal systems: examples from northern Iberian Peninsula. PhD dissertation. Universitat Autònoma de Barcelona

Piqué, A., Canals, A., Grandia, F., Banks D.A., 2008. Mesozoic fluorite veins in NE Spain record regional base metal-rich brine circulation through basin and basement during extensional events. Chemical Geology 257, 139-152.

Pous, J., Sugrañes, L.S., Badiella, P., 1990. Estudio geoeléctrico de la depresión de La Selva (Girona). Acta Geológica Hispánica 25, 261-269.

Rock, L., Mayer, B., 2002. Isotopic assessment of sources and processes affecting sulfate and nitrate in surface water and groundwater of Luxembourg. Isotopes in Environtal and Health Studies 38, 191-206.

Stober, I., Bucher, 1999. Origin of salinity of deep groundwater in crystalline rocks. Terranova 11, 181-185.

Tóth, J., 1995. Hydraulic continuity in large sedimentary basins. Hydrogeology Journal 3, 4–16.

Tóth, J., 2000. Las aguas subterráneas como agente geológico: Causas, procesos y manifestaciones. Boletín Geológico y Minero 111, 9–26.

Utrilla, R., Pierre, C., Ortí, F., Pueyo, J.J., 1992. Oxygen and sulphur isotope compositions as indicators of the origin of Mesozoic and Cenozoic evaporites from Spain. Chemical Geology: Isotope Geoscience Section 102, 229–244.

Van Stempvoort, D.R., Krouse, H.R., 1994. Controls of d18O in sulphate. In: Alpers, C.N., Blowes, D.W. (Eds.), Environmental Geochemistry of Sulphide Oxidation. American Chemical Society, Washington, pp. 446–480.

Vehí, M., 2000. Geologia ambiental de la depressió de la Selva. PhD dissertation. Universitat Autònoma de Barcelona. Spain

Vengosh .A, Pankratov, S., 1998. Chloride/bromide and chloride/ fluoride ratios of domestic sewage effluents and associate contaminated groundwater. Ground Water 36, 815–824.

Vitòria, L., 2004. Estudi multi-isotòpic ($\delta^{15}N$, $\delta^{34}S$, $\delta^{13}C$, $\delta^{18}O$, δD i $^{87}Sr/^{86}Sr$) de les aigües subterrànies contaminades per nitrats d'origen agrícola i ramader. PhD dissertation. 188 pp. Universitat de Barcelona. Spain.

Vitòria, L., Grandia, F., Soler, A., 2004a. Evolution of the chemical (NH_4) and isotopic (^{15}N-NH_4) composition of pig manure stored in an experimental pit. In: IAEA (Eds.), Isotope Hydrology and Integrated Water Resources Management. Conference & Symposium Papers, Vienna, pp. 260–261.

Vitòria, L., Otero, N., Canals, A., Soler, A., 2004b. Fertilizer characterization: isotopic data (N, S, O, C and Sr). Environmental Science Technology 38, 3254–3262.

Wittemore, D.O., Davis, S.N., 1995. Patterns of Cl/Br with Cl concentration in the hydrosphere. Geological Society of America, Abstract with Programs, vol. 27, 465-466.

Chapter V

Conclusions

Hydrogeological flow systems in range-and-basin areas are governed by the heterogeneity inherent in their geological evolution. Their study requires a large-scale approach to determining the origin of the flow systems; i.e. the location of all the recharge zones that provide the basin area with water resources, as well as the way it discharges. Moreover, in regions with considerable human development, groundwater withdrawal has a varying seasonal effect on flow systems, from a regional to local scale. This alteration of hydrogeological dynamics affects the recovery of water resources, and therefore their future availability.

In this dissertation, the Selva Basin has been studied as a paradigmatic case of a range-and-basin area with severe pressure on groundwater resources. The conclusions of the research conducted in this area provide various insights into the problem of water management in these geological environments. First of all, it presents the outcome of different methodologies ranging from fieldwork to numerical modeling, together with the analysis of hydraulic head, hydrochemical and isotopical data records. Second, it describes the behavior of potentiometric evolution in different geological settings, and the hydrochemical/isotopical features and related geochemical processes that define groundwater samples and each of the recharge end-members in particular. Finally, this research shows the effect of human pressures even on large-scale flow systems, and therefore provides some strategies for the assessment of water resources management in these hydrogeological systems.

This final chapter summarizes the features from a hydrogeological perspective that support the conceptual model for the Selva Basin aquifer system which also illustrate the contribution and the possibilities for each methodology applied. Finally, these results enable an approach to water resource assessment in tectonic hydrogeological contexts.

As is usual in range-and-basin areas, the groundwater dynamics in the Selva basin are controlled by the tectonic structure and the sedimentary infilling of the basin. In this area, groundwater recharge of the basin is attributed to various hydrological flow systems; i.e., local, intermediate and regional. Nevertheless, this flow field is largely affected by withdrawal rates, which disturb natural flow patterns and lead to water mixing that affects groundwater quality and quantity. Human pressures are thus identified as one of the main governing forces on the overall flow system, and a key factor in its interpretation.

Furthermore, human activities modify the natural flow system according to the water withdrawal regimes in two different ways:

- At deep aquifer levels, they modify the natural hydrodynamics of the aquifer that cause:
    - Mixing of different flow systems depending on the season.
    - Introduction of pollutants (nitrate) at deeper aquifer levels decreasing the quality of the water resources.
    - Increasing of fluoride content over safe drinking levels in some deep supply wells.
- For shallow, water-table aquifers, by introducing pollution to the system in the form of nitrogen compounds, and to a lesser extent, sulphates and chlorides into groundwater from fertilizers (mainly pig manure) and wastewater.

One of the main goals of a regional hydrogeological study is to identify the recharge areas of the system. In the Selva basin, recharge occurs on the basin's surface and by hydrological continuity between the basin and the surrounding range areas. Regional fault zones act as preferential flow paths that control recharging flows originating in the mountain ranges.

Moreover, the tectonic structure of the Selva basin determines the large-scale distribution of hydrogeological flow systems. In this regard, it is possible make a distinction between two main hydrogeological systems: 1) the Onyar River Basin (ORB), that occupies the northern half of the tectonic basin, associated with the fault system that defines the northern and eastern limits of the basin, and 2) the Santa Coloma River Basin (SCRB), with a flow system mainly controlled by the regional fault zone that defines the western limit of the area. The structural features are thus essential in understanding the influence of the surrounding ranges as recharge areas, as well as the flow rates towards the Neogene sedimentary infilling of the basin. Hydrochemical and isotopical characteristics will therefore differ according to this structural control, and, as mentioned above, depending on the effects of groundwater withdrawal in the flow field.

This structural control defines the local, intermediate and regional flow systems which are responsible for the large-scale hydrodynamics of the basin and, more importantly, the recovery of drawdown after the main withdrawal period (summer). The origin of the recharge

of the large-scale, regional flow systems is assigned to the Transversal range in the ORB and to the Guilleries range in the SCRB, especially in its western part. (Figure 5.1). These hydrogeological systems involve a groundwater flow within the basement and an upward vertical recharge from the basement to the overlying Neogene sedimentary layers.

Moreover, local and intermediate flow systems originate in the basin itself or in the less-elevated surrounding ranges, and the fault system has a minor effect on their flowpaths. For instance, local flow systems involve the recharge in the upper Neogene sedimentary layers and alluvial formations in most of the area, with the exception of the SCRB alluvial deposits that also receive some contribution from regional recharge because of their geomorphological setting along the fault zone. Recharge from the Gavarres range and the Selva Marítima range, due to their lower elevation and their structural setting, only contributes to intermediate flow systems that recharge the Neogen infilling of the basin by a lateral flow on the edge of the basin. There is also an upward vertical recharge from the basement in some areas close to the main faults along the edge of the basin.

As mentioned above, each flow system has its own hydrochemical and isotopical features that enable end-members to be identified in the overall hydrogeological system, flow paths, and mixing processes. Regional flows are also different in the two basins – the ORB and the SCRB - except for their isotopic values ($\delta^{18}O$), of below -6 ‰, showing similar recharge altitudes above 500-800 m asl, and in some cases showing the effects of CO_2 interaction. In the Santa Coloma basin, with low or high mineralization, the flow system shows lower Cl content (70 mg/l or less), a Cl/Br ratio of 130 or less, negligible NO_3, up to 8 mg/l of F and no TOC content. However, in the Onyar river basin, the regional flow shows higher Cl content (over 200 mg/l), a Cl/Br ratio of about 200, TOC of up to 3 mg/l, F of up to 15 mg/l, negligible NO_3 and $\delta^{34}S\text{-}SO_4$ of over 20 ‰, related with the sulphate reduction process.

Intermediate flow systems show variable hydrochemical and isotopical values, depending on the recharge area and their flow path. These flow systems usually show hydrochemical facies between regional and local flow systems, consistent with the groundwater recharged in the Gavarres range and/or the lower part of the most elevated range areas. The range of water isotopes is between the basin's surface and the most elevated zones of the range areas, with $\delta^{18}O$ values of between 5.5 and 5.9‰. Furthermore, the intermediate flow systems related to regional faults in the Gavarres range show F content of between 0.5 and 3.0 mg/l.

Local recharge and/or flow systems can be divided into three different categories: present recharge in alluvial and Neogene sediments, old recharge in Neogene sediments and recharge in granite outcrops.

Present recharge in the Santa Coloma River Basin is characterized by a mineralization with low Cl (< 30 mg/l), low nitrate, and a Cl/Br ratio similar to rain water. Due to the aquifer-river interaction, the δD and $\delta^{18}O$ values vary as a result of the mixing between local rainfall and stream contributions. Tritium values show a variability of between 3 and 5.6 TU. Present local recharge can have similar characteristics in both basins, and especially in the ORB, it is characterized by pollution with high nitrate, and to a lesser extent, high sulphate and chloride, with an isotopic value ($\delta^{18}O$) of between 4.7 and 5.3 ‰ consistent with the range of isotopic values of the basin's surface rainfall. The Cl/Br ratio is between 350-600, attributed to sewage waters, with a $\delta^{34}S\text{-}SO_4$ of between 5 and 9 ‰.

Old recharge, localized mainly in the Onyar River basin, is groundwater partially recharged before bomb testing period, with tritium values below 3 TU. It is has low or zero nitrate content, and a Cl content about 70 mg/L. The $\delta^{18}O$ values are also within the range of the basin's surface (4.7-5.3 ‰), with even lower values that indicate the influence of intermediate flow systems in some areas.

The groundwater recharged in the granite outcrops of the Selva or the surrounding areas may have low or high mineralization levels depending on water-rock interaction and/or pollution. The groundwater samples from wells drilled in weathered granite usually present low mineralization, whereas those sampling points associated with fractures have higher mineralization and Cl content. Nevertheless, wells related to fractured areas usually present a lower yield. Their isotopic value ($\delta^{18}O$) mainly falls within the basin's surface range, except in the SE of the basin (the Llagostera area), where the isotopic content denotes evaporative processes in the vadose zone.

Finally, groundwater samples arising from a mixing of different flow systems have also been identified. Various mixing processes occur in the Selva basin. In specific terms, the Santa Coloma fault plays an important role that enables mixing between water recharged in the surface formations and groundwater belonging to regional flow systems, and those originating in the Guilleries range in particular. The proportion of water coming from every flow system

will be determined by the particular geological and hydrogeological features and, in some cases, the screen intervals and pumping rates of each well.

In the Onyar River basin, mixing processes also occur. As in the Santa Coloma area, regional faults play an important role and this contribution is mainly related to the groundwater withdrawal regime. In areas where the sedimentary infilling of the basin acts as a single, unique aquifer, and where exploitation levels are high, groundwater extraction creates downward vertical flows that recharge the deeper sedimentary layers of the aquifer with water from the upper levels. Simultaneously, deep wells located near fracture zones in the basement can generate upward vertical flows that recharge the Neogene aquifer levels with groundwater related to regional flowpaths. This behavior varies throughout the year, depending on seasonal extraction rates.

The hydrochemical characteristics of the end-members in the ORB will therefore determine large nitrate concentrations (>50 mg/L) in groundwater. If there is a groundwater contribution from the basement, fluoride content over 0.4 mg/L must be expected. Furthermore, wells with several screen intervals may even show a more complex hydrochemistry related to the mixing within the pumping well. The occurrence of these mixing processes reveals the effect of pumping on the quality of the resources withdrawn, which under predevelopment conditions show neither nitrate nor fluoride in their composition. This observation highlights how human pressures disturb natural groundwater hydrodynamics.

Under post-development conditions, the integrated application of several hydrogeological approaches (modeling, hydrochemistry, isotopes, etc.) is necessary for a full understanding of the how this kind of flow system behaves. Furthermore, because of the variability of groundwater withdrawal during the year, a complete understanding of the groundwater behavior can only be achieved by applying these approaches during the different seasons.

In conclusion, this dissertation supports the characterization of hydrogeological systems based on the study of flow systems contributing to their water resources, rather than a mere description of their hydrogeological properties. An analysis of flow systems provides an integrated understanding of the entire hydrodynamics, which is essential for a sound assessment for water resources planning. Furthermore, this research highlights the strong influence of human pressure upon the entire flow system. Seasonal groundwater monitoring

reflects these effects, and provides an interesting insight into the behavior of the whole system under stress.

This perspective is particularly relevant at a time when river district management plans are being produced as part of the implementation of the Water Framework Directive. The hydrogeology of groundwater mass bodies, and especially the extent of human pressures upon them, can be more fully understood when they are described from a flow system perspective: this enables allows reasonable knowledge of the potential alterations to their recharge and their quality. Both aspects are fundamental in achieving the goal of sustainable water resources management.

Moreover, as shown here, many hydrogeological systems consist of several geologic formations and/or geographic locations. These assumptions have to be considered before the establishment of water bodies (Water Framework Directive 2000/60/CE), as in some cases they are not simply defined by the complete hydrogeological system(s) in which they work. Studies based on integrated methodological approaches that involve distinct spatial scales are therefore essential for an appropriate understanding of the hydrogeological dynamics of groundwater bodies and their adequate water resources management.

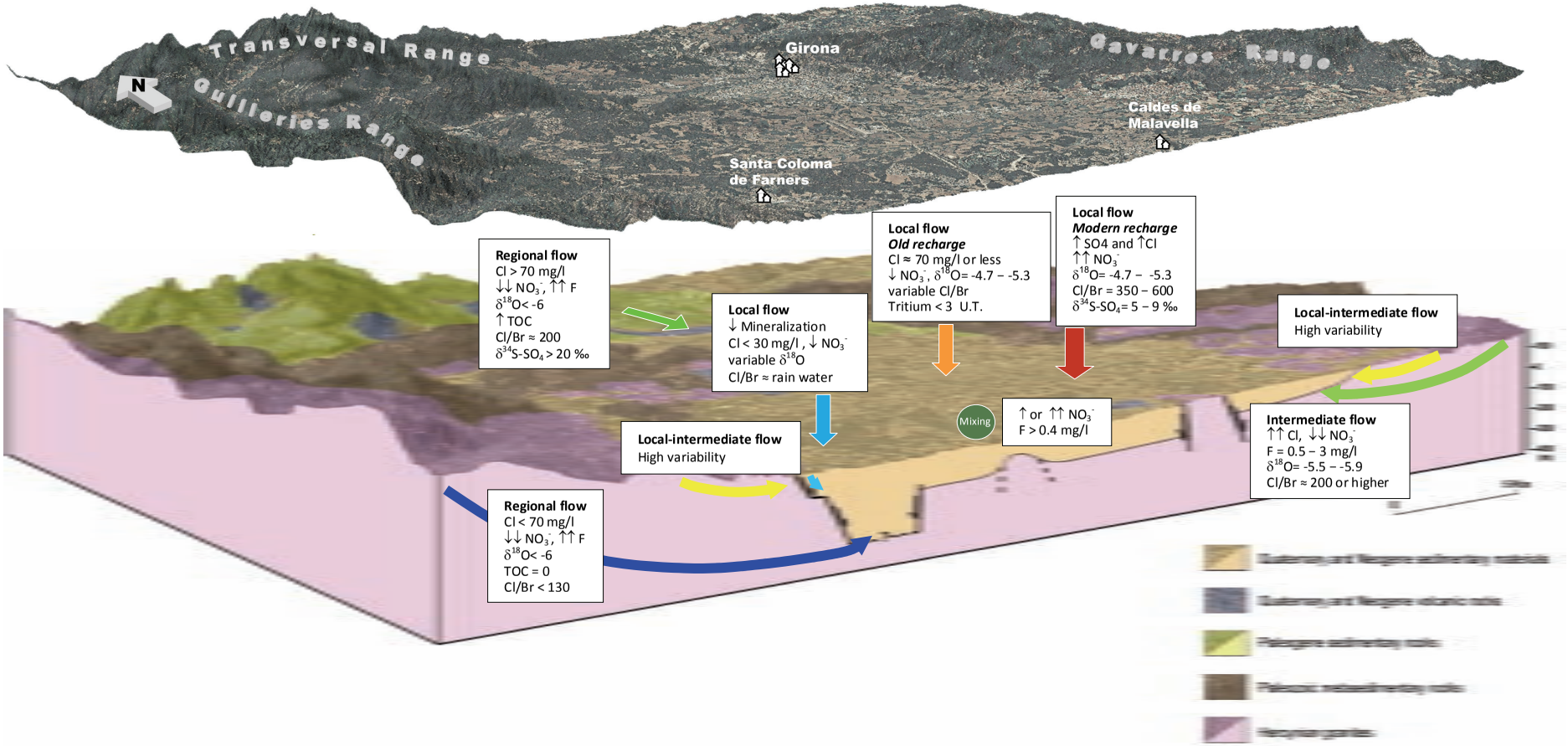

Figure 5.1. Block diagram of Northern side of the Selva basin and surrounding range areas. The arrows indicate the different flow systems that contribute to the basin's recharge, and their most significant hydrochemical and isotopic characteristics. Recharges in granite outcrops and by hydraulic continuity between the various geological formations have not been shown.

Annex

Published articles

Folch, A., Mas-Pla, J., 2008. Hydrogeological interactions between fault zones and alluvial aquifers in regional flow systems. Hydrological Processes 22, 3476-3487.

Mencio, A., Folch, A., Mas-Pla, J., 2010. Analyzing hydrological sustainability through water balance. Environmental Management. DOI 10.1007/s00267-010-9461-y.

Folch, A., Casadellà, L., Astui, O., Mencio, A., Massana, J., Vidal-Gavilan, G., Pérez-Paricio, A., Mas-Pla, J., 2010. Veryfing conceptual flow models in a river-connected alluvial aquifer for management purposes using numerical modelling. XVIII International Conference on Water Resources, CMWR 2010, J. Carrera (Ed), CIMNE, Barcelona (accepted).